RECENT ADVANCES IN ENGINEERING, SCIENCE AND CONSTRUCTION

EDITED BY: Assist. Prof. Dr. Cüneyt YÜCELBAŞ

AUTHORS

Asghar Abbas
Aslı AKSOY
Akram Ismael Shehata
Cengiz BOZADA
Deepa SONAL
Ebru TARIM
Ferit KARGIN
Guangwen Yin
Hafiz Muhammad Waqar Ahmad
Halime PEHLİVANOĞLU
Hikmet Y. ÇOĞUN
Huseyin Cagan KILINC
Mehmet Erbil ÖZCAN
Melahat GÖKTAŞ
Mikail ASLAN
Muhammad Mohsin
Muhmmad Tahir Aleem
Muhammad Zeeshan Afzal
Nelam Sajjad, Zohaib Shahid
Liliana Aguilar- Marcelino
Rao Zahid Abbas
Rizwan Abdul Aleem
Sudi APAK
Yunus OZTURK
Yusuf Jibril Habib

İKSAD
Publishing House

RECENT ADVANCES IN ENGINEERING, SCIENCE AND CONSTRUCTION

EDITED BY

Assist. Prof. Dr. Cüneyt YÜCELBAŞ

AUTHORS

Asghar Abbas
Aslı AKSOY
Akram Ismael Shehata
Cengiz BOZADA
Deepa SONAL
Ebru TARIM
Ferit KARGIN
Guangwen Yin
Hafiz Muhammad Waqar Ahmad
Halime PEHLİVANOĞLU
Hikmet Y. ÇOĞUN
Huseyin Cagan KILINC
Mehmet Erbil ÖZCAN
Melahat GÖKTAŞ
Mikail ASLAN
Muhammad Mohsin
Muhmmad Tahir Aleem
Muhammad Zeeshan Afzal
Nelam Sajjad, Zohaib Shahid
Liliana Aguilar- Marcelino
Rao Zahid Abbas
Rizwan Abdul Aleem
Sudi APAK
Yunus OZTURK
Yusuf Jibril Habib

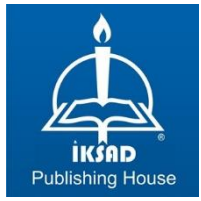

(The Licence Number of Publicator: 2014/31220)
TURKEY TR: +90 342 606 06 75
USA: +1 631 685 0 853
E mail: iksadyayinevi@gmail.com
www.iksadyayinevi.com

ISBN: 978-625-7562-95-9
Cover Design: İbrahim KAYA
September / 2021
Ankara / Turkey
Size = 16x24 cm

CONTENTS

PREFACE

This book presents the recent advances in engineering, science, and construction. The matters discussed and presented in the chapters of this book cover a wide spectrum of topics and research methods in the field of engineering, science, and technology.

The book contains eight chapters: estimations of river flows by use of artificial intelligence methods, investigation of quality criteria during the storage of vacuum dried minced meat and powder soup, using in the density functional method in material science, investigation of coating efficiency in friction surfacing process, synthesis and characterization of graft copolymers by atom transfer radical polymerization, the effects of nitrilotriacetic acid (nta) on some plasma enzymes of nile tilapia, necrotic enteritis: A re-emerging economically important issue and alternatives to antibiotics, and application of IoT in agriculture.

This book, which consists of studies covering the fields of artificial intelligence, engineering, science, construction, materials, and metallurgical, will constitute an academic data source for academicians and researchers.

I believe that this book, which consists of different scientific fields, will make significant contributions to the world of science and I would like to thank the authors who have contributed.

Sincerely Yours
Assist. Prof. Dr. Cüneyt YÜCELBAŞ[1]
Sep 2021

[1] Hakkari University, Electrical and Electronics Engineering Department, Hakkari, TURKEY.
E-mail: cuneytyucelbas@hakkari.edu.tr ORCID ID: 0000-0002-4005-6557

CHAPTER 1

COMPARISON OF AKDERE FLOW MEASUREMENT STATION DATA BASED DEEP-LEARNING MODELS IN PREDICTION OF STREAM-FLOW FOR WATER RESOURCES APPROACH

Assist. Prof. Dr. Huseyin Cagan KILINC[1],
Assist. Prof. Dr. Yunus OZTURK[2] , Prof. Dr. Sudi APAK[3]
MSc Ebru TARIM[4*]

[1] İstanbul Esenyurt University, Engineering Faculty, Civil Engineering Department, İstanbul, Turkey. huseyincagankilinc@esenyurt.edu.tr , ORCID ID 0000-0003-1848-2856
[2] Kilis 7 Aralık University, Engineering Faculty, Civil Engineering Department, Kilis, Turkey. ynsemre@kilis.edu.tr , ORCID ID 0000-0001-8032-9292
[3] İstanbul Esenyurt University, Engineering Faculty, Industrial Engineering Department, İstanbul, Turkey. sudiapak@esenyurt.edu.tr , ORCID ID 0000-0003-4333-8266
[4] Hasan Kalyoncu University, Engineering Faculty, Civil Engineering Department, Gaziantep, Turkey. tarmebru@gmail.com , ORCID ID 0000-0001-6980-1891

1. INTRODUCTION

Water is a source of life that is vital for humans and brings life almost to a halt in case of lack. It faces many negativities that will jeopardize its sustainability day by day. For this reason, predicting water resources enables water to be used in every future in a planned, efficient and economical way. Water resources management extends to the rainwater collected in river basins and the transfer of these rainwater to consumers. In the management of river basins, evaluation of land soil is of great importance along with accurate estimation of current measurement stations. The main goal should be to protect, plan and sustain river basins. In this context, planning of water resources management can be done strategically by creating many prediction models. ANN and deep learning models, one of the AI techniques, are among these prediction methods. Estimates can provide suitable planning opportunity for both the producer and the user for water resources, living things, irrigation, hydroelectric power generation and transfer of water to future generations.

Accurate estimation of flow is an necessary component for both water amount and amount direction. In last years, AI techniques have been evidented as a computer science branch to model a vast variety of hydrological handle. A number of research studies are conducted to find a more fruitful approach in terms of correctness and acticality (Mehr et al., 2013).

DL is a develope branch of AI consisting of a large number of layers of neurons that symbolize the learning handle. DL can get over with large-scale data and excel in several fields. Accordingly, surveyors pay more notice to investigating DL for intrusion detection (Aldweesh et al., 2020). DL is one of the developed touches to machine learning and has been gaining more and more note in last years (Boulemtafes et al., 2020). With the rapid growth of DL algorithms, many high-correctness models were developed and implemented in the real world space. DL is parallel and suitable for distributed computing, which can significantly increase system efficiency. A kind of distributed computing system is proposed for deep learning. The design concept of cache pre-transmission aims to use reinforcement learning to train a pre-forward policy to increase the cache hit rate. Due to the characteristics of reinforcement learning, this policy can be adapted and applied to different computer environments. Finally, this system has been demonstrated experimentally (Cheng et al., 2020).

Terzi and Köse (2012), in the flow estimation of Göksu River, ANN models are developed by using the current values of the stations no.1714, 1, 2, 3, 4 and 5 days ago and the current values of the stations no 1719 and 1720 as input. It is observed that the developed model's coefficient of clarity and average absolute error value gives better conclusions compared to other models.

Yurdusev et al., (2008), estimation of monthly flows in the closed basin of Akarçay river from rain and flow observations using the ANN method, models are designed in 4 different categories depending on

the parameters such as the location of the precipitation observation stations present in the basin and the observation interval. The conclusions obtained are compared with the conclusions of multivariate regression analysis and it is revealed that ANN can be successfully applied to the flow prediction problem from the flow and precipitation observations and produces safe estimates.

The flow rate of the Lower Sakarya River gives the highest determination coefficient (R^2) of the four-day time shift using flow data obtained from Doğançay Current Observation Station using Feed Forward Back Propagated Neural Networks from ANN models. This study on the Sakarya river is thought to help future energy planning and flood studies (Kızılaslan et al., 2013).

An ANN model is developed and applied to the daily flows of the Coruh River in the Coruh basin. The ANN model created successfully represents the daily flows of the Coruh River; Thus, it is thought that the developed model structure can be used successfully in the estimation of daily flows of other river basins (Okkan and Mollamahmutoğlu, 2010).

Gündüz (2011), daily flow data in 1968-2006 period is used for ANN and wavelet transformation models developed to estimate river flow in Fırat-Dicle basin. Crosscheck conclusions show that AI techniques can be used successfully in river flow prediction. It is observed that the Köprüçay currents estimated by the forward feed backward propagation ANN method give better conclusions when compared

with the conclusions of the linear regression (LR) model (Demirpençe, 2005).

In this study, estimations of river flows are made with the data obtained from current measurement stations. Prediction is realized by making use of AI methods ANN and DL models. As a conclusion of the crosscheck, the best prediction model can be determined and can be a guide in similar studies.

2. STUDY AREA AND DATA

In this study, the daily streamflow information used was collected from the Euphrates River located in the southeast region of the Turkey. The daily flow values of a flow measurement stations in the Fırat Basin, one of the 25 basins in Turkey, were examined and evaluated for performance analyses using DL optimizers (Figure 1).

Figure1: Location of Euphrates river basin

This basin is located in the eastern part of Turkey with a 127304 km^2 area –making it the biggest wetland area in the country. River Murat and River Karasu are important rivers supplying Euphrates River with water (Figure 2).The data used in this study was flow measurement stations taken from General Directorate of State Water Affairs (DSI) which are the most accurate data in the Euphrates river and they are located at the same basin area. Euphrates Basin has area of 127 304 km^2, with an average elevation of 1009.87m. The average rainfall is 540.1 mm / year. According to the records in the beginning and middle of the 20th century, the average annual natural flow of the Euphrates River is 20.9 cubic kilometers. The station are D21A183 (Akdere Çayı Aşağıköprülü Village). The daily discharge data taken into account for this study covered the period of 2011-2018 for.

The flow of the river was measured by calculating the water level pressure with a sensor placed in the target area of the river. In the study, 70% of the flow data was used as training data and 30% as test data.

Figure 2: Euphrates river basin and its drainage network

3. METHODOLOGY

In this study, the DL method was performed by Keras library to predict the stream flow. Standardization of a dataset is a common requirement for many machine learning estimators.

The mentioned machine learning bookcase is actually a bookcase of program the systems. There is more than one system in the library. Python Deep Learning Aplication (PDLA) is a python library for deep learning. Besides this bookcase it also works with Tensorflow librariy which can be helpful for DL usage. Because it is a high-level bookcase, the user can develop application more easily than Tensorflow. For this reason, it is widely used. This bookcase can be used by many developers around the world.

3.1. Artificial Intelligence

The idea of creating smart machines, especially smart systems that can learn and predict, was put forward in the 1980s. Artificial intelligence, which has become a part of our daily life with the development of technology; expert systems have become structures that can learn, reason, make use of past information, plan, offer suggestions and communicate with fuzzy logic, genetic algorithms and artificial neural networks. While AI systems are used for different purposes in many disciplines, the methods developed during this widespread use continue to contribute to the development of other fields (Arslan, 2020). AI has the capabilities to analyze complex medical data. The ability of AI methods to reveal meaningful relationships within a data set is used in many clinical scenarios to predict diagnosis, treatment and outcome. The main AI methods that are widely used today; expert systems are fuzzy logic, genetic algorithms and artificial neural networks (Demirhan et al., 2010).

3.2. Deep Learning

The history of DL goes back to 1943, when Walter Pitts and Warren McCulloch imitated the human brain and developed a computer model based on neural networks. They used a combination of mathematics and an algorithm they called "threshold logic" to imitate the thinking process. DL allows computational models consisting of multiple processing layers to learn representations of data with multiple levels of abstraction. These methods have significantly improved the latest

technology in many other areas, such as speech recognition, visual object recognition, object detection, drug discovery and genomics. DL explores the complex structure in large datasets by using the re propagation algorithm to specify how a machine must change the internal parameters used to calculate the representation on each layer from the representation in the previous layer. Deep-eve networks have made breakthroughs in the processing of images, videos, speeches and sounds, while repetitive networks have shed light on sequentive data such as text and speech (LeCun et al., 2015). DL has serious potential to change and improve many things in our lives, and research is supported in every way by making significant investments (Keleş, 2018).

3.3. Optimizers

Adam optimization is an algorithm for first order gradient based optimization of stochastic functions based on predictions of lower order moments. The method can be easily used in non-stationary problems and has a minimum memory requirement. The success rate is much higher in efficient parameters. While creating the probability distribution of the outputs, it statistically optimizes the input-output map (Kingma and Ba, 2014).

Adamax is a variation of Adam dependent on the unendingness standard. It is a variant of Adam based on the infinity norm. Default parameters follow those provided in the paper. Adamax is sometimes

superior to adam, specially in models with embeddings (Kingma and Ba, 2015).

3.4. Evaluation Criteria

3.4.1. MAD (Mean Absolute Deviation)

It is the average of the absolute deviations of the data at a given information point or simply the "mean absolute deviation" (MAD) in the data set. In global form, the central point can be the conclusion of a randomly selected data point associated with the data set given by the median, mode, mean, or any central trend measure. The absolute values of the difference between the data points and their central tendencies can be summed and divided by the number of points in the data set (Konno and Koshizuka, 2005).

3.4.2. MAPE (Mean Absolute Percentage Error)

MAPE, where the actual value is not zero but is quite small, will often get extremely high values. The precision of this scale makes MAPE insignificant as a measure of error when using it for low volume data. MAPE is the most commonly used summary measure to assess the correctness of population estimates. Although MAPE has many desirable criteria, it argues that, from both normative and relative perspectives, the common practice of using it only to evaluate population estimates should be changed. It is normally considered that MAPE does not meet the validity criterion because it exaggerates the error found in a population estimate as a summary measure (Tayman and Swanson, 1999).

3.4.3. MEAN (Actual / Predicted)

For statistics, a forecast error is the difference between the actual value of a time series and the predicted or predicted value. With the prediction error derived from the same data scale, crosschecks between prediction errors of different series can only be made on the same serial scale.

3.4.4. STD (Standard deviation)

Standard deviation is a measure used in probability theory and statistical science to summarize the propagation of data values, a sample, a probability distribution, or a random variable. In other words, it is a measure that shows how high each data in a study group is compared to the average and how common the distribution is in another frequency.

3.4.5. Correlation

Correlation analysis is an analysis technique used to examine the relationships between two sets of variables, each with at least two variables. In analysis, one variable set can be defined as a descriptive or argument set, and the other can be defined as a dependent variable set. However, variable sets do not have to be defined in this way. In the broadest sense correlation is any statistical association, though it commonly refers to the degree to which a pair of variables are linearly related.

4. RESULT AND DISCUSSIONS

While analyzing the performance of the model, the proximity between the real values and the estimated values was examined. Correlation, R^2, MSE, MAE, RMSE and MAD, Std, among the methods used for the evaluation of models in the literature, were used as evaluation methods. The evaluation conclusions obtained by comparing the deep learning conclusions with the real conclusions were shown in Table 1. Regression chart, which is one of the most important charts comparing the real values with the estimated values, were shown in Figure 3 separately according to the training and test conclusions for the 4-shift scenario. The more linear the actual and predicted values shown in this type of chart, the closer the values are. According to the chart in the figure, the conclusions with the closest to real values are the training conclusions of the scenario with the highest correlation value. According to these conclusions, it can be called that the MAE loss is more accomplished for the test in the DL model.

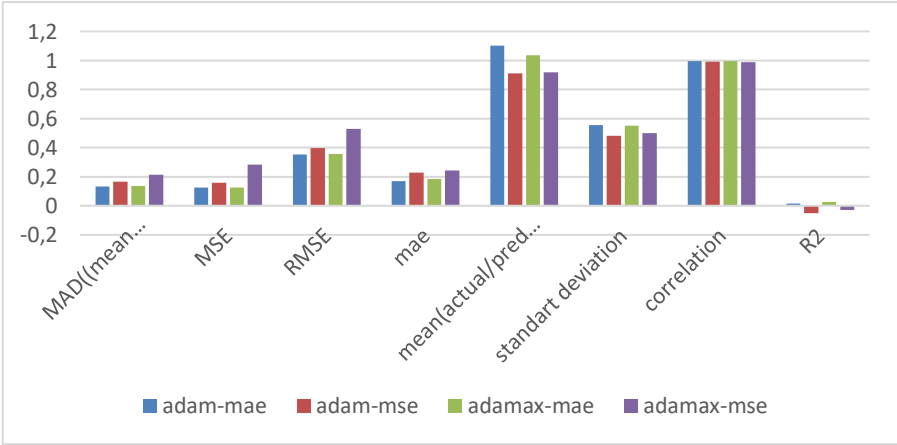

Figure 3: Crosscheck of statistical conclusions for Akdere station

Table 1: Crosscheck of All Remedial Conclusions for Statistical Evaluation for Akdere Station

AKDERE				
Statistics	ADAMAX-MAE	ADAMAX-MSE	ADAM-MAE	ADAM-MSE
MAD	0,137982	0,214168	0,134152	0,164533
MSE	0,126381	0,282030	0,124868	0,159106
RMSE	0,356134	0,531065	0,353367	0,398880
MAE	0,183245	0,243009	0,169879	0,228568
MEAN	1,035630	0,917398	1,100508	0,912371
STD	0,550444	0,501119	0,556797	0,841517
Correlation	0,994584	0,987941	0,994630	0,993660

5. CONCLUSIONS

The data set used in this study taken from the daily measurements of DSI flow measurement station from Akdere, the village of Aşağıçöplü No D21A183 (2011-2018) on the Göksu River. The data set of 4 time-shifted scenarios, the flow values starting from 4 days before to one day before were used as input in the 5th day forecast. In the study, the Sequential Model was created by using Python DL Aplication Bookcase, which is a DL bookcase. The model used in the study consists of 1 input layer, 4 hidden layers and 1 output layer. The Epoch (Iteration) number is 1024 for the 4-shift scenario. 70% of the data belonging to 4 shifting scenarios used for training and 30% for testing. In this study, in the south of Turkey and one of the major water sources of a DL model to predict current values of the Euphrates River branch were formed. While analyzing the performance of the model, the proximity between the real values and the estimated values was examined.

The more linear the actual and predicted values shown in this type of chart, the closer the values are. According to the chart in the figure, the conclusions with the closest to real values are the training conclusions of the scenario with the highest correlation value. Correlation values of the training and test conclusions obtained from the model for the 4-shifting scenario were found as 0.9946 for Akdere-Adam MAE. One-to-one conclusions were obtained in places that seem like a single line. The model was run many times by creating hidden layers with different numbers and properties. As a conclusion of these studies, the conclusions of the four-shift scenarios were compared separately and the conclusions of the experiment of the best conclusions were used in the study. In order to examine the realism of the conclusions, the model using this information was run repeatedly and it was observed that similar conclusions were obtained in each run.

Considering all the conclusions, it was observed that the success of the 4 translational scenarios and the DL model was very good. The use of this scenario and the DL model in future studies will guide the forecast of current values. In this study, an forecast was made based on single current values and successful conclusions were obtained. When the input parameters are increased, it will be useful to use them in future studies with different scenarios. In addition, with these estimated flow values, an important data was obtained in terms of designing and feasibility of a potential dam that is planned to be built on different rivers.

REFERENCES

Aldweesh, A., Derhab, A., Emam, A. Z. (2020). Deep learning approaches for anomaly-based intrusion detection systems: A survey, taxonomy, and open issues. *Knowledge-Based Systems*, 189, 105124.

Arslan, M. (2020). Projective Draw a Person Test system design based on Artificial Intelligence. Istanbul University-Cerrahpasa, Master Thesis.

Boulemtafes, A., Derhab, A., Challal, Y. (2020). A review of privacy-preserving techniques for deep learning. *Neurocomputing*, 384, 21-45.

Cheng, S. T., Hsu, C. W., Horng, G. J., Lin, C. H. (2020). Adaptive cache pre-forwarding policy for distributed deep learning. Computers & Electrical Engineering, 82, 106558.

Demirhan, A., Kılıç, Y. A., İnan, G. (2010). Artificial intelligence applications in medicine. *Turkish Journal of Intensive Care Medicine*, *9*(1), 31-41.

Demirpençe, H. (2015). Estimation of Köprüçay Currents with Artificial Neural Networks. *Congress of Civil Engineering Problems of Antalya Region*, Antalya.

Gündüz, A. (2011). Estimation of daily river flows in the Euphrates-Tigris basin using different artificial intelligence methods. Fırat University Graduate School of Natural and Applied Sciences, Department of Civil Engineering Master Thesis (no: 284732).

Keleş, A. (2018). Deep Learning and Its Applications in Health. Information Technologies & Applied Sciences, *Electronic Turkish Studies*, 13(21).

Kingma, D., Ba J. (2014). On the Convergence of Adam and Beyond, Cornell University *computer science.* arXiv:1412.6980.

Kingman, D. P., Ba, J. (2015). Adam: A Method for Stochastic Optimization. Conference paper, *In 3rd International Conference for Learning Representations*, Cornell University, arXiv:1412.6980.

Kızılaslan, M., Sağın, F., Doğan, E., Sönmez, O. (2014). Estimation of Sakarya River currents with artificial neural networks. *Sakarya University Institute of Science Journal*, 18(2), 99-103.

Konno, H., Koshizuka, T. (2005). Mean-absolute deviation model. *Iie Transactions*, *37*(10), 893-900.

LeCun, Y., Bengio, Y., Hinton, G. (2015) Deep learning. *nature*, 521 (7553), 436-444.

Mehr, A. D., Butler, E., Olyaie, E. (2013). Streamflow prediction using linear genetic programming in crosscheck with a neuro-wavelet technique. *Journal of Hydrology*, 505, 240-249.

Okkan, U., Mollamahmutoğlu, A. (2010). Modeling of Yiğitler Creek daily flows with Artificial Neural Networks and Regression Analysis. *Dumlupınar University Journal of the Institute of Science*, (023), 33-48.

Tayman, J., Swanson, D. A. (1999). On the validity of MAPE as a measure of population forecast accuracy. *Population Research and Policy Review*, *18*(4), 299-322.

Terzi, Ö., Köse, M. (2012). Current Prediction of Göksu River By Artificial Neural Networks Method. *International Journal of Technological Sciences*, 4(3), 1-7.

Yurdusev, M. A., Müserref, A. C. I., Turan, M. E., İçağa, Y. (2008). Estimation of Akarçay river monthly flows with artificial neural networks. *Celal Bayar University Journal of Science*, 4(1), 73-88.

CHAPTER 2

INVESTIGATION OF QUALITY CRITERIA DURING THE STORAGE OF VACUUM DRIED MINCED MEAT AND POWDER SOUP DEVELOPED FROM IT

Assist. Prof. Dr. Aslı AKSOY[1],
Assist. Prof. Dr. Halime PEHLİVANOĞLU[2]

[1] Halic University, Faculty of Fine Arts, Department of Gastronomy and Culinary Arts, Istanbul, Turkey, asliaksoy@halic.edu.tr, ORCID ID 0000-0002-7775-6514
[2] Tekirdag Namık Kemal University, Faculty of Veterinary Medicine, Department of Food Hygiene and Technology, Tekirdag, Turkey, hpehlivanoglu@nku.edu.tr, ORCID ID 0000-0003-3138-9568

INTRODUCTION

Meat and meat products are a very valuable food since they contain especially B vitamins, high amount of protein, essential fatty acids and minerals such as iron, zinc and phosphorus (Djordjevic et al, 2016; Doulgeraki et al, 2012). In addition, it is very susceptible to microbial spoilage due to its high water activity (Casaburi et al, 2015). Especially meat products with small pieces and large surface area, such as minced meat, are not resistant to spoilage. Ensuring food safety in these products is possible with the application of a suitable drying technique. The shelf life of meat can be extended with the drying process, which is one of the old and reliable methods. In addition, since the weight and volume of the product decrease at the end of the drying process, storage and shipping costs decrease (Doymaz et al., 2016). Dried meat is generally obtained in cube, sliced or powder form by drying with hot air, and it is also included as a component in the formulation of products such as bouillon, instant soup, noodle etc. (Aykın Dinçer and Erbaş, 2019).

Hot air, which is widely used in conventional drying, can cause denaturation, especially in heat-sensitive foods, and reduce nutritional and sensory properties (Doymaz et al., 2016). For this reason, the drying method should be chosen carefully for drying foods with high nutritional and economic value such as meat and meat products (Laopoolkit and Suwannaporn, 2011). In this regard, vacuum drying has some advantages over conventional hot air drying. In this method, since it is operated at low temperatures and there is no oxygen in the

environment, foods sensitive to heat and oxygen can be dried safely. Thus, it is possible to obtain products with the best preserved color, flavor and nutrients (Mousa and Farid, 2002).

Instant powder soups, in which dried meat products are used as an ingredient, have become a product with high added value, which is frequently used by military units, some aid organizations and also by working people and students who have limited time. At the same time, the production of instant soup in powder form is quite simple.

According to the type of soup to be produced, production can be carried out by mixing and packaging suitable generally pre-treated or dried raw materials (grain, legumes, vegetables, spices, flavorings, yoghurt powder, milk powder or whey powder, etc.) (Apaydın, 2015).

Consumption of ready to eat soups (liquid) that only require heating, ready to cook soup or instant powder soups that can be prepared in minutes are increasing day by day. Ready-to-cook powder soups have an important production potential in the food industry with their low cost in storage and transportation stages due to their low volume and weight, as well as long shelf life. In addition, it has advantages such as not requiring a cold chain for its storage, being able to be stored for a long time without taking up space, and being practical for its preparation. Therefore, different soup formulations are developed and produced by the producers in the food industry, taking into account the consumer demands and tastes (Coksaygili and Basoglu, 2011). Since the raw materials in its formulation are dry and have low water activity, ready to cook powder soups are resistant to enzymatic and

microbial spoilage (Raitio et al, 2011). If dried meat is to be used in the product formulation, a drying technique should be used that will affect the product properties to the least extent.

Meat and meat products, which is used as an ingredient in instant powder soup, bouillon, noodle etc. in the market are thermal dried products. However, meat is sensitive to heat in terms of nutrients. For this reason, minced meat as the most commonly used meat product in this study was dried using a non-thermal method, unlike the products on the market.

In this study, minced meat was dried with vacuum drying technique at room temperature and ready to cook powder soup was developed by using this dried meat product as a component. It was aimed to examine the quality criteria during the storage of the dried minced meat and the developed powder soups. For this purpose, the dried minced meat samples were stored at 0 ^{o}C, 4 ^{o}C and 25 ^{o}C for 12 months, and the developed powder soups were stored at 25 ^{o}C for 12 months, and their microbial and physicochemical properties were periodically examined.

1. MATERIAL and METHOD

1.1. Material

Minced meat to be dried and ready-to-cook powder soup to be used as control were purchased from a local market in Istanbul. Minced meat samples were kept in refrigerator conditions until the drying process. Except dried minced meat, the raw materials were obtained from Soyyiğit Gıda San. ve Tic. A.Ş. used in powder soup production.

1.2. Method

1.2.1. Drying, Storage and Rehydration of Minced Meat

Drying of minced meat was carried out using a vacuum dryer (DaihanWOV-30, South Korea) in a private food testing laboratory in Istanbul. The vacuum in the cabin is provided by a vacuum pump (EVP 2XZ-2C, China) with a pump speed of 2 L/s and a pressure of 60 mbar (Başlar et al, 2014). The minced meat was laid on a non-stick surface (silicone) with a thickness of 5 mm, placed in the vacuum dryer cabinet with trays, and the system was operated at 25 °C and -760 mm Hg pressure. The drying process was continued until the water activity of the minced meat fell below 0.6.

Dried minced meat samples were analyzed on day 0 immediately after drying. In addition, the samples were taken into bags suitable for vacuum, sealed with vacuum and made ready for storage. A climate cabinet adjusted to 75% humidity was used for storage at 25 ^{o}C. Samples stored at 0 ^{o}C were analyzed at the end of the 6th and 12th months, and samples stored at 4 ^{o}C and 25 ^{o}C were at the end of 2nd, 4th, 6th, 8th, 10th and 12th months.

Rehydration of dried minced meat was performed before acidity, pH, TBARS and microbiological analyses. For this purpose, sterile distilled water was added to the samples as much as the amount of moisture lost during drying, and they were kept for 2 hours in the refrigerator and rehydrated product was obtained. Thus, it is ensured that the moisture content of the product is brought to the initial moisture level.

1.2.2. Production of Ready to Cook Powder Soup

The soup (B) sample was developed using by minced meat dried in vacuum dryer at 25°C and also wheat flour, corn starch, oil powder (palm oil, glucose syrup, milk protein, stabilizer-triphosphate, anti-caking-silicon dioxide), whey powder, salt, onion powder, yeast extract, soy granules and protein, yoghurt powder, guar gum, black pepper, white pepper and flavoring (onion, vinegar). In addition, the other soup (A) produced with the same formulation without using dried meat was evaluated as a control. Soup samples were stored in a climate cabinet adjusted to approximately 75% humidity at 25°C after after first day analyzes were performed.

1.2.3. Analyzes

Moisture, water activity, acidity, pH, color values (L*,a*,b*), thiobarbituric acid reactive products (TBARS), total mesophilic aerobic bacteria (TMAB), mold – yeast, coliform bacteria, *Staphylococcus aureus, Salmonella spp. and Eschericha coli* O157 analyzes were performed for dried minced meat.

Moisture, water activity, color values (L*,a*,b*), peroxide number, total mesophilic aerobic bacteria (TMAB), mold – yeast, coliform bacteria, *Clostridium perfiringens, S.aureus, Bacillus cereus* and *Salmonella* analyzes were performed for ready to cook powder soup (hereafter referred to as powder soup) developed using dried minced meat. For microbiological analysis, the parameters defined in the TS 3190 Dry Soup Mix (Anon, 2014) were performed.

Moisture determination was carried out by the method of AOAC 950.46 (2006). Water activity values were determined using the water activity device (Novasina Labtouch-Aw). Fat percent of the samples was calculated according to the AOAC 960.39 (2012). Acidity (%) and pH analysis were done according to the methods defined by Gökalp et al. (1999). Color values (L*,a*,b*) were measured as stated by Tekin (2015), TBARS values were calculated as stated by Ulu (2014). The peroxide number was determined according to the TS 3960 method.

The methods used for microbiological counts are: FDA-BAM methods for TMAB (Maturin and Peeler, 2001) mold-yeast (Tournas et al.) and *E. coli* O157 (Feng et al, 2020); BS ISO 4882:2006 (BS 2006) method for coliform bacteria count, BS EN ISO 6886-1:1999 (BS 1999) method for *S. aureus* analysis, ISO 6579-1:2017 (ISO 2017) method for *Salmonella* count, BS EN ISO 7932:2004 (BS 2014a) method for *B. cereus* and BS EN ISO 7937:2004 (BS 2104b) method for *C. perfiringens.*

For statistical analysis, data were subjected to analysis of variance (ANOVA) using JMP 9 (SAS, Cary, NC, USA). For the significant ($p<0.05$) differences, the mean values were further analyzed using Duncan's Multiple Range Test (comparison test).

2. RESULTS – DISCUSSION

2.1. Results Obtained by Drying Minced Meat

The properties of the minced meat before and after drying are shown in Table 1.

Table 1: The Properties of the Minced Meat Before and After Drying

Analyses	**Before drying**	**After drying**
Moisture (%)	76.10[a]	12.91[b]
Water activity (a_w)	0.952[a]	0.586[b]
Acidity (%)	0.57[b]	0.70[a]
pH	5.65[a]	5.07[b]
Fat (%, in dry matter)	24.31[a]	24.14[a]
L*	36.05[b]	43.40[a]
a*	20.43[a]	17.18[b]
b*	3.95[b]	10.06[a]
TBARS (mg MDA/kg)	0.151[b]	0.283[a]
TMAB (log kob/g)	3.79[b]	4.39[a]
Mold - yeast (log kob/g)	2.25[b]	2.92[a]
S. aureus (log kob/g)	*ND	*ND
Coliform bacteria (log kob/g)	*ND	*ND
Salmonella (log kob/g)	*ND	*ND
E. coli O157 H7 (log kob/g)	*ND	*ND

a-b: Different letters in the same line show statistical differences between drying methods ($p< 0.05$).
(*): Not detected

The value specified in the Turkish Food Codex Microbiological Criteria Communiqué (2011) for TMAB, which is one of the most important microbial parameters in terms of food safety, is $5x10^6$ cfu/g. When Table 1 is examined, the increase in TMAB and mold-yeast load of minced meat after drying is less than 1 log. It was determined that the obtained values for TMAB are in accordance with the Codex. As a result of drying, the moisture content was reduced from 76.10% to 12.91%, and the water activity was reduced to values lower than 0.6

(0.586), which is important for food safety. After drying the minced meat, acidity increased and pH decreased. TBARS results were detected higher than before drying. The color of the product became similar to the color of cooked meat after drying. L* (brightness) value increased, a* value (redness value) decreased, and b* value (yellowness value) increased. Coliform bacteria, *C. perfiringens, S. aureus, E.coli* O157 and *Salmonella* were not detected in the products.

There are no product on the market that was exactly the same as the product obtained in this study. The moisture content of a ready-to-eat product sold in the market that dried with hot air, which has a shelf life of 3 months and is sold under the name of "dried meat", was measured as around 35%. In this study, the moisture value of the product, which does not contain spices, salt, etc. and is dried without applying heat treatment, is much more suitable in terms of food safety. It is thought that this product can be preferred both for use in the food industry as a raw material and as a food stuff in kitchens.

2.2. Results Obtained by Storage of Dried Minced Meat

The results obtained by storage at 0°C of dried minced meat are given in Table 2, the results obtained by storage at 4°C are given in Table 3, and the results obtained by storage at 25°C are given in Table 4.

Table 2: The Results Obtained by Storage at 0°C of Dried Minced Meat

Analyses	Months		
	0	6	12
Moisture (%)	12.91^{b}	12.93^{b}	13.22^{a}
Water activity (a_w)	0.586^{b}	0.581^{b}	0.593^{a}
Acidity (%)	0.70^{a}	0.72^{a}	0.69^{a}
pH	5.67^{a}	5.71^{a}	5.69^{a}
L*	43.40^{a}	43.01^{a}	42.19^{b}
a*	17.18^{a}	14.20^{b}	14.11^{b}
b*	10.06^{a}	9.92^{a}	9.89^{a}
TBARS (mg MDA/kg)	0.283^{a}	0.288^{a}	0.284^{a}
TMAB (log kob/g)	4.39^{a}	4.45^{a}	4.50^{a}
Mold - yeast (log kob/g)	2.92^{a}	2.88^{a}	2.91^{a}
S. aureus (log kob/g)	*ND	*ND	*ND
Coliform bacteria (log kob/g)	*ND	*ND	*ND
Salmonella (log kob/g)	*ND	*ND	*ND
E. coli O157 H7 (log kob/g)	*ND	*ND	*ND

a-b: Different letters in the same line show statistical differences between drying methods ($p< 0.05$).
(*): Not detected

Table 3: The Results Obtained by Storage at 4°C of Dried Minced Meat

Analyses	Months						
	0	2	4	6	8	10	12
Moisture (%)	12.91^{b}	12.88^{b}	12.92^{b}	13.25^{ab}	15.58^{a}	13.62^{a}	13.58^{a}
Water activity (a_w)	0.586^{b}	0.601^{b}	0.603^{b}	0.627^{a}	0.633^{a}	0.631^{a}	0.633^{a}
Acidity (%)	0.70^{c}	0.78^{b}	0.77^{b}	0.80^{b}	0.86^{a}	0.85^{a}	0.82^{a}
pH	5.67^{a}	5.51^{b}	5.56^{b}	5.01^{c}	5.05^{c}	5.04^{c}	5.05^{c}
L*	43.40^{a}	42.62^{ab}	41.94^{b}	41.48^{b}	41.60^{b}	41.58^{b}	41.61^{b}
a*	17.18^{a}	15.11^{b}	12.67^{c}	10.44^{d}	8.33^{e}	8.89^{e}	8.42^{e}
b*	10.06^{a}	10.11^{a}	8.94^{b}	8.87^{b}	7.55^{c}	7.61^{c}	7.58^{c}
TBARS (mg MDA/kg)	0.283^{d}	0.287^{d}	0.375^{c}	0.401^{b}	0.434^{a}	0.467^{a}	0.458^{a}
TMAB (log kob/g)	4.39^{a}	4.31^{a}	3.75^{b}	2.56^{c}	1.79^{d}	1.73^{d}	1.75^{d}
Mold - yeast (log kob/g)	2.92^{a}	2.01^{b}	1.98^{b}	1.11^{c}	0.98^{c}	0.92^{c}	0.99^{c}
S. aureus (log kob/g)	*ND	*ND	*ND	*ND	*ND	*ND	*ND
Coliform bacteria (log kob/g)	*ND	*ND	*ND	*ND	*ND	*ND	*ND
Salmonella (log kob/g)	*ND	*ND	*ND	*ND	*ND	*ND	*ND
E. coli O157 H7 (log kob/g)	*ND	*ND	*ND	*ND	*ND	*ND	*ND

a-e: Different letters in the same line show statistical differences between drying methods ($p< 0.05$).
(*): Not detected

Table 4: The Results Obtained by Storage at 25°C of Dried Minced Meat

Analyses	Months						
	0	**2**	**4**	**6**	**8**	**10**	**12**
Moisture (%)	12.91^{b}	12.88^{b}	13.78^{a}	13.75^{a}	13.77^{a}	13.81^{a}	13.75^{a}
Water activity (a_w)	0.586^{b}	0.598^{b}	0.619^{a}	0.629^{a}	0.638^{a}	0.635^{a}	0.632^{a}
Acidity (%)	0.70^{b}	0.85^{a}	0.87^{a}	0.85^{a}	0.83^{a}	0.82^{a}	0.83^{a}
pH	5.67^{a}	5.19^{b}	5.16^{b}	5.19^{b}	5.11^{b}	5.13^{b}	5.11^{b}
L*	43.40^{c}	44.51^{b}	44.58^{b}	53.63^{a}	53.65^{a}	53.71^{a}	53.69^{a}
a*	17.18^{a}	11.55^{b}	9.22^{c}	9.25^{c}	9.16^{c}	9.18^{c}	9.16^{c}
b*	10.06^{d}	12.45^{c}	16.34^{b}	20.41^{a}	20.52^{a}	20.48^{a}	20.50^{a}
TBARS (mg MDA/kg)	0.283^{d}	0.348^{c}	0.551^{b}	0.648^{a}	0.655^{a}	0.658^{a}	0.657^{a}
TMAB (log kob/g)	4.39^{a}	3.22^{b}	2.48^{c}	2.55^{c}	1.87^{d}	1.95^{d}	1.85^{d}
Mold - yeast (log kob/g)	2.92^{a}	2.02^{b}	1.27^{c}	0.77^{d}	0.17^{e}	0.12^{e}	0.15^{e}
S. aureus (log kob/g)	*ND	*ND	*ND	*ND	*ND	*ND	*ND
Coliform bacteria (log kob/g)	*ND	*ND	*ND	*ND	*ND	*ND	*ND
Salmonella (log kob/g)	*ND	*ND	*ND	*ND	*ND	*ND	*ND
E. coli O157 H7 (log kob/g)	*ND	*ND	*ND	*ND	*ND	*ND	*ND

a-e: Different letters in the same line show statistical differences between drying methods ($p< 0.05$).
(*): Not detected

When the analysis values in Table 2, Table 3 and Table 4 are examined, the following conclusions are reached: It was determined that the moisture and water activity values increased from the 6th month in 0°C storage, from the 6th month in the 4°C storage, and from the 4th month in the 25°C storage. It is thought that this increase in humidity values is due to the air permeability of the packaging material and the lack of industrial packaging material (laminated, composite, etc.) structure and feature. While the acidity and pH values did not change in storage at 0°C, the acidity increased over time from the 2nd month in storage at 4°C and 25°C, while the pH value decreased proportionally.

It was observed that the L* (brightness) value decreased during storage at 0°C and 4°C, and increased during storage at 25°C. The a* (redness-greenness) value decreased during storage at 0°C, 4°C and 25°C, the b* (yellowness-blueness) value did not change at 0°C, decreased at 4°C storage, and at 25°C storage. While the TBARS values, which are indicators of fat oxidation in meat products, did not change in storage at 0°C, but increased from the 4th month in storage at 4°C and from the first month in storage at 25°C. However, this value was never detected above 1 mg MDA/kg.

While the TMAB number did not change in 0°C storage, it started to decrease from the 4th month in 4°C storage and from the 2nd month in 25°C storage. It was thought that providing an anaerobic environment with the drying process and vacuum packaging negatively affected the viability of aerobic bacteria. The value specified in the Turkish Food Codex Microbiological Criteria Communiqué (2011) for TMAB, which is one of the most important microbial parameters in terms of food safety, is $5x10^6$ cfu/g for minced meat. It was determined that the analysis results obtained during the storage were in accordance with the Codex. While the mold-yeast number did not change at 0°C, it started to decrease from the second month on storage at 4°C and 25°C. *S. aureus, Salmonella, E. coli* O157 H7 and coliform bacteria were not detected at any temperature and storage period.

2.3. Results Obtained by Storage of Powder Soup

Fat content of the developed soups detected as 13,52 % for sample A and as 13,73% for sample B. Also the results of soup samples A (with meat) and B (without meat) obtained at the end of storage at 25°C of are given in Table 5.

When Table 5 is analyzed in terms of analysis parameters; it was determined that the moisture and water activity values of soup sample A (without meat) and sample B (with meat) increased during storage. It is thought that this increase in humidity values is due to the air permeability of the packaging material and the lack of industrial packaging material (laminated, composite, etc.) structure and feature. When the peroxide numbers of the samples were examined, it was determined that they did not change during storage. This suggested that the packaging material might be resistant to oxygen permeability. In addition, all the values obtained are lower than 10 meq O_2 / kg, the value specified as the maximum limit according to the TS 11342 Instant Soup (2005).

L*, a*, b* values did not change in soup sample A (meatless). On the other hand, L* values decreased over time, a* value did not change, and b* value increased especially from the 8th month in the soup sample B (with meat) It is thought that the change in color values is due to the fat content of the minced meat used in the formulation.

TMAB counts decreased in both soup samples. It was thought that the drying process and vacuum packaging, providing an anaerobic environment, adversely affected the viability of aerobic bacteria. It is

known that the value considered critical for food safety for TMAB in foods is 10^4-10^5 log. In addition, no significant change was detected in the mold-yeast counts of the samples during storage. *S. aureus*, *Salmonella*, *E. coli* O157 H7 and coliform bacteria were not detected at any temperature and storage period.

Table 5: Analysis Values Obtained During the Storage of Soup Samples A (without meat) and B (with meat)

Analyses	12. Month		10. Month		8. Month		6. Month		4. Month		2. Month		0. Month	
	B	A	B	A	B	A	B	A	B	A	B	A	B	A
Moisture (%)	4.62^{A}	3.93^{a}	4.51^{A}	3.84^{a}	4.54^{A}	3.80^{a}	3.55^{B}	3.77^{a}	3.51^{B}	3.15^{b}	3.47^{B}	3.11^{b}	3.45^{B}	3.22^{b}
Water activity	0.548^{A}	0.492^{a}	0.529^{A}	0.501^{a}	0.534^{A}	0.455^{a}	0.375^{B}	0.441^{a}	0.381^{B}	0.365^{b}	0.355^{B}	0.371^{b}	0.372^{B}	0.330^{b}
Peroxide value (meg O_2 /kg)	0.64^{A}	0.70^{a}	0.65^{A}	0.70^{a}	0.65^{A}	0.72^{a}	0.65^{A}	0.70^{a}	0.64^{A}	0.70^{a}	0.64^{A}	0.69^{a}	0.65^{A}	0.71^{a}
L*	88.05^{B}	91.69^{a}	88.18^{B}	91.45^{a}	88.02^{B}	91.75^{a}	88.55^{A}	91.13^{a}	88.61^{A}	91.45^{a}	88.87^{A}	91.11^{a}	89.11^{A}	91.53^{a}
a*	-0.49^{A}	-0.82^{a}	-0.51^{A}	-0.84^{a}	-0.44^{A}	-0.85^{a}	-0.41^{A}	-0.89^{a}	-0.57^{A}	-0.81^{a}	-0.59^{A}	-0.89^{a}	-0.57^{A}	-0.85^{a}
b*	12.10^{A}	11.51^{a}	12.01^{A}	11.47^{a}	11.95^{A}	11.45^{a}	9.81^{B}	11.41^{a}	9.85^{B}	11.33^{a}	9.79^{B}	11.27^{a}	9.86^{B}	11.35^{a}
TMAB (log kob/g)	3.37^{B}	3.34^{b}	3.49^{B}	3.25^{b}	3.41^{B}	3.37^{b}	3.34^{B}	3.22^{b}	3.15^{B}	3.47^{b}	4.65^{A}	4.11^{a}	4.82^{A}	4.64^{a}
Mould - yeast (log kob/g)	3.25^{A}	3.15^{a}	3.30^{A}	3.09^{a}	3.34^{A}	3.11^{a}	3.27^{A}	3.18^{a}	3.19^{A}	3.11^{a}	3.28^{A}	3.15^{a}	3.22^{A}	3.12^{a}
Coliform bacteria (log kob/g)	*ND	*ND	*ND	*ND	*ND	*ND	*ND	*ND	*ND	*ND	*ND	*TE	*ND	*ND
C. perfiringens (log kob/g)	*ND	*ND	*ND	*ND	*ND	*ND	*ND	*ND	*ND	*ND	*ND	*ND	*ND	*ND
S. aureus (log kob/g)	*ND	*ND	*ND	*ND	*ND	*ND	*ND	*ND	*ND	*ND	*ND	*ND	*ND	*ND
B. cereus (log kob/g)	*ND	*ND	*ND	*ND	*ND	*ND	*ND	*ND	*ND	*ND	*ND	*ND	*ND	*ND
Salmonella (log kob/g)	*ND	*ND	*ND	*ND	*ND	*ND	*ND	*ND	*ND	*ND	*ND	*ND	*ND	*ND

Each type of soup was evaluated in itself during storage. Small letters were used to mark the soup sample A (without meat) and capital letters were used to mark the soup sample B (with meat).a-b and A-B: Different letters in the same line show statistical differences between drying methods ($p< 0.05$).
(*): Not detected

3. CONCLUSION

Meat and meat products are foods that have high nutritional and economic value and are prone to microbial spoilage. It is possible to preserve this valuable food, to use it as a raw material in the production of some foods and to ensure food safety by drying method. In the market, meat dried by heat treatment can be used as raw material in products such as dry soup powder, bouillon, noodle etc. However, the method chosen for drying should be able to preserve the product properties in the best way. In this context, it is possible to prevent oxidation and loss of nutrients, since drying can be performed in an oxygen-free environment and at low temperature with vacuum drying method. Therefore, in this study, minced meat was dried at room temperature by vacuum drying method. The dried minced meat sample was stored at 0 ^{o}C, 4 ^{o}C and 25 ^{o}C for 12 months and evaluated by analyzing quality criteria at certain periods. In this way, it was determined that food safety was ensured with the least change in product characteristics. In addition, different from the soup samples on the market, ready to cook powder soup formulations have been developed using and without using vacuum-dried minced meat without the use of heat treatment. Soup samples were stored at 25 ^{o}C for 12 months and their microbial and physicochemical properties were periodically examined. As a result, the data obtained in this study revealed that the meat dried with vacuum drying technique as a non-thermal preservation method, when packaged in vacuum, preserves its properties for 12 months even at 25 ^{o}C, and that the meat

dried in this way can be used in industrial products such as powder soup mixes.

REFERENCES

AOAC, (2006). AOAC 950.46. Official methods of analysis Proximate Analysis and Calculations Moisture (M) Meat - item 108, Association of Analytical Communities, Gaithersburg, MD, 17th edition.

AOAC, (2012). AOAC 960.39 Fat (crude) or ether extract in meat. In Official Methods of Analysis of AOAC International;Association of Analytical Communities: Gaithersburg, MD.

Apaydın, H. (2015) Inhibition effect of Propolis (bee gum) against Staphylococcus aureus isolated from instant soup, Master Thesis, Namık Kemal University, Natural Sciences Institue, Tekirdag, Turkey.

Aykın Dinçer, E., Erbaş, M. (2019). Quality Characteristics of Dried Meat Products, Gıda, c.44, s.3, ss. 472-482.

Baslar, M. Kilicli, M., Toker, O.S., Sagdic, O., Arici, M. (2014). Ultrasonic vacuum drying technique as a novel process for shortening the drying period for beef and chicken meats. Innov. Food Sci. Emerg. Technology, 26, 182–190.

BS (1999). BS EN ISO 6886-1:1999, Microbiology of food and animal feeding stuffsHorizontal method for the enumeration of coagulase-positive *Staphylococc*i (*Staphylococcus aureus* and other species).

BS (2004a). BS EN ISO 7932:2004 Microbiology of food and animal feeding stuffs-Horizontal method for the enumeration of presumptive *Bacillus cereus*-Colony-count technique at 30°C, 2004.

BS (2004b). BS EN ISO 7937:2004, Microbiology of food and animal feeding stuffs- Horizontal method for the enumeration of *Clostridium perfringens*-Colony count technique.

BS (2006). BS ISO 4882:2006, Microbiology of food and animal feeding stuffsHorizontal method for the enumeration of coliforms -Colony-count technique.

Casaburi, A., Piombino, P., Nychas, G.J., Villani, F., Ercolini, D. (2015). Bacterial populations and the volatilome associated to meat spoilage, Food Microbiology, c. 45, ss. 83-102.

Çoksaygılı, N., Başoğlu, F. (2011). Bursa Piyasasında Satılan Hazır Toz Çorbaların Mikrobiyolojik ve Bazı Kimyasal Özellikleri, Uludag University. Journal of Agricultural Faculty, c. 25, sayı 1, ss. 87-95.

Djordjevic, J., Boskovic, M., Dokmanovic, M., Lazic, I., Ledina, T., Suvajdzic, B., Baltic, M. (2016). Vacuum and Modified Atmosphere Packaging Effect on *Enterobacteriaceae* Behaviour in Minced Meat: Vacuum and Modified Atmosphere Packaging Effect, Journal of Food Processing and Preservation c. 41, s. 2.

Doulgeraki, A. I., Ercolini, D., Villani, F., Nychas, G. J. E. (2012). Spoilage microbiota associated to the storage of raw meat in different conditions, International Journal of Food Microbiology, c.157, sayı 2, ss. 130-141.

Doymaz, İ., Karasu, S., Başlar, M. (2016). Effects of infrared heating on drying kinetics, antioxidant activity, phenolic content, and color of jujube fruit, Journal of Food Measurement and Characterization, c.10, sayı 2, ss. 283-291.

Feng, P, Weagent, S.D., Jinneman, K. (2020). Bacteriological Analytical Manual, Chapter 4A, Diarrheagenic *Escherichia coli*.

Gökalp, H.Y., Kaya, M., Tülek, Y. ve Zorba, Ö. (1999). Et ve ürünlerinde kalite kontrolü ve laboratuar Uygulama Klavuzu" (3. Edt.) Atatürk University, Faculty of Agriculture Press, Erzurum.

ISO (2017). ISO 6579-1:2017. Horizontal method for the detection, enumeration and serotyping of *Salmonella* - Part 1: Detection of *Salmonella* spp.

Laopoolkit, P., Suwannaporn, P. (2011). Effect of pretreatments and vacuum drying on instant dried pork process optimization, Meat Science, c. 88, sayı 3, ss. 553-558.

Maturin L.J, Peeler J.T. (2001). Aerobic plate count. In: Food and Drug. Administration (FDA), Bacteriological analytical manual online.

Mousa, N., Farid, M. (2002). Microwave Vacuum Dryıng Of Banana Slices. Drying Technology, C. 20, Sayı 10, Ss. 2055-2066.

Raitio, R., Orlien, V., Skibsted, L. H. (2011). Storage Stability of Cauliflower soup powder: The Effect of Lipid Oxidation and Protein Degradation Reactions, Food Chemistry, 128, 371-379.

Tekin, H. (2015). Application of ultrasound assisted vacuum drying for improving quality properties during peppers dehydration, Master Thesis, Institute of Natural Sciences, Yıldız Technical University, Istanbul, Turkey.

Turkish Food Codex (2017). Regulation on Nutrition and Health Claims.

Turkish Food Codex (2011). Regulation on Microbiological Criteria.

Tournas, V., Stack, M.E., Mislivec, P.B., Koch H.A., Bandler R. (2001). Chapter 18. Yeast, mold and mycotoxins. In: Food and Drug Administration (FDA), Bacteriological Analytical Manual Online.

TS (2018). TS 3190 Dry Soup Mix. Ankara.

TS (2017). TS EN ISO 3960. Animal and vegatable fats and oils- Determination of peroxide value – Iodometric (visual) endpoint determination. Ankara.

TS (2005). TS 11342 Instant Soup. Ankara.

Ulu, H. (2004). Evaluation of three 2-thiobarbituric acid methods for the measurement of lipid oxidation in various meats and meat products. Meat Science ,67, 683–687.

CHAPTER 3

THE USE IN THE DENSITY FUNCTIONAL METHOD IN MATERIAL SCIENCE FOR RARE METAL HEXABORIDES

Cengiz BOZADA[1] , Asst. Prof. Dr. Mikail ASLAN[2]

[1]Gaziantep University, Faculty of Engineering, Department of Physics Engineering, Gaziantep, Turkey
[2] Gaziantep University, Faculty of Engineering, Department of Metallurgical and Material Science Engineering, Gaziantep, Turkey. aslanm@gantep.edu.tr
ORCID ID 0000-0003-0578-5049

1.INTRODUCTION

Rare-Earth Hexaboride (REB_6) have fascinated a lot of attention due to their important properties containing thermionic emission, chemical stability, hardness, high melting point, magnetic characteristics, low work function, efficiency, low volatility, narrow band semiconductivity and superconductivity. Hence such properties have been used in a variety of applications, such as electron emitters, photonic and electronic applications. REB_6 materials is in a simple cubic CsCl-type structure (Pm-3m symmetry), in which rare earth element occupies the Cs site and octahedral borides are located on the Cl site (Ji et al., 2011). REB_6 (RE = La, Ce, Y, Gd, Pr, Ho, Nd, Sm, Tb, Dy) has attracted a lot of attention for its important features. LaB_6 is an superb electron emitter material.Its high melting point is 2715 °C (Yu et al., 2018). CeB_6 is a intense Kondo substance and exhibits heavy fermions performance (Bai & Ma, 2010). PrB_6 is antiferromagnetic substance (Onuki et al., 1989). NdB_6 exhibits an antiferromagnetic behavior and this material order antiferromagnetic at 7,8 K (Kubo et al., 1993). SmB_6 is a Kondo insulator. Kondo insulators have properties of heavy fermion f-electron compounds (Wolgast et al., 2013). EuB_6 is as a ferromagnetic semiconductor (Süllow et al., 1998). GdB_6 is antiferromagnetically at T_N = 15,5 K (Semeno et al., 2018). YbB_6 is topological crystalline Kondo insulator and is a typical complex valence narrow bandgap semiconductor .This material have large band gap (Weng et al., 2014). ErB_6 is a metallic (Gernhart et al., 2012). PmB_6 is a topologically nontrivial compound (Hung & Jeng, 2020). TbB_6 is antiferromagnetically at 21 K (Luca et

al., 2004). DyB_6 is an antiferromagnetic metal. The antiferro-quadrupolar ordering occurs in DyB_6 at T_N = 26 K (Takahashi et al., 1998). HoB_6 shows a ferroquadrupole ordering at T_Q=6,1K (Yamaguchi et al., 2003).

Density Functional Theory (DFT) is one of the fundamental usually preferred computational methods for examining and investigating the features of systems such as isolated clusters and molecules, nanoparticles (NP), crystal structures, interfaces and periodic surfaces in the gas state. There are two important factors in choosing the DFT method. The first is that DFT gives satisfactory answers to challenging scientific questions available in different fields, while another is the acquisition of important information that can't be determined by experiments (Neugebauer & Hickel, 2013). In addition, DFT is one of the basic techniques commonly used to calculate atoms, molecules, crystals, surfaces and their interactions by ab initio (Argaman & Makov, 2000). The optical, mechanical characteristics, electronic structures, hardnesses (Li et al., 2009), thermal expansion coefficient, bulk modulus, heat capacity (Guo-Liang et al., 2009), second-order elastic constants (SOEC) and third-order elastic constants(TOEC) (Zeng et al., 2017), the work functions of REB_6 can be calculated by using DFT. Also, DFT is used to obtain energetic and dynamic donne of the atoms in different structures and surroundings (Schmidth et al., 2015). Generally, the properties of REB_6 are studied by first- principles calculation connected to DFT. Thus DFT plays an significantt mission in REB_6.

2. RESULT AND DISCUSSION

The optical, mechanical features, electronic structures and hardnesses of REB_6 can be calculated by using DFT (Li et al., 2009). Xiao et al. have examined the electronic structure, theoretical hardness, optical and mechanical features of mixed-valence SmB_6 by first principles using DFT. The band structures of the SmB_6 are semiconductors with a minimum gap. Also, their calculated results exhibit SmB_6 is a brittle material (Xiao et al., 2017). In another study, Qi et al. synthesized the nanocrystalline Ca-doped CeB_6 powders by using a solid state method. They found that Ca doped causes the absorption valleys to change to a longer wavelength direction and decreases the all kinetic energy of the electrons of CeB_6 (Qi et al., 2018). In the low energy region the calculated energy loss function of $Ce_{0.875}Ca_{0.125}B_6$ is shown in Figure 1. The plasma excitation frequency energy of CeB_6 and $Ce_{0.875}Ca_{0.125}B_6$ can be found to be 1.98 eV and 1.54 eV respectively, illustrating that the plasma excitation energy of CeB_6 is decreased with Ca doped. This could describe the absorption valley of nanocrystalline $Ce_{1-x}Ca_xB_6$ red-shifts if the Ca doping content straightly enhances. The total kinetic energy of the electrons depends on the change of the plasma frequency. They found from the first principle consequences that the numerical values of the Fermi energies for CeB_6 and $Ce_{0.875}Ca_{0.125}B_6$ were 9.11230 eV and 8.55953 eV, respectively. Ca doping causes both nanocrystal $Ce_{1-x}Ca_xB_6$ to the red shift in the absorption valley and reduce the total kinetic energy of electrons.

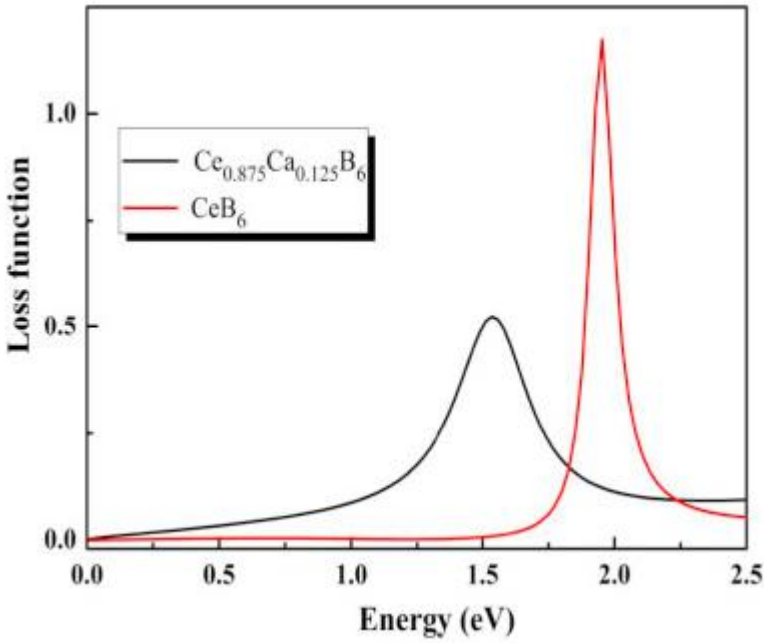

Figure 1: The energy loss function of $Ce_{0.875}Ca_{0.125}B_6$ Adopted from (Qi et al, 2018) Copyright© 2017 Elsevier B.V.

In another study, Chao et al. have produced SmB_6 , LaB_6 and Sm doped LaB_6 via a solid state technique. The shift of the position of the minimum numerical value of LaB_6 in the long wave direction is caused by increasing the amount of sm doped. They used DFT to commentate the optical features of Sm doped LaB_6. According to their calculated consequences, the decreased number of conduction electrons causes the absorption spectra to alter and after Sm doped the Sm4f states alter DOS near the Fermi surface of LaB_6 (Chao et al., 2015).

In a different study, Liang et al. have analyzed the coefficient of thermal expansion, bulk modulus and thermal capacity of LaB_6 by the plane-wave pseudopotential technique, which uses a GGA within the framework of DFT. They applied a semi-harmonic Debye model that uses the total energy set against volume acquired by the plane wave pseudopotentenial technique to investigate thermal features and vibration impact (Guo-Liang et al., 2009). In a separate study, Gürel et al. have investigated the lattice-dynamical, elastic, structural, and thermodynamical features of LaB_6 and CeB_6 by ab initio study. Their calculations were performed within linear-answer formalism and DFT performing pseudopotentials and a plane-wave basis.They obtained the thermodynamics properties of CeB_6 and LaB_6 by a quasiharmonic approximation (Gürel & Eryiğit, 2010). In another study, Schmidt et al. have examined the improvement of the interatomic potentials of LaB_6 through a combination of DFT and molecular dynamics simulations. DFT is used to obtain energetic and dynamical data from atoms in a variety of configurations and environments (Schmidt et al., 2015). The lattice energy is shown in Fig.2. The atomization is called as cohesive energy. According to their calculated the atomization energy derived from the DFT and lattice sum yielded 20.130 eV and 20.177 eV respectively.

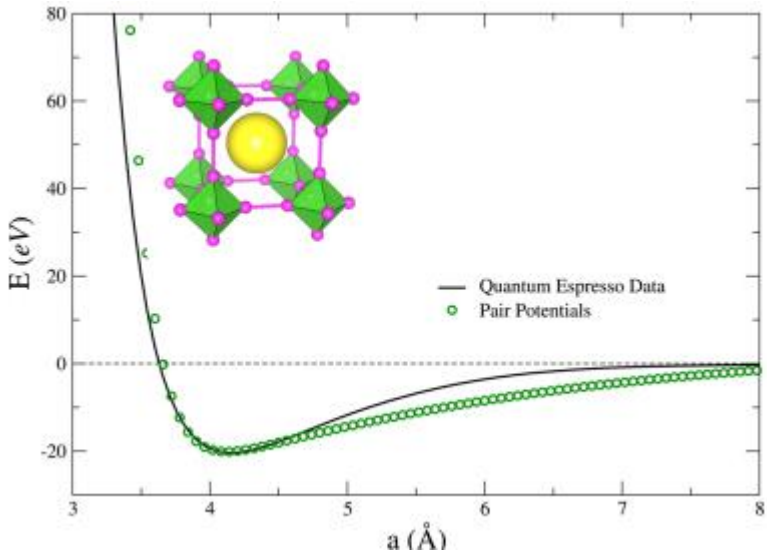

Figure 2: Atomization (Cohesive) energies from DFT for LaB_6 Adopted from (Schmidt et al., 2015) Copyright© 2015 American Chemical Society

In a different study, Zeng et al. have studied the complete set of the independent second-order elastic constants (SOEC) and third-order elastic constants (TOEC) of LaB_6 and CeB_6 by homogeneous deformation theory and the combination technique of first-principles calculations within the framwork of DFT (Zeng et al., 2017). SOECs and TOECs are used to model the mechanical answer of crystalline under high pressure. Fig.3. illustrated the strain–energy relations of LaB_6 and CeB_6. The solid lines and the discrete points represent the results acquired from fitted polynomials and the first-principles calculations within the framework of DFT, respectively. Resilience energy is also known as strain energy. The resilience energy with positive tensions is every time smaller than that negative tensions and hence the TOECs are classically negative.

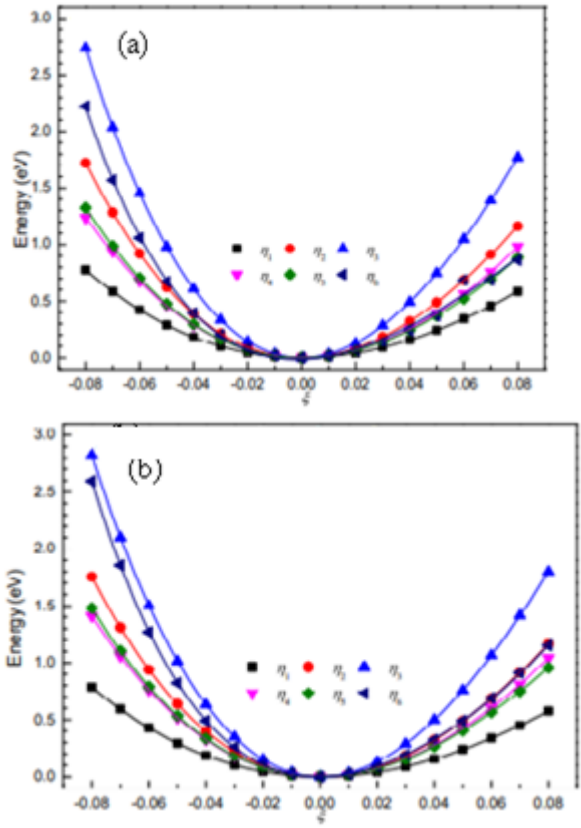

Figure 3: The resilience energy relations of (a) CeB_6 and (b) LaB_6. The solid lines and the discrete points symbolize the consequences of third-order polynomial appropriating DFT results, respectively. Adopted from (Zeng et al., 2017) Copyright© 2017 MDPI

In a separate study, Bai et al. have calculated the chemical bond and structural features of CeB_6 and EuB_6 employing an all-electron full-potential linearized augmented plane wave (FPLAPW) and GGA+U technique. Several 4f electrons in the Ce atom is dissimilar from that of the Eu atom. The Ce-Ce and Eu-Eu bonds are generally ionic bonds, Ce (Eu)−B bonds contains covalent and ionic bond properties (Bai & Ma, 2010). In another study, Chao et al. have studied the

optical features of Yb- doped LaB_6 with first-principle calculations based on DFT. According to their results, Yb-doping reduces the plasmon energy of LaB_6, it causes the position of the transmission peak to red shift in the visible-near infrared region, and the Yb 4f states on the near Fermi surface affect the optical characteristics. Also, the number of charge carriers, the all kinetic energy of the electrons, and the plasma frequency are decreased (Chao et al., 2016). In a different study, Ning et al. systematically studied the work functions of LnB_6 (Ln = Gd, Pr, Nd) at (100) plane by first-principles calculation within the framework of DFT. It exhibits that the work function of LnB_6 at (100) plane fits the connection of $\Phi(GdB_6) > \Phi(NdB_6) > \Phi(PrB_6)$. They have proven that doping rare-earth improves the thermionic emission performance of CeB_6 and decreases its work function (Ning et al., 2019). The work functions illustrated on the (001) surface of LnB6 (Ln = Gd, Pr, Nd) is in Fig.4. The work functions of GdB_6, NdB_6 and PrB_6 shown in black dots are 2.96 eV, 2.87 eV and 2.84 eV respectively. The values of the work functions shown in red dots reduce to 2.71 eV, 2.47 eV and 2.38 eV, respectively after geometry optimization.

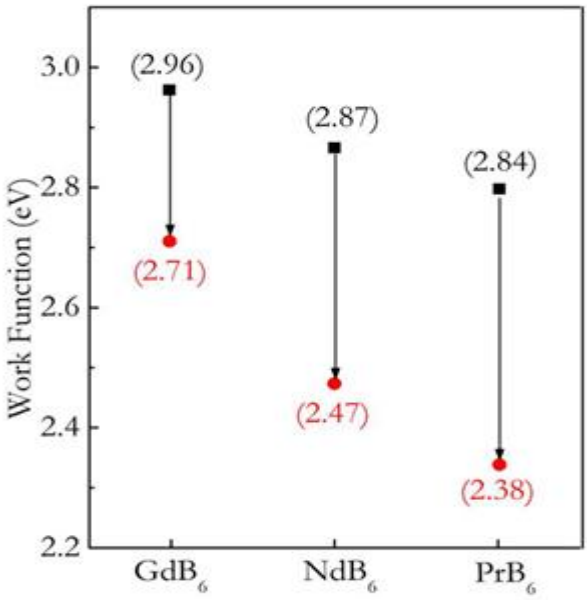

Figure 4: The work function on (001) surfaces of LnB6 (Ln = Pr, Nd and Gd) Adopted from (Ning et al., 2019) Copyright© 2019 John Wiley & Sons

In a separate study, Liu et al. have systematically studied the work functions and the crystal electronic structures of binary and ternary REB_6 (LaB_6, CeB_6, GdB_6, NdB_6, $La_{0.75}Ce_{0.25}B_6$, $La_{0.75}Nd_{0.25}B_6$, $La_{0.75}Gd_{0.25}B_6$, $Ce_{0.75}Gd_{0.25}B_6$) by the first-principles calculations based on DFT. REB_6 indicates the big DOS close Fermi level. REB_6 with d orbital have superb emission performance and d orbital of RE effect the electronic states of electron emission near the Fermi level. Electron emission also known as field emission.

They found that REB_6 (RE = La, Ce, Gd) has a low work function. Doped of RE with effective d orbital electrons considerably reduces the work function of REB_6. First principles calculations based on DFT ensure an excellent method for the investigation of field emission

features of REB_6 (Liu et al., 2018). In another study, Liu et al. have systematically studied the bandgap, DOS and work functions of LaB_6 crystal surfaces by the first-principles calculations within the framework of DFT. According to their electronic structure calculations, they determined that LaB_6 has a metallic feature and the big dos near the Fermi level of LaB_6 are large consists of La 5d, 6s, and B 2p (Liu et al., 2017).

Fig.5a and b exhibit the computed and total density of states (DOS) and partial density of states (PDOS) of LaB_6. The valence configurations is (La:$5s^2 5p^6 5d^1 6s^2$), (B:$2s^2 2p^1$). The value of DOS near to the Fermi energy (-5 eV–5 eV) are large compared to another energy regions, in which the big DOS has been activated by La s, La p, La d, and B p orbitals and La d orbital electron are the major contributor. In the energy regions 0eV to 10 eV, –5eV–0eV, -10 eV to -5 eV, several levels of hybridization are seen between La d and B p electrons, and La d electrons have the main contribution in the 2eV–5eV energy regions. The substances with electron emission are generally related with a big DOS near the Fermi level. The big DOS near the Fermi level of LaB_6 will be accountable for its features of field emission. Fig.5c. illustrated the calculated energy band structure for the LaB_6. The Fermi level is taken as 0 eV, another energy levels are described by comparing it with the Fermi level. They calculated the value of the bandgap as 0.038 eV and stated that the value of this small bandgap explains the metallic behavior. Fig.5d illustrated the crystal structure of LaB_6. The lattice parameter is defined

experimentally at approximately c = 4.153 Å, with a boron positional constant of approximately z=0.1993.

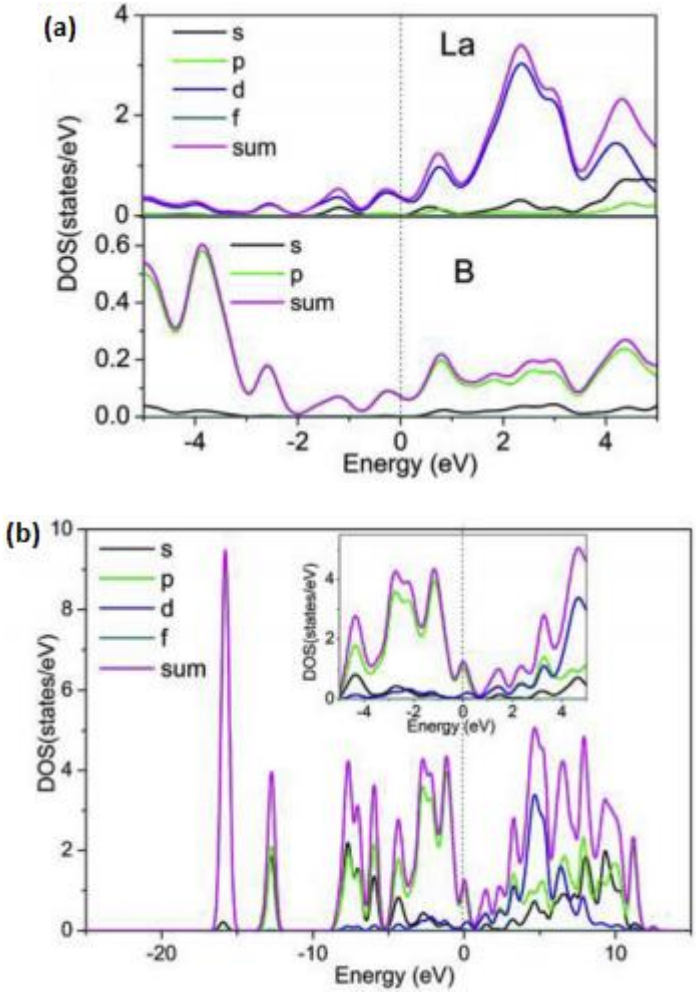

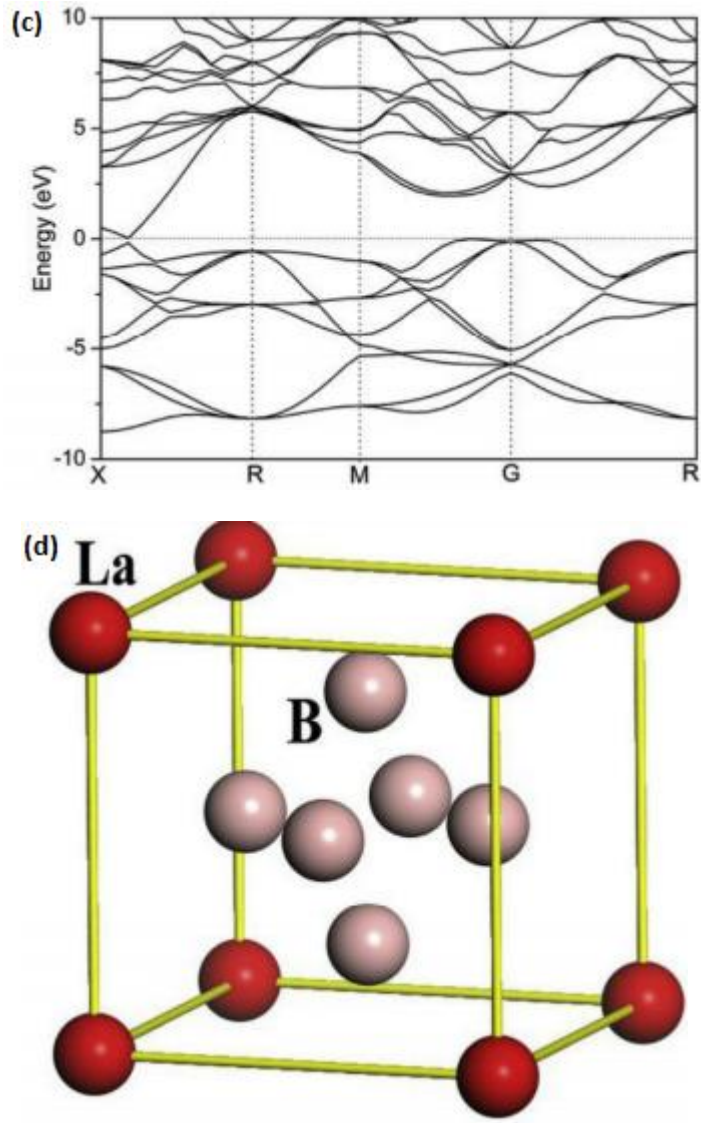

Figure 5: (a) The partial DOS of LaB_6, (b) total DOS, (c) electronic band structure and (d) Crystal structure Adopted from (Liu et al., 2017) Copyright© 2017 Elsevier Ltd

3. CONCLUSIONS

The optical and mechanical features, hardnesses and electronic structure, elastic, lattice-dynamic, and thermodynamic properties of REB_6 were calculated from basic principles based on the DFT. DFT is preferred to understand the optical features of rare-earth element-doped REB_6. The results show that before conducting experiments, for REB_6 materials, DFT can provide information about the band structures of materials and whether the material is brittle and show conductive behavior or not. Furthermore, DFT can provide information that can not be obtained by experiments. For example, in the mentioned study, the Sm 4f states decreased a number of conduction electrons and change the DOS on the Fermi surface of Sm doped-REB_6. Moreover, in another study, Yb-doping leads to a decrease in the all kinetic energy of the electrons, the number of charge carriers, and the plasmon energy of REB_6. It also causes the position of the transmission peak in the visible-near infrared to be redshifted. Thus, by employing DFT, the mechanical, optical properties, electronic structures and hardnesses of REB_6 can be examined detailly. This technique provides important advantages for studying REB_6 materials at the nano/atomic scale.

REFERENCES

Ji, X. H., Zhang, Q. Y., Xu, J. Q., & Zhao, Y. M. (2011). Rare-earth hexaborides nanostructures: recent advances in materials, characterization and investigations of physical properties. Progress in Solid State Chemistry, 39(2), 51-69.

Yu, Y., Wang, S., Li, W., & Chen, Z. (2018). Low temperature synthesis of LaB6 nanoparticles by a molten salt route. Powder Technology, 323, 203-207.

Bai, L., & Ma, N. (2010). GGA+ U method investigating structural and chemical bond properties of CeB6 and EuB6. Physica B: Condensed Matter, 405(22), 4634-4637.

Onuki, Y., Umezawa, A., Kwok, W. K., Crabtree, G. W., Nishihara, M., Yamazaki, T., ... & Komatsubara, T. (1989). High-field magnetoresistance and de Haas–van Alphen effect in antiferromagnetic PrB 6 and NdB 6. Physical Review B, 40(16), 11195.4

Kubo, Y., Asano, S., Harima, H., & Yanase, A. (1993). Electronic structure and the Fermi surfaces of antiferromagnetic NdB6. Journal of the Physical Society of Japan, 62(1), 205-214.

Wolgast, S., Kurdak, Ç., Sun, K., Allen, J. W., Kim, D. J., & Fisk, Z. (2013). Low-temperature surface conduction in the Kondo insulator SmB 6. Physical Review B, 88(18), 180405.

Süllow, S., Prasad, I., Aronson, M. C., Sarrao, J. L., Fisk, Z., Hristova, D., ... & Gibbs, D. (1998). Structure and magnetic order of EuB 6. Physical Review B, 57(10), 5860.

Semeno, A. V., Gil'manov, M. I., Sluchanko, N. E., Shitsevalova, N. Y., Filipov, V. B., & Demishev, S. V. E. (2018). Antiferromagnetic resonance in GdB 6. JETP Letters, 108(4), 237-242.

Weng, H., Zhao, J., Wang, Z., Fang, Z., & Dai, X. (2014). Topological crystalline Kondo insulator in mixed valence ytterbium borides. Physical review letters, 112(1), 016403.

Gernhart, Z. C., Jacobberger, R. M., Wang, L., Brewer, J. R., Dar, M. A., Diercks, D. R., ... & Cheung, C. L. (2012). Existence of erbium hexaboride nanowires. Journal of the American Ceramic Society, 95(12), 3992-3996.

Hung, S. H., & Jeng, H. T. (2020). Topological Phase and Strong Correlation in Rare-Earth Hexaborides XB6 (X= La, Ce, Pr, Nd, Pm, Sm, Eu). Materials, 13(19), 4381.

Luca, S. E., Amara, M., Galéra, R. M., Givord, F., Granovsky, S., Isnard, O., & Beneu, B. (2004). Neutron diffraction studies on GdB6 and TbB6 powders. Physica B: Condensed Matter, 350(1-3), E39-E42.

Takahashi, K., Nojiri, H., Ohoyama, K., Ohashi, M., Yamaguchi, Y., Motokawa, M., & Kunii, S. (1998). Neutron-scattering study of DyB6. Journal of magnetism and magnetic materials, 177, 1097-1098.

Yamaguchi, T., Akatsu, M., Nakano, Y., Washizawa, T., Nemoto, Y., Goto, T., ... & Nakamura, S. (2003). Thermal expansion and ultrasonic measurements of ferroquadrupole ordering in HoB6. Physica B: Condensed Matter, 329, 622-623.

Neugebauer, J., & Hickel, T. (2013). Density functional theory in materials science. Wiley Interdisciplinary Reviews: Computational Molecular Science, 3(5), 438-448.

Argaman, N., & Makov, G. (2000). Density functional theory: An introduction. American Journal of Physics, 68(1), 69-79.

Li, C., Wang, B., Li, Y., & Wang, R. (2009). First-principles study of electronic structure, mechanical and optical properties of V4AlC3. Journal of Physics D: Applied Physics, 42(6), 065407.

Guo-Liang, X., Jing-Dong, C., Yao-Zheng, X., Xue-Feng, L., Yu-Fang, L., & Xian-Zhou, Z. (2009). First-principles calculations of elastic and thermal properties of lanthanum hexaboride. Chinese Physics Letters, 26(5), 056201.

Zeng, X., Ye, Y., Zou, S., Gou, Q., Wen, Y., & Ou, P. (2017). First-Principles Study of the Nonlinear Elasticity of Rare-Earth Hexaborides REB6 (RE= La, Ce). Crystals, 7(11), 320.

Schmidt, K. M., Graeve, O. A., & Vasquez, V. R. (2015). Ab initio and molecular dynamics-based pair potentials for lanthanum hexaboride. The Journal of Physical Chemistry C, 119(25), 14288-14296.

Xiao, L., Su, Y., Peng, P., & Tang, D. (2017, June). First-principles study of electronic, mechanical and optical properties of mixed valence SmB6. In IOP Conference Series: Materials Science and Engineering (Vol. 207, No. 1, p. 012084). IOP Publishing.

Qi, X., Bao, L., Chao, L., & Tegus, O. (2018). Experimental and theoretical investigation on tunable optical property of nanocrystalline Ca-doped CeB6. Physica B: Condensed Matter, 530, 312-316.

Chao, L., Bao, L., Shi, J., Wei, W., Tegus, O., & Zhang, Z. (2015). The effect of Sm-doping on optical properties of LaB6 nanoparticles. Journal of Alloys and Compounds, 622, 618-621.

Gürel, T., & Eryiğit, R. (2010). Ab initio lattice dynamics and thermodynamics of rare-earth hexaborides LaB 6 and CeB 6. Physical Review B, 82(10), 104302.

Chao, L., Bao, L., Wei, W., & Tegus, O. (2016). Optical properties of Yb-doped LaB6 from first-principles calculation. Modern Physics Letters B, 30(07), 1650091.

Ning, S. Y., Iitaka, T., Xu, D. D., Li, Z., Wang, Y., Yang, X. Y., & Zhang, J. X. (2019). Preparation and Properties of High-Quality CexLayPryNd0. 05Gd0. 05B6 Single Crystal by Optical Float-Zone Technique. physica status solidi (a), 216(4), 1800706.

Liu, H., Zhang, X., Xiao, Y., & Zhang, J. (2018). The electronic structures and work functions of (100) surface of typical binary and doped REB6 single crystals. Applied Surface Science, 434, 613-619.

Liu, H., Zhang, X., Ning, S., Xiao, Y., & Zhang, J. (2017). The electronic structure and work functions of single crystal LaB6 typical crystal surfaces. Vacuum, 143, 245-250.

CHAPTER 4

INVESTIGATION OF COATING EFFICIENCY IN FRICTION SURFACING PROCESS

Dr. Mehmet Erbil ÖZCAN [1]

[1] Fırat University, Mechanical Engineering Department, Elazığ, TURKEY
meozcan@firat.edu.tr , ORCID ID 0000-0003-1641-8279

INTRODUCTION

It was estimated that annual financial losses caused by wear in the world are around 200 billion dollars (Savaşkan, 1999). In order to reduce these losses, improve the surface properties of the materials, and gather the desired properties, coating processes are carried out with different methods. Surface coating processes are used in many areas such as automotive, aircraft, electronics and health sector in order to improve and improve properties such as abrasion, corrosion, optics and beautify the external appearance. Instead of the entire substrate material, only the surface is improved using various coating methods such as PVD, CVD, thermal spray and friction. Friction surfacing, which is one of these coating methods, is based on the principle of coating by reaching high temperatures as a result of pressing the consumable rod, which performs rotational movement on the substrate material, with a certain axial force (Batchelor et al., 1996).

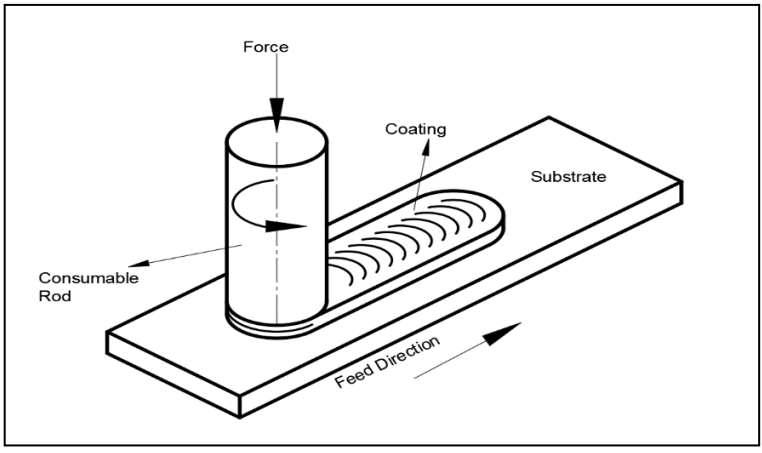

Figure 1: Schematic representation of the friction coating method

Friction surfacing, also known as friction deposition, is performed to improve and develop the properties of the substrate by depositing many materials such as tool steels, stainless steels, aluminum alloys and hardfacing materials on the surface. Friction surfacing, which continues to be used in many areas such as repairing axles, agricultural vehicles and anchor chains, increasing the wear resistance of materials, coating low carbon steels with high carbon steels, repairing the wearing parts of aircraft turbine blades and railway vehicles, continues to be a highly important coating method today (Rafi et al., 2011; Govardhan et al., 2012). In addition, one of the most important reasons for choosing this method can be shown as the coating process by reaching the plastic deformation temperature of the material without the need for an additional heating source.

Figure 2: Friction surfacing process

RESEARCH AND FINDINGS

Coating efficiency is the ratio of the total material deposited on the substrate to the amount of material consumed from the consumable rod (Fitseva et al., 2015). One of the most important factors in determining the amount of material deposited on the coating is the accumulation that occurs in the flange area. When the number of revolutions exceeds a certain level, the accumulation in the flange area increases and the efficiency of the coating decreases (Fitseva et al., 2015). The fact that the efficiency of the coating depends on the amount of material accumulating in this flange area sets the goal of minimizing the material accumulating in this area. In other words, the smaller the flange area at the end of the consumable rod, the higher the coating efficiency. The amount of material deposited on the coating is obtained by calculating the volume. The volume is calculated by measuring the width, length and height values of the material accumulated on the substrate material. After the volumetric calculations, the efficiency of the coating is obtained according to Equation 1.

$$\eta_{coating} = \left(\frac{deposited\ material}{concumed\ material\ from\ rod}\right) * 100\% \qquad (1)$$

In the graph in Figure 3, the yields of the coatings made at 800, 1000 and 1200 rpm rotational speeds and Vh=120 mm/min horizontal feed and Vv=160 mm/min vertical feed rates are compared. Considering the efficiency of coatings made without powder addition, the highest

efficiency is 32.29% at 800 rpm. When we look at the 10% B4C added coatings, the highest efficiency is again at 800 rpm; When the efficiency of the coatings with 20% B4C added is examined, it is observed that the highest efficiency is at 1000 rpm and when the values of the coatings with 30% B_4C addition are examined, the highest efficiency is again at 800 rpm. When the graph of Figure 3 is examined, the lowest efficiency was obtained in the 20% B4C powder added coating.

In Figure 4, the efficiencies of B_4C and TiC powder added coatings with n=1000 rpm, Vv=160 mm/min and 10% reinforcement ratio were compared. When the effect of horizontal feed rate on TiC and B_4C powder-reinforced coating efficiencies was examined, it was seen that the efficiency of TiC-reinforced coatings was higher than the efficiency of B4C-reinforced coatings. In Figure 5, the comparison of coating efficiencies of B4C added coatings according to horizontal and vertical feed rate rates was given. When the effect of horizontal feed on the coating efficiency was examined, the best efficiency was obtained as 35.86% at a vertical feed rate of Vv=140 mm/min and a horizontal feed rate of Vf=140 mm/min. When the efficiencies of the coatings made with 160 mm/min vertical feed rate were examined, it was seen that the coating with the highest efficiency was obtained with Vf=100 mm/min horizontal feed rate. Likewise, in coatings made at a vertical feed rate of Vv=180 mm/min, the horizontal feed rate with the highest efficiency was 35.91% and Vf=120 mm/min. According to these results, it was seen that the horizontal and vertical

feed rates do not have a direct effect on the efficiency, and the most important parameters affecting the efficiency are the number of revolutions and the material combination (Fitseva et al., 2015).

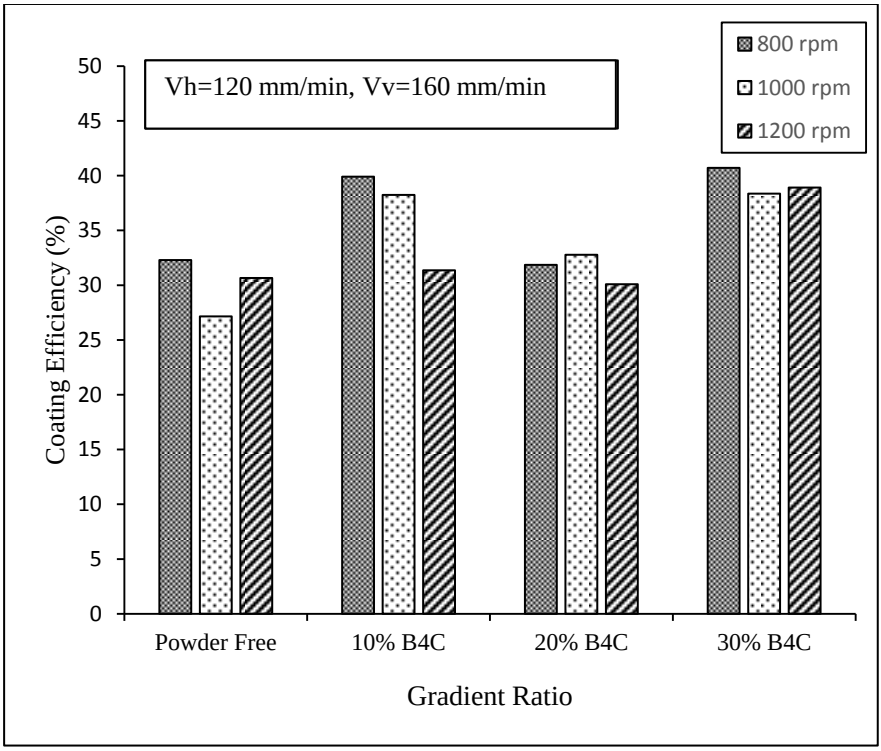

Figure 3: Comparison of coating efficiencies of coatings with and without B_4C addition at 800, 1000 and 1200 rpm, Vf=120 mm/min, Vv=160 mm/min conditions

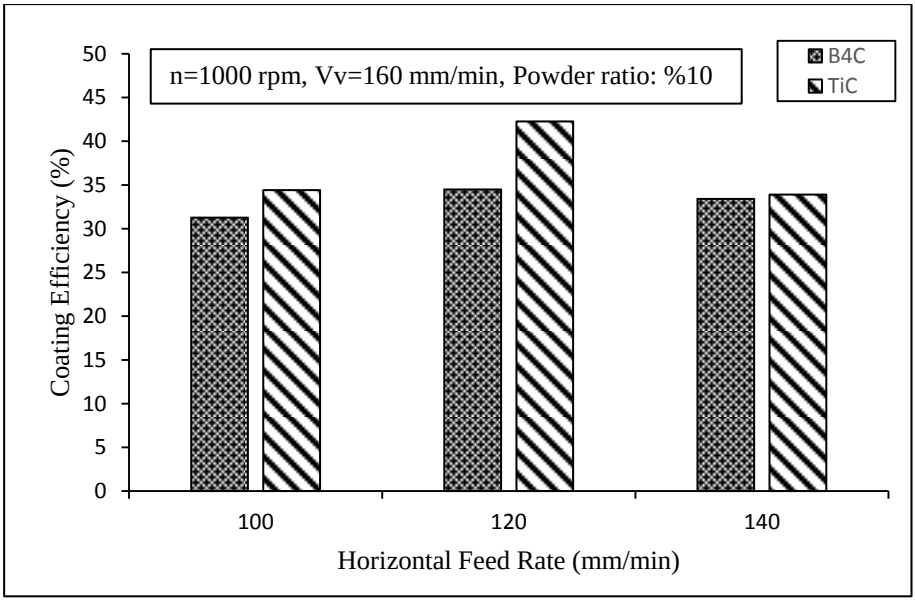

Figure 4: Comparison of the efficiency of S=1000 rpm, Vv=160 mm/min, 10% powder added B_4C and TiC coatings

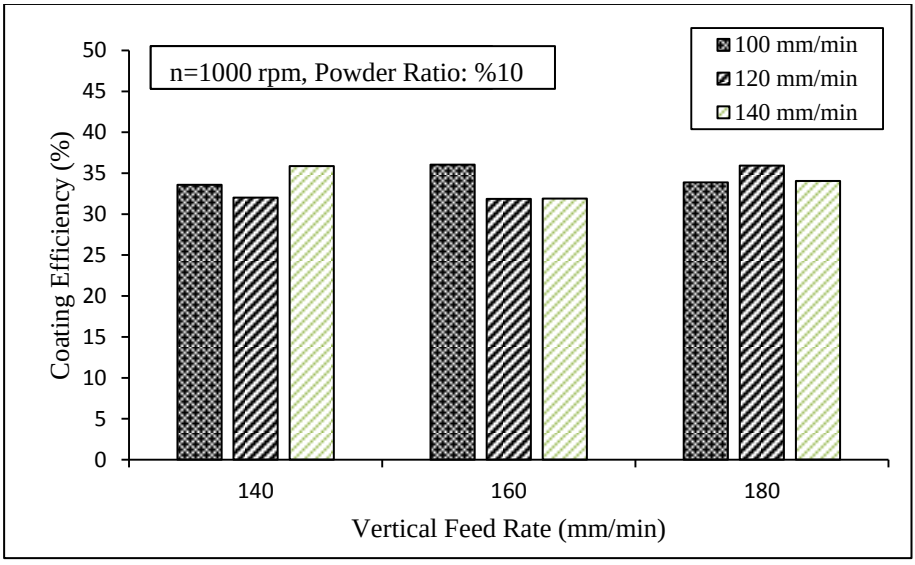

Figure 5: Variation of coating efficiency of B_4C added samples according to horizontal and vertical feed rate

CONCLUSIONS

The efficiency of the materials coated with the friction coating method gives the ability of the coating material to accumulate on the surface on the substrate. The results obtained as a result of the comparison of the coating efficiencies as a result of the coatings are given below.

- When the coating efficiencies were compared depending on the rotation speed during the coating of the material, it was seen that the highest efficiency was obtained in the coating made at 800 rpm.
- When a comparison was made according to the proportions of the powders, it was seen that the best efficiency was obtained in the 30% B4C addition. The highest reinforcement rate is due to the very good transfer of the consumable rod on the substrate and the good adhesion properties of B_4C powder after the sintering process.
- When a comparison is made according to the vertical and horizontal feed rates, it is seen that the highest coating efficiency is achieved at a vertical feed rate of 160 mm/min and a horizontal feed rate of 120 mm/min. Depending on these two parameters, vertical and horizontal feed rates make a positive contribution to the efficiency up to a certain limit speed, and adversely affect the efficiency when exceeding the limit speed.
- When the coating efficiencies of TiC and B_4C reinforced materials were compared, it was seen that the efficiency of TiC powder reinforced coating was higher at all three speeds. This

difference between B_4C and TiC is thought to be related to the atomic structure and adhesion properties of the material.

REFERENCES

Savaşkan, T. (1999). Material Information and Inspection. Birsen Publishing.

Batchelor, A. W., Jana, S., Koh, C. P., & Tan, C. S. (1996). The effect of metal type and multi-layering on friction surfacing. Journal of materials processing technology, 57(1-2), 172-181.

Rafi, H. K., Ram, G. J., Phanikumar, G., & Rao, K. P. (2011). Microstructural evolution during friction surfacing of tool steel H13. Materials & Design, 32(1), 82-87.

Govardhan, D., Kumar, A. C. S., Murti, K. G. K., & Reddy, G. M. (2012). Characterization of austenitic stainless steel friction surfaced deposit over low carbon steel. Materials & Design (1980-2015), 36, 206-214.

Fitseva, V., Krohn, H., Hanke, S., & Dos Santos, J. F. (2015). Friction surfacing of Ti–6Al–4V: Process characteristics and deposition behaviour at various rotational speeds. Surface and Coatings Technology, 278, 56-63.

CHAPTER 5

SYNTHESIS AND CHARACTERIZATION OF GRAFT COPOLYMERS BY ATOM TRANSFER RADICAL POLYMERIZATION

Dr. Melahat GÖKTAŞ [1]

[1]Yüzüncü Yıl University, Department of Science Education, Van, Turkey
melahat_36@hotmail.com

INTRODUCTION

Poly(vinyl chloride) (PVC) is one of the more used up thermoplastic polymers worldwide because of its general versatility and inexpensive. It is currently utilized in various applications ranging from construction to packaging. PVC is only synthesized on an industrial scale by free-radical polymerization (FRP) (Abreu et al., 2018). For the successful carrying out of a new polymerization technology for preparation of the PVC materials, it is very important to sustain the needed reactions conditions in the FRP process, which have been optimized for decades (Abreu et al., 2018; Fang et al., 2018). Poly(vinyl chloride) (PVC), the second most synthesized thermoplastic polymer after polyethylene, has been one of the most importantmaterials in our daily life for years with wide applications such as engineering materials, medical devices, rigid pipes, flooring, window frames and filtration materials (Huang et al., 2016; Fang et al., 2015).

Since it was first brought out in 1995, Atom transfer radical polymerization (ATRP) has been importantly utilized for block/graft copolymers synthesis and evaluated (Wang&Matyjaszewski, 1995; Wu et al., 2018; Lanzalaco et al., 2015; Brown et al., 2016; Wang et al., 2018; Okada& Matyjaszewski, 2015). The living/controlled radical polymerization techniques such as, which many research groups have focused heavily on perform studies, nitroxide-mediated polymerization (NMP), atom transfer radical polymerization (ATRP), and reversible addition fragmentation chain transfer polimerization

(RAFT) (YK&Ercole, 1998; Göktaş, 2020; Göktaş, 2019a; Yildiko et al., 2020).

Graft copolymers which combined of different properties monomers are used in various fields of technology. Graft copolymers is an significant field of study in macromolecular chemistry such as polymer chemistry and polymer technology. Macromonomeric initiators have been widely used for synthesis various graft copolymers via a set of processes of the living/controlled radical polymerization (Göktaş, 2019b; Göktaş, 2019c; Göktaş&Olgun, 2019; Göktaş&Deng, 2018; Göktaş et al., 2014; Öztürk et al., 2010; Öztürk et al., 2014; Öztürk et al., 2020; Savaş&Öztürk, 2020; Tukur et al., 2020;Öztürk&Cakmak; 2008; Coşkun&Seven; 2011; Paik et al., 1998). A great number of graft copolymers synthesized by atom transfer radical polymerization (ATRP) is available in the macromolecular literature. For example, Paik et al. Graft copolymers of poly(viny1 chloride) with styrene and (meth)acrylates were prepared by atom transfer radical polymerization (Paik et al., 1998). Poly(vinyl chloride) (PVC) containing graft copolymers, such as poly(vinyl chloride) (PVC), hydroxyethyl methacrylate (HEMA), (Fang et al., 2018) poly(vinyl chloride) (PVC), methyl methacrylate (MMA), pentafluorophenyl methacrylate (PFMA), and oligo (ethylene glycol) methyl ether methacrylate (OEGMA), (Huang et al., 2016) poly(vinyl chloride) (PVC), poly(*N*,*N*-dimethylaminoethyl methacrylate) (PDMA), (Fang et al., 2015) poly(vinyl chloride) (PVC), poly (ethylene glycol) methyl ether methacrylate, (Wu et al., 2018) poly(vinyl chloride) (PVC), hydroxyethyl methacrylate

(HEMA), (Lanzalaco et al., 2015) poly(vinyl chloride) (PVC), bis(2-bromo-2-methylpropanoatoethyl)amino vinyl (DEAB), methyl methacrylate (MMA), (Coşkun&Seven, 2011) poly(vinyl chloride) (PVC), *n*-butyl acrylate (BA), 2-ethyl hexyl acrylate (EHA), (Bicak&Ozlem, 2003) were also synthesized by atom transfer radical polymerization (ATRP).

In this study, poly(vinyl chloride) (PVC) based graft copolymer PVC-g-poly(acrylamide) was synthesized by copolymerization of acrylamide (AAm) monomers onto chains of PVC via ATRP using PVC macro initiator.

EXPERIMENTAL

Materials

Acrylamide (AAm), copper(I) chloride (CuCl), PVC (approximately Mn= 99,000 g/mol) were received from Aldrich. *N,N,N′,N″,N″*-Pentamethyldiethylenetriamine (PMDETA) was supplied by Acros. Methanol, *N*,*N*-dimethylformamide (DMF), ether were received from Sigma-Aldrich and used as received. All other chemicals were supplied by fluka and used as received.

Purification of PVC

PVC was purified as shown in literatures, (Öztürk et al., 2014) 2.5 g of PVC (approximately Mn= 99,000 g/mol) was solved in 40 mL of THF in 24 h and precipitated in methanol and dried under vacuum at 25 ^{o}C for 48 h before use.

The synthesis procedure of PVC-*g*-poly(AAm) graft copolymers

Graft copolymer PVC-*g*-poly(acrylamide) was prepared via ATRP. In accordance with ATRP mechanism, First, PVC (macro initiator) and monomers were spread out in *N*,*N*-dimethylformamide (DMF) as a solvent in a tube. Second, PMDETA and CuCl were filled into the flask. Finally, polymerization was carried out in a 90 °C oil bath. At the end of polymerization, the reaction mixture was droped into an excess of methanol to separate of the PVC-*g*-poly(acrylamide) graft copolymer. The obtained polymers were dried in a vacuum oven and the graft copolymer yield was found out gravimetrically.

RESULTS AND DISCUSSION

Purification of PVC

Before being used of the PVC (macro initiator) in the polymerization processes, it was purified and then its molecular weight was determined by GPC ($M_{n,GPC}$ = 85931 g/mol) in Figure 1. The FTIR spectra of PVC in Figure 2a displays 2909 and 2968 cm^{-1} for $–CH_2$ and –CH bands. The ^{1}H-NMR spectrum of PVC in Figure 4a shown the typically signals at 4.5 ppm for –C<u>H</u> and at 2.2 ppm for –C<u>H</u>$_2$.

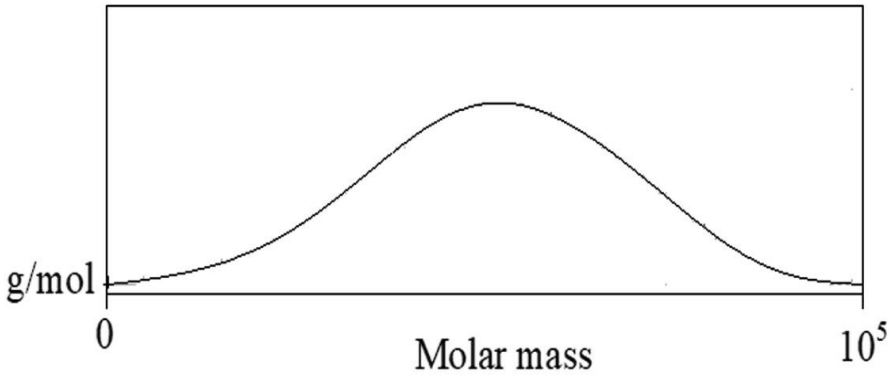

Figure 1: GPC molar mass diagram of PVC (macro initiator).

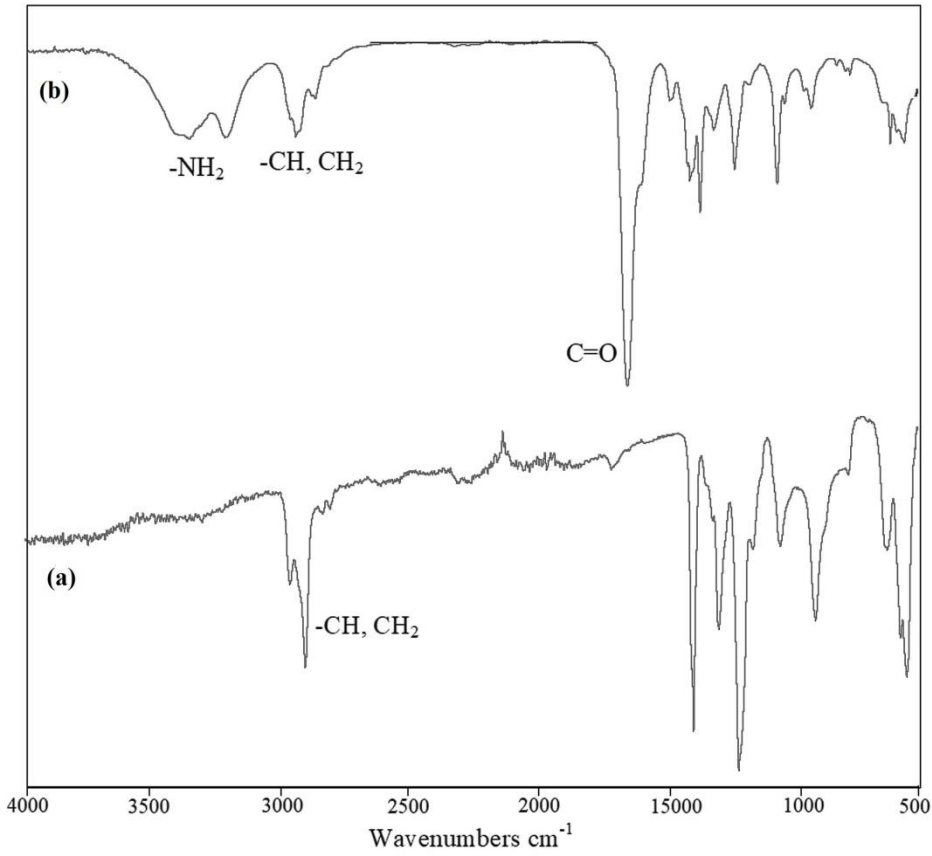

Figure 2: FTIR spectra of PVC **(a)**, PVC-*g*-poly(AAm) graft copolymers **(b)**.

The synthesis procedure of PVC-*g*-poly(AAm) graft copolymers

In the present study, a common vinyl monomer can be easily grafted onto PVC via ATRP due to the labile chlorine in PVC macroinitiator. The ATRP launched to synthesis PVC-*g*-poly(AAm) graft copolymers using the macroinitiator (PVC). The synthesis route of the PVC-*g*-poly(AAm) graft copolymers is displayed in Figure 3. ATRP was assessed by altering the amount of monomer and macroinitiator in the attendance of PVC (macroinitiator). The results of the graft copolymerization of AAm which obtained by ATRP is presented in Table 1,2. The conversion of the graft copolymers decreased from 60.10 wt% to 14. 86 wt% (Table 1) and increased from 13.94 wt% to 54.06 wt% (Table 2) over time.

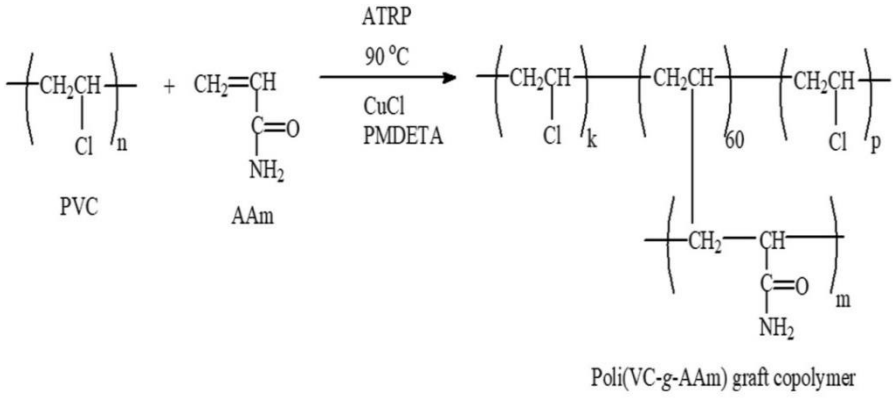

Figure 3: Synthetic route PVC-*g*-poly(AAm) graft copolymers.

The FTIR spectra of the P(VC-*g*-AAm) graft copolymers is presented in Figure 2b. The bands at 3198 and 3338 cm^{-1} for $–NH_2$ bands, 2930

cm^{-1} for $–CH_2$ and –CH bands, 1723 cm^{-1} for –C=O bands. Typical ^{1}H-NMR spectra of the PVC-*g*-poly(AAm) graft copolymers in Figure 4b displays 2.4 ppm for $–C\underline{H}_2$ of PAAm and PVC block, 3.2 ppm for –C<u>H</u> of PAAm and PVC block, 4.5 ppm for –C<u>H</u> of PVC block, 6.0, 6.1, 7.0 and 7.4 ppm for $–N\underline{H}_2$ of PAAm block.

The block lengths of PVC-*g*-poly(AAm) graft copolymers were arranged utilizing the ^{1}H-NMR spectrum. The block lengths of the graft copolymers was arranged utilizing the integral ratios of the signals corresponding to the $–N\underline{H}_2$ of poly-AAm (δ=6.0ppm), –C<u>H</u> of poly-PVC (δ=4.5 ppm). The block size of the graft copolymers can be designed by varying the amount of AAm and macromonomeric initiator (in Table 1-2).

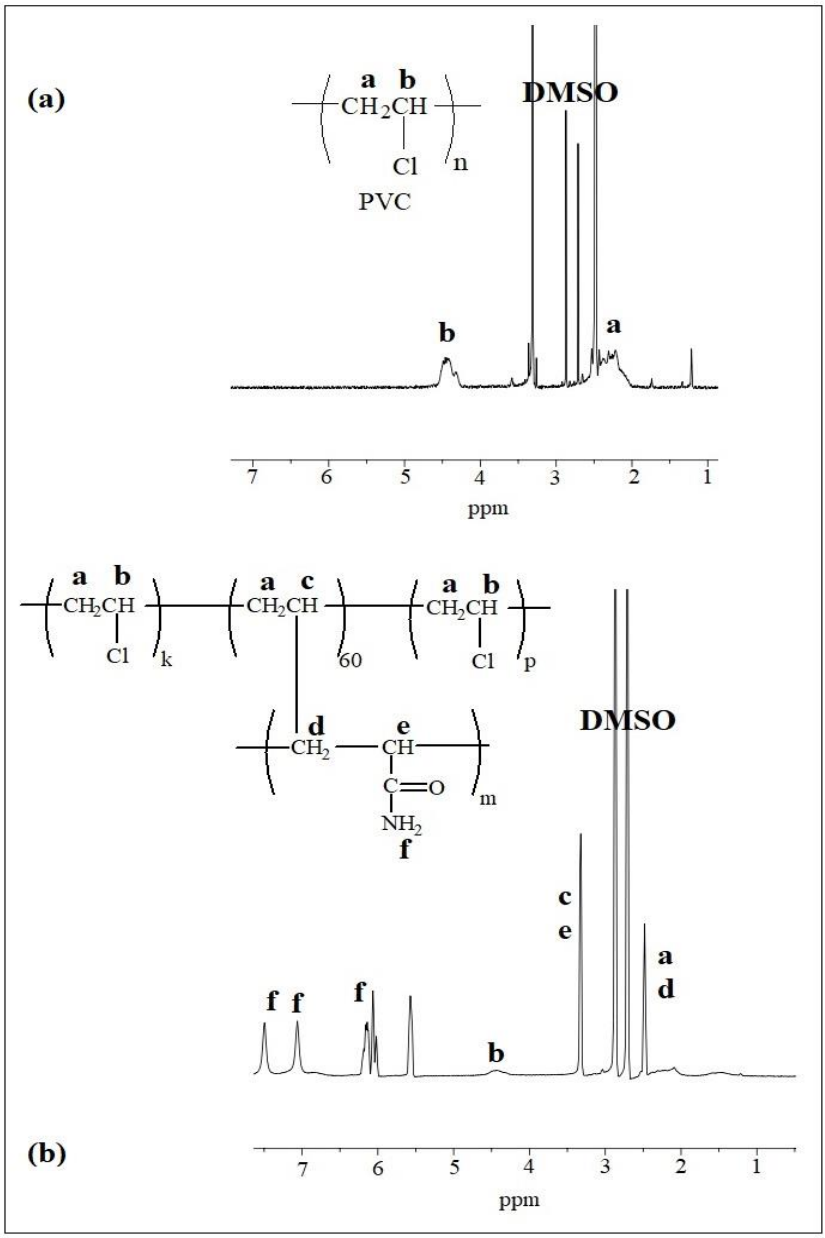

Figure 4: ^{1}H-NMR spectrum of PVC **(a)**, PVC-*g*-poly(AAm) graft copolymers **(b)**.

Thermal analysis of graft copolymers

The thermal properties of PVC-*g*-poly(AAm) graft copolymers were inquired into by thermogravimetric analysis (TGA), differential scanning calorimetry (DSC). The thermal decomposition temperature of PVC-*g*-poly(AAm) graft copolymers were proved via TGA. TGA curves of the graft copolymers was acquired by noting their weight loss curves with increasing temperature (in Figure 5). Weight loss of the graft copolymer with TGA analysis started at 25 ^{o}C and ended with two decays at 550 ^{o}C (in Figure 5). With the help of TGA characterization, it was observed that the weight loss and decomposition temperatures (Td) of the graft copolymers were 160 ^{o}C for the PAAm, 260 ^{o}C for the PVC, respectively.

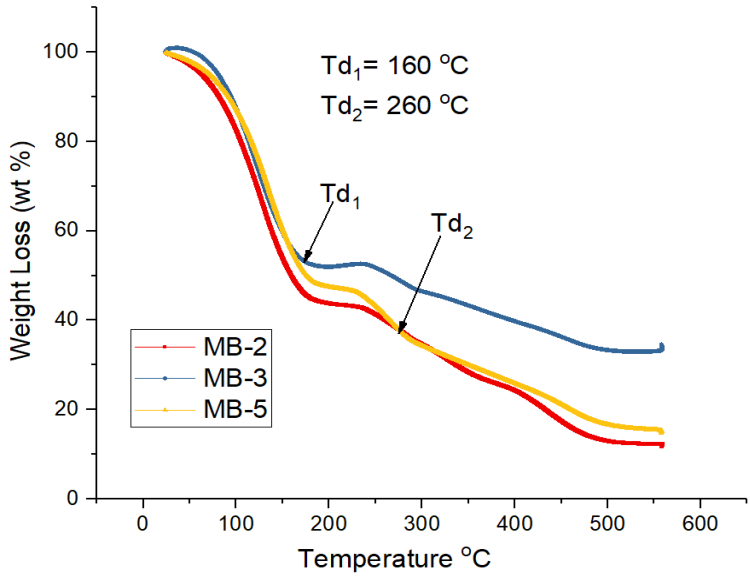

Figure 5: TGA curves of the PVC-*g*-poly(AAm) graft copolymers (MB series).

DSC analysis of the PVC-*g*-poly(AAm) graft copolymers were also carried out (Figure 6). Graft copolymers (MB-2 and MB-5 in Table 2) shown glass transition temperature (T_g) value about 40 ^{0}C. The glass transition temperature of the graft copolymers was different from the homo polymers. The glass transition temperature results for the graft copolymer show the miscibility of the homopolymers.

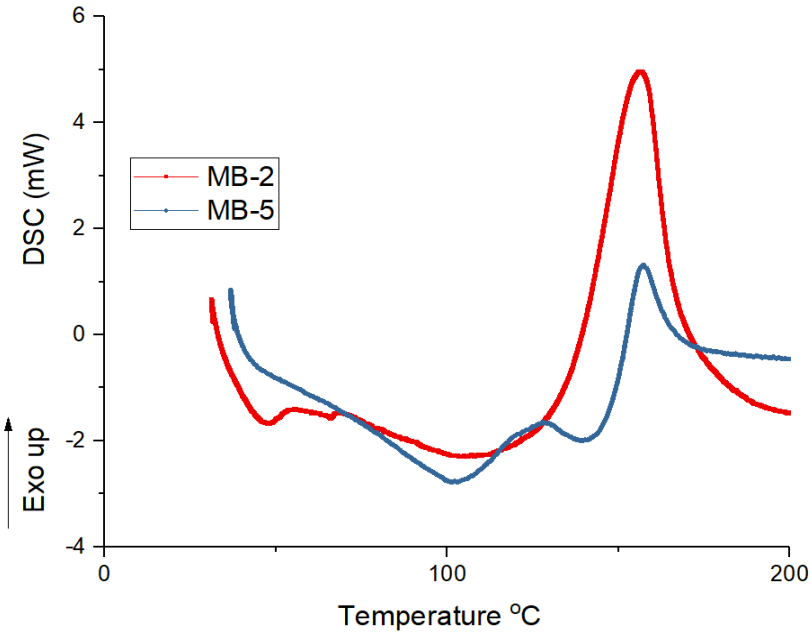

Figure 6: TGA curves of PVC-*g*-poly(AAm) graft copolymers (MB-2, MB-5 in Table 2).

SEM analysis was performed to examine the surface morphology of the graft copolymers. According to SEM analysis of PVC-*g*-poly (AAm) graft copolymers, it was observed that the distribution of graft copolymers within each other was good. SEM pictures of the graft copolymers were demonstrated in Figure 7.

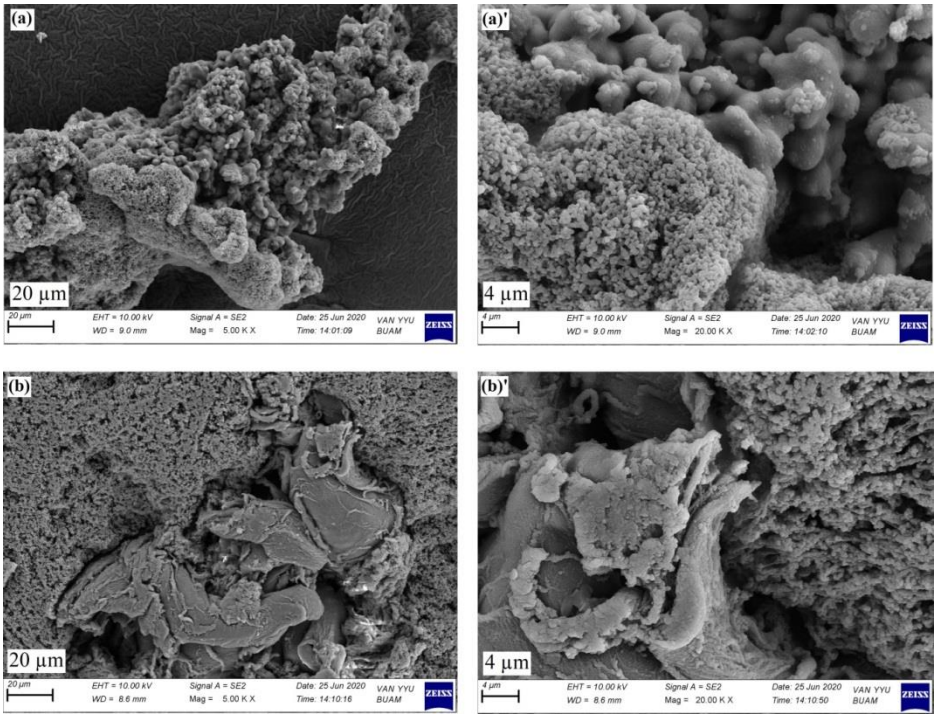

Figure 7: SEM micrographs of the PVC-*g*-poly(AAm) graft copolymers: BM-1 (a, a'), BM-5 (b, b'), (in Table-1).

CONCLUSIONS

In here, PVC based graft copolymers, PVC-*g*-poly(acrylamide) P(VC-*g*-AAm) graft copolymers, were synthesized by atom transfer radical polymerization (ATRP). High molecular weight PVC, which is an initiator suitable for ATRP polymerization, was used in the study. PVC is not a polymer prone to being processed as it is produced, but after the plasticizer, colorant, filler are added, they are shaped as a material. In our study, we synthesized and evaluated PVC-g-poly (acrylamide) graft copolymers by binding acrylamide monomer to PVC with ATRP. High molecular weight polymers such as block and

graft copolymers synthesized using macro initiators such as PVC can make a great contribution to materials science and polymer technology. The products were characterized using spectroscopic methods and multi-instruments.

Table 1: Effect of AAm amount on graft copolymerization. Polym. temp.= 90 ^{0}C; polym. time = 6 h; DMF= 3 mL.

Code	*PVC (g)*	*CuCl (g)*	*PMDETA (g)*	*AAm (g)*	*Yield (g)*	*Conv. (%)*	*Poly-AAm/poly-VC segment (mol/mol)*
BM-1	0.1000	0.0045	0.0160	1.2500	0.8114	60.10	0.39/0.15
BM-2	0.1000	0.0045	0.0160	1.5000	0.8867	55.41	0.54/0.15
BM-3	0.1000	0.0045	0.0160	1.7500	0.4847	30.29	0.46/0.15
BM-4	0.1000	0.0045	0.0160	2.0000	0.4049	19.28	0.52/0.15
BM-5	0.1000	0.0045	0.0160	2.2500	0.3492	14.86	0.64/0.15

Table 2: Effect of macromonomeric initiator (PVC) on graft copolymerization. Polym. temp.= 90 ^{0}C; polym. time = 6 h; DMF= 3 mL.

Code	*PVC (g)*	*CuCl (g)*	*PMDETA (g)*	*AAm (g)*	*Yield (g)*	*Conv. (%)*	*Poly-AAm/poly-VC segment (mol/mol*
MB-1	0.1000	0.0015	0.0020	2.5000	0.3625	13.94	-
MB-2	0.2000	0.0023	0.0040	2.5000	0.6086	22.54	0.52/0.75
MB-3	0.3000	0.0034	0.0060	2.5000	0.6573	23.47	0.50/0.84
MB-4	0.4000	0.0046	0.0080	2.5000	-	-	0.50/0.78
MB-5	0.5000	0.0057	0.0100	2.5000	1.6218	54.06	0.54/0.90

REFERENCES

Abreu, C. M., Fonseca, A. C., Rocha, N. M., Guthrie, J. T., Serra, A. C., & Coelho, J. F. (2018). Poly (vinyl chloride): current status and future perspectives via reversible deactivation radical polymerization methods. Progress in Polymer Science, 87, 34-69.

Fang, L. F., Matsuyama, H., Zhu, B. K., & Zhao, S. (2018). Development of antifouling poly (vinyl chloride) blend membranes by atom transfer radical polymerization. Journal of Applied Polymer Science, 135(6), 45832.

Huang, Z., Feng, C., Guo, H., & Huang, X. (2016). Direct functionalization of poly (vinyl chloride) by photo-mediated ATRP without a deoxygenation procedure. Polymer Chemistry, 7(17), 3034-3045.

Fang, L. F., Wang, N. C., Zhou, M. Y., Zhu, B. K., Zhu, L. P., & John, A. E. (2015). Poly (N, N-dimethylaminoethyl methacrylate) grafted poly (vinyl chloride) s synthesized via ATRP process and their membranes for dye separation. Chinese Journal of Polymer Science, 33(11), 1491-1502.

Wang, J. S., & Matyjaszewski, K. (1995). Controlled/" living" radical polymerization. Halogen atom transfer radical polymerization promoted by a Cu (I)/Cu (II) redox process. Macromolecules, 28(23), 7901-7910.

Wu, H., Li, T., Liu, B., Chen, C., Wang, S., & Crittenden, J. C. (2018). Blended PVC/PVC-g-PEGMA ultrafiltration membranes with enhanced performance and antifouling properties. Applied Surface Science, 455, 987-996.

Lanzalaco, S., Galia, A., Lazzano, F., Mauro, R. R., & Scialdone, O. (2015). Utilization of poly (vinylchloride) and poly (vinylidenefluoride) as macroinitiators for ATRP polymerization of hydroxyethyl methacrylate: Electroanalytical and graft-copolymerization studies. Journal of Polymer Science Part A: Polymer Chemistry, 53(21), 2524-2536.

Brown, S., Yue, Y., Kuo, L. J., Mehio, N., Li, M., Gill, G., ... & Dai, S. (2016). Uranium adsorbent fibers prepared by atom-transfer radical polymerization (ATRP) from poly (vinyl chloride)-co-chlorinated poly (vinyl

chloride)(PVC-co-CPVC) fiber. Industrial & Engineering Chemistry Research, 55(15), 4139-4148.

Wang, Z., Wang, Z., Pan, X., Fu, L., Lathwal, S., Olszewski, M., ... & Matyjaszewski, K. (2018). Ultrasonication-induced aqueous atom transfer radical polymerization. ACS Macro Letters, 7(3), 275-280.

Okada, S., & Matyjaszewski, K. (2015). Synthesis of bio-based poly (N-phenylitaconimide) by atom transfer radical polymerization. Journal of Polymer Science Part A: Polymer Chemistry, 53(6), 822-827.

YK, C. J. C., & Ercole, F. (1998). Living free-radical polymerization by reversible addition− fragmentation chain transfer: the RAFT process. Macromolecules, 31, 5559-5562.

Göktaş, M. (2020). Synthesis and characterization of temperature-responsive block copolymers using macromonomeric initiator. Chemical Papers, 74(7), 2297-2307.

Göktaş, M. (2019a). Synthesis and characterization of various block copolymers using PMMA-Br macroinitiator. Chemical Papers, 73(9), 2329-2339.

Yildiko, Ü., Ata, A. C., & Cakmak, İ. (2020). Synthesis, spectral characterization and DFT calculations of novel macro MADIX agent: mechanism of addition-fragmentation reaction of xanthate compound. SN Applied Sciences, 2(10), 1-14.

Göktaş, M. (2019b). Copolymer synthesis with redox polymerization and free radical polymerization systems. In Redox. IntechOpen.

Göktaş, M. (2019c). Synthesis and characterization of poly (styrene-b-methyl methacrylate) block copolymers via ATRP and RAFT. Journal of the Institute of Science and Technology, 9(1), 139-149.

Göktaş, M., & Olgun, B. (2019). One-step synthesis and characterization of poly (ε-caprolactone)-b-poly (N-isopropylacrylamide) thermo-responsive block copolymers via RAFT and ROP techniques. Polymer Science, Series B, 61(4), 421-429.

Göktaş, M., & Deng, G. (2018). Synthesis of poly (methyl methacrylate)-b-poly (N-isopropylacrylamide) block copolymer by redox polymerization and atom

transfer radical polymerization. Indonesian journal of chemistry, 18(3), 537-543.

Göktaş, M., Öztürk, T., Atalar, M. N., Tekeş, A. T., & Hazer, B. (2014). One-step synthesis of triblock copolymers via simultaneous reversible-addition fragmentation chain transfer (RAFT) and ring-opening polymerization using a novel difunctional macro-RAFT agent based on polyethylene glycol. Journal of Macromolecular Science, Part A, 51(11), 854-863.

Öztürk, T., Göktaş, M., & Hazer, B. (2010). One-step synthesis of triarm block copolymers via simultaneous reversible-addition fragmentation chain transfer and ring-opening polymerization. Journal of applied polymer science, 117(3), 1638-1645.

Öztürk, T., Göktaş, M., Savaş, B., Işıklar, M., Atalar, M. N., & Hazer, B. (2014). Synthesis and characterization of poly (vinyl chloride-graft-2-vinylpyridine) graft copolymers using a novel macroinitiator by reversible addition-fragmentation chain transfer polymerization. e-Polymers, 14(1), 27-34.

Öztürk, T., Meyvacı, E., & Arslan, T. (2020). Synthesis and characterization of poly (vinyl chloride-g-ε-caprolactone) brush type graft copolymers by ring-opening polymerization and "click" chemistry. Journal of Macromolecular Science, Part A, 57(3), 171-180.

Savaş, B., & Öztürk, T. (2020). Synthesis and characterization of poly (vinyl chloride-g-methyl methacrylate) graft copolymer by redox polymerization and Cu catalyzed azide-alkyne cycloaddition reaction. Journal of Macromolecular Science, Part A, 57(12), 819-825.

Tukur, A., Pekdemir, M. E., Haruna, H., & Coşkun, M. (2020). Magnetic nanoparticle bonding to PVC with the help of click reaction: characterization, thermal and electrical investigation. Journal of Polymer Research, 27, 1-12.

Özturk, T., & Cakmak, I. (2008). Synthesis of poly (ethylene glycol-b-styrene) block copolymers by reverse atom transfer radical polymerization. Journal of Polymer Research, 15(3), 241-247.

Coşkun, M., & Seven, P. (2011). Synthesis, characterization and investigation of dielectric properties of two-armed graft copolymers prepared with methyl methacrylate and styrene onto PVC using atom transfer radical polymerization. Reactive and Functional Polymers, 71(4), 395-401.

Paik, H. J., Gaynor, S. G., & Matyjaszewski, K. (1998). Synthesis and characterization of graft copolymers of poly (vinyl chloride) with styrene and (meth) acrylates by atom transfer radical polymerization. Macromolecular rapid communications, 19(1), 47-52.

Bicak, N., & Ozlem, M. (2003). Graft copolymerization of butyl acrylate and 2-ethyl hexyl acrylate from labile chlorines of poly (vinyl chloride) by atom transfer radical polymerization. Journal of Polymer Science Part A: Polymer Chemistry, 41(21), 3457-3462.

CHAPTER 6

THE EFFECTS of NITRILOTRIACETIC ACID (NTA) on SOME PLASMA ENZYMES of NILE TILAPIA (*Oreochromis niloticus* Linnaeus, 1758*)* in ACUTE LEAD EXPOSURE

Prof. Dr. Hikmet Y. ÇOĞUN[1] , Prof. Dr. Ferit KARGIN[2]

[1] Cukurova University, Ceyhan Veterinary Medicine, Department of Physiology, Adana, Turkey. hcogun@cu.edu.tr , ORCID ID 0000-0001-6559-4397
[2] Cukurova University, Faculty of Science and Letters, Department of Biology, Adana, Turkey. fkargin@cu.edu.tr , ORCID ID 0000-0003-4315-5689

INTRODUCTION

Naturally occurring lead (Pb) in the environment is produced by mining and manufacturing activities (Health, 1987). In addition, it is agreed that metals such as lead, which are toxic and non-biodegradable, accumulate in many aquatic creatures and cause various diseases such as kidney, liver lesions, endocrine disorders and the effect of cell membrane lipids on central nervous system cells (Lliopoulou-Georgudaki and Kotsanis 2001).

Nitrilotriacetic acid (NTA), the formula $N(CH_2CO_2H)_3$, is a colorless solid and used as a chelating agent, which forms coordination compounds with metal ions (chelates) such as Ca^{2+}, Cu^{2+}, and Fe^{3+}. The nitrilotriacetic acid (NTA) seems to be a promising "anti-pollutant", to prevent fish-kills in case of short-term breakdown of normal pollution controls in the aquatic environment (Sprague, 1968). NTA, known as a powerful chelating agent, can affect heavy metals in the aquatic environment even at very low concentrations in aquatic environments (Zitko and Carson 1972).

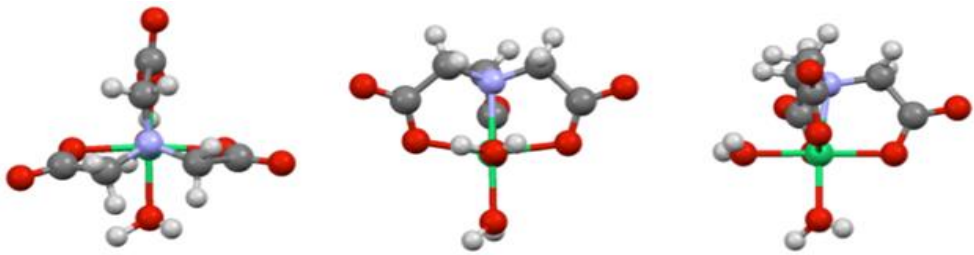

Figure 1: Structure of the NTA (URL1)

Blood biochemical parameters are among the factors that determine the health status of fish (Blaxhall and Daisley 1973; Desai et al., 2002). It is known that the energy requirement increases under stress conditions such as environmental pollution where fish are affected. Fish provide these energy requirements from sources such as glucose, glycogen, protein and lipids (Wandelaar Bonga, 1997; Levesque et al., 2002).

Plasma enzyme activities (cortisol, AST - aspartate aminotransferase and ALT - alanine aminotransferase) have been widely used an indicator of environmental and aquatic pollution (Nemcsok and Hughes 1988; Pelgrom et al., 1985; Shah and Altindag 2004). Biochemical parameters such as cortisol, ALT and AST in fish are good markers for fish metabolism under the influence of heavy metals.

The purpose of this study,was the effects of Pb and Pb+NTA on selected biochemical parameters (cortisol, ALT and AST) in Nile fish (*O. niloticus)* exposed to the sublethal concentration of Pb and Pb+NTA.

MATERIALS AND METHODS

Nile fish *O. niloticus* was obtained from fish production ponds of Cukurova University and adapted to the environment at 25 ± 1 ° C for 2 months in the laboratory. At the end of this adaptation period, the average body measurements and body masses of the animals were 13.3 ± 1.57 cm and 47.6 ± 3.25 g, respectively. Fish were exposed to

1.0 mg/L Pb and 1.0 mg/L Pb + 1.0 mg/L NTA at 2, 4 and 6 days. Experiments were carried out in three groups. In the first group, the fish were left at 1.0 mg / L Pb concentrations, in the second group 1.0 mg / L Pb + 1.0 mg / L NTA concentrations, and in the third group they were used as control.

Fish in experiments were carried out in three replicates, with two fish per repeat. After 2, 4 and 6 days, the fish were removed from the aquarium, after anesthesia with MS-222, the water droplets on it were removed with blotter paper and the tail section was cut and their blood was taken. Blood was centrifuged at 4000 rpm over 10 min at 15 ^{0}C. ALT and AST activities were determined using the UV test technique (Bergmeyer et al., 1985) and determined by ROCHE Hitachi E-170 and DPP. Cortisol level was measured by an electrochemiluminometric technique (Chiu et al., 2003).

Data are presented as mean ± standard error. For the statistical analysis, it was used one-way analysis of variance (ANOVA) followed by Student Newman–Keul's test using SPSS 10.0 statistical software (SPSS Inc., Chicago, IL). Differences were considered significant if $P < 0.05$.

RESULTS AND DISCUSSION

During the experiments, no death was observed in the ambient lead and lead-NTA mixture effects. Statistical analysis was done with the "SNK" test, the difference between groups was measured to be significant at $P < 0.05$.

Measuring blood cortisol levels in fish are good indicator of metal stress on fish. It has been shown that cortisol, a stress hormone, increases glucose production in fish through both gluconeogenesis and glycogenolysis in the presence of stress in the environment and possibly plays an important role in the stress-related increase in plasma glucose concentration (Iwama et al., 1999). In our study, it was determined that both Pb alone and the mixture of Pb + NTA caused an increase in cortisol levels compared to the control group (Table 1). In a similar study, Monteiro et al. (2005) observed that the blood cortisol level of *O. niloticus* increased under the effect of copper exposure. The decrease in blood cortisol levels under the Pb + NTA effect compared to the Pb effect alone indicates that NTA has a chelating effect.

Biochemical parameters such as ALT and AST in fish are good markers for fish metabolism under the influence of metal and are widely used in veterinary medicine in the diagnosis of physiological conditions and diseases of fish. And also, serum ALT and AST levels are important markers used especially in the diagnosis of damage to fish tissues (gill, muscle, liver) (De La Tore et al., 2000). These markers have been useful to determine in the diagnosis of liver and kidney diseases in fish (Maita et al., 1984; Adel et al., 2006). These enzymes of *O. niloticus* increased in response to lead exposures when compared to control during 2, 4 and 6 days (Figure 2 and 3). In our study, a significant increase was observed in blood ALT and AST levels under the effect of lead concentrations. Many researchers found

in their studies that these increases in fish serum ALT and AST levels were highly affected by environmental stress factors (De La Tore et al., 2000; Adel et al., 2006). It is thought that the increased ALT and AST levels in the serum of *O. niloticus* may have as a result of meeting the excess energy needed to combat stress caused by heavy metals such as lead. The presence of NTA in the environment is thought to reduce the toxic effect of lead in the environment due to its chelating effect on metal. While these decreases in the presence of NTA were observed as an increase or decrease in the lead effect alone, it was observed that these changes in the NTA effect approached the control level. The changes in these parameters show statistical significance.

In conclusion, the data obtained in this study show that lead causes an increase in plasma enzymes (cortisol, ALT and AST). NTA in combination with Pb caused a decrease in the toxic effect of Pb on plasma enzyme parameters. The present results show that NTA has an inhibitory effect against Pb-induced toxicity.

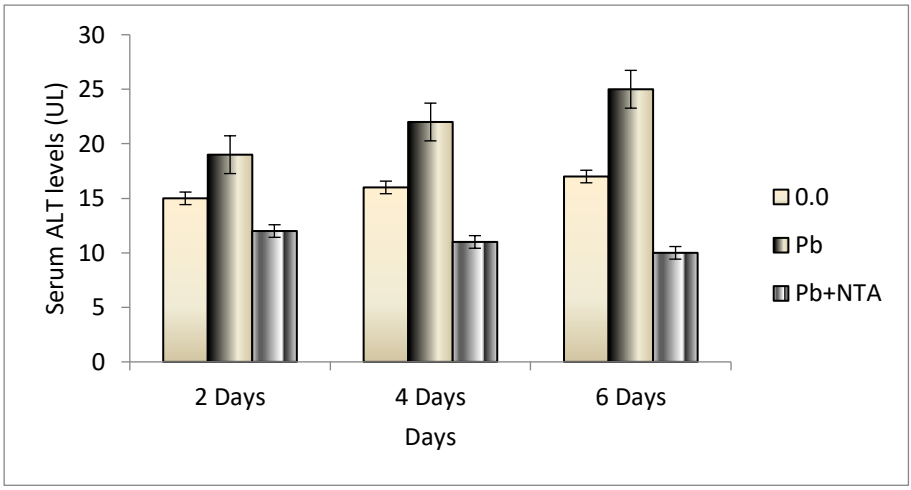

Figure 2: Serum ALT levels (UL) of Nile fish *O. niloticus* exposed to Pb, Pb+NTA for 2, 4 and 6 days.

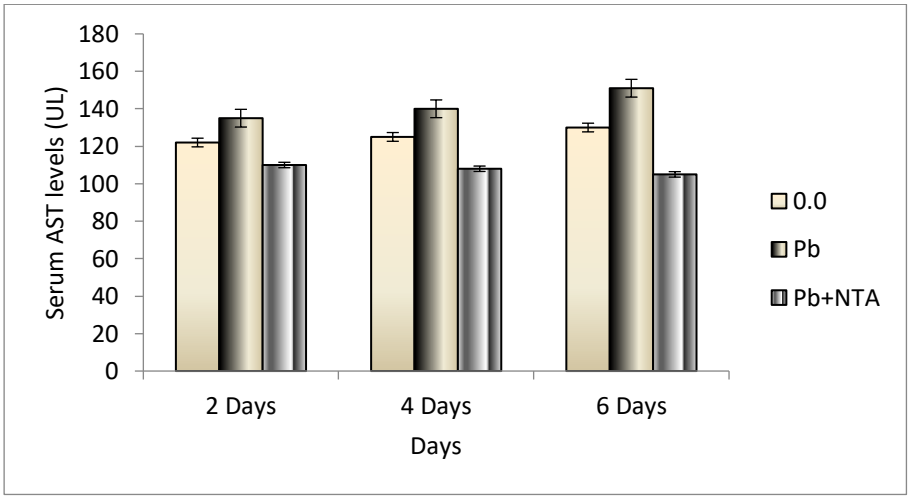

Figure 3: Serum AST levels (UL) of Nile fish *O. niloticus* exposed to Pb, Pb+NTA for 2, 4 and 6 days.

Table 1: Serum Cortisol (ng/dL) levels of *O. niloticus* under the exposure of Pb and Pb+NTA for 2,4 and 6 days. Letters a,b and c show the differences between groups at the same time ($p<0.05$)

Days	Control		1.0 ppm Pb		1.0 ppm Pb + 1.0 ppm NTA	
2	6.11± 0.03	a	7.13 ± 0.61	b	7.2± 0.30	b
4	5.90± 0.01	a	6.41 ± 0.22	b	5.8± 0.09	a
6	6.00± 0.04	a	7.75 ± 0.11	b	5.0± 0.80	c

REFERENCES

Adel, M.S., Ahmed M.E. and Salah, E.M. (2006). Reproductive and Patho-Physiological Responses of Blue Tilapia (*Oreochromis aureus*) Exposed to Chromium with or Without Chelating Substances. The Egyptian Journal of Experimental Biology (Zoology), 2, pp 195-205.

Bergmeyer, H.U., Horder, M. and Rej, R. (1985). International Federation of Clinical Chemistry (IFCC) Scientific Committee. Journal of Clinical Chemistry and Clinical Biochemistry, 24, pp 481–495.

Blaxhall, P.C. and Daisley, K.W. (1973). Routine Haematological Methods for use with Fish Blood. The Journal of Fish Biology, 5, pp 771-781.

Chiu, S.K., Collier, C.P., Clark, A.F., Wynn-Edwards, K.E. (2003). Salivary cortisol on ROCHE Elecsys immunoassay system: pilot biological variation studies. Clin Biochem, 36, pp 211–214.

De La Tore, F.R., Salibian, A., Ferrari, L. (2000). Biomarkers Assessment in Juvenile *Cyprinus carpio* Exposed to Waterborne Cadmium. Environmental Pollution, 109, pp 227–278.

Desai, H. S., Balram, N., Panigrahi, J. (2002). Toxicological Effects on Some Biochemical Parameters of Freshwater Fish *Channa punctatus* (Bloch) under the Stress of Nickel. Journal of Environmental Biology, 23(3), pp 275-277.

Health, A.G. (1987) Water Pollution and Fish Physiology. CRC Pres. Florida USA, pp 24.

Iwama, G.K., Vijayan, M.M., Forsyth, R.B. (1999). Ackerman PA. Heat shock proteins and physiological in fish. Am Zool, 39, pp 901–909.

Levesque, H.M., Moon, T.W., Campbell, G.C., Hontela, A. 2002. Seasonal Variation in Carbohydrate and Lipid Metabolism of Yellow Perch (*Perca flavescens*) Chronically Exposed to Metals in the Field. Aquatic Toxicology. 60: 257-267.

Lliopoulou-Georgudaki, I.J. and Kotsanis, N. (2001) Toxic Effects of Cadmium and Mercury in Rainbow Trouth (*Oncorhynchus mykiss*): A Short-term

Bioassay. The Bulletin of Environmental Contamination and Toxicology, 66, pp 77-85.

Maita, M., Shiomitsu, K. and Ikeda, Y. (1984). Health Assessment by the Climogram of Hemochemical Constituents in Cultured Yellowtail. Bulletin of the Japanese Society of Scientific Fisheries, 51, pp 205-211.

Nemcsok, J.G. and Hughes, G.M. (1988). The Effect of Copper Sulphate on Some Biochemical Parameters of Rainbow trout. Environmental Pollution, 49, pp 77-85.

Pelgrom, S.M.G.S., Lock, R.A.C., Balm, P.H.M. and Wendelaar Bonga, S.E. (1995). Effects of Combined waterbone Cd and Cu Exposures on Ionic and Plasma Cortisol in Tilapia *Oreochromis mossambicus*. Comparative Biochemistry & Physiology, 111C, pp 227-235.

Shah, S.L. and Altindag, A. (2004). Hematological Parameters of Tench (*Tinca tinca* L.) After Acute and Chronic Exposure to Lethal and Sublethal Mercury Treatments, The Bulletin of Environmental Contamination and Toxicology, 73, pp 911-918.

Sprague, J. B. (1968). Promising Anti-pollutant: Chelating Agent NTA protects Fish from Copper and Zinc. Nature 220, pp 1345 – 1346.

URL1:https://en.wikipedia.org/wiki/Nitrilotriacetic_acid#/media/File:Ni(NTA)(aq)23views.png

WendelaarBonga, S.E., 1997. The Stres Response in Fish. Physiological Reviews. 7, pp 591–625.

Zitko, V., & Carson, W. V. (1972). Release of heavy metals from sediments by nitrilotriacetic acid (NTA). Chemosphere, 1(3), 113-118.

CHAPTER 7

NECROTIC ENTERITIS: A RE-EMERGING ECONOMICALLY IMPORTANT ISSUE AND ALTERNATIVES TO ANTIBIOTICS FOR PREVENTION IN THE POULTRY INDUSTRY

Muhammad Zeeshan Afzal[§1]; Muhammad Mohsin*[§1,2]; Hafiz Muhammad Waqar Ahmad[§4]; Muhmmad Tahir Aleem*[§1]; Rizwan Abdul Aleem[1]; Nelam Sajjad[2], Zohaib Shahid[5]; Asghar Abbas[6]; Akram Ismael Shehata[2,3]; Yusuf Jibril Habib[2]; Liliana Aguilar- Marcelino[7]; Rao Zahid Abbas[1]; Guangwen Yin[2]*

[1] Faculty of Veterinary Science, University of Agriculture, Faisalabad, Pakistan
[2] College of Life Science, College of Animal Sciences (College of Bee Science), Fujian Agriculture and Forestry University, Fuzhou, Fujian Province, China
[3] Department of Animal and Fish production, Faculty of Agriculture (Saba-Basha), Alexandria University, Alexandria, Egypt
[4] Veterinary Research Institute, Lahore, Pakistan
[5] College of Veterinary and Animal Sciences, Jhang, Pakistan
[6] Department of Veterinary and Animal Sciences, Muhammad Nawaz Shareef University of Agriculture, Multan, Pakistan
[7] Centro Nacional de Investigacion Discliplinaria en Salud Animal e Inocuidad, INIFAB, Km 11 Carretera Federal Cuernavaca, No. 8534, Col. Progreso, Jiutepec, Morelos, C.P. 62550, Mexico
§ Equally contributed authors
*Corresponding Authors: onlymohsindvm@gmail.com; yinguangwen000@sina.com; dr.tahir1990@gmail.com

INTRODUCTION

Poultry has enormous importance as a rich source of animal protein for the human. The poultry industry is overgrowing day by day. Worldwide, its share of annual meat production is about 34% (M'Sadeq et al., 2015). However, the poultry industry faces huge production losses due to infectious diseases, including necrotic enteritis (Van Immerseel et al., 2016). Enteric infections are of particular concern to the poultry industry due to high mortality, losses in production, reduced weight gain and increased contamination of poultry products anticipated for human consumption (Hafez et al., 2011). Among the enteric diseases of the poultry, Necrotic enteritis (NE) caused by *Clostridium perfringes* is considerably important, causing widespread intestinal necrosis (Moore, 2016). The recent years have seen a marked increase in severity and occurrence of NE. Its re-emergence is a considerable alarm for the poultry industry as clinical forms of the disease are associated with high mortality, and subclinical conditions adversely affect feed conversion ratio and growth performance. The disease is worldwide, and birds are most susceptible in the first 3-4 weeks of age, economically the most important period for a broiler farmer (Zahoor et al., 2018). It adversely affects the feed growth performance of the birds, but in severe cases, can result in 10-40% mortality in infected flocks (McDevitt et al., 2006). The NE-infected birds suffer poor FCR and estimated 12% decreased body weight compared with normal healthy birds (Skinner et al., 2010). According to an estimate, about 6 billion USD losses are due to NE (Umar et al., 2016).

The accurate diagnosis of NE is essential for the correct interpretation of scientific studies and possible infectious disease prevention. The correct and definite diagnosis of the clostridial disease is necessary for its proper treatment. Previously, antimicrobials were routinely used for prophylactic control of NE in poultry. However, the recent banning of their use and modern and effective alternatives due to drug resistance is essential for successfully managing NE. Preventive treatment involves controlling predisposing factors, including diet modifications, and improving the overall hygiene of the environment. The control strategies should also target the causative agent by controlling the colonization, proliferation, and survival of lethal strains of the microbes and controlling the pathogenicity and virulence factors of the microbes. Vaccination against the disease is an effective approach. However, live vaccines can trigger the disease spread due to poor poultry management system and weak immune status of the birds.

The use of plants (Engberg et al., 2013) and other feed additives, including probiotics (bacteria and yeasts), essential oils (Liu et al., 2016; Timbermont et al., 2010), enzymes (Caly et al., 2015), organic acids (Geier et al., 2010; Timbermont et al., 2010), lysozyme (Liu et al., 2010). Annatto extracts (Galindo-Cuspinera et al., 2003) and antimicrobial peptides (Fig.1) are appealing approaches against *C. perfringens.* This manuscript focuses on pathogenicity and the control of NE by probiotics and prebiotics and vaccination against *C. perfringens*. The non-conventional control measures for NE are also covered in the manuscript.

Predisposing factors

NE in poultry was first reported in the 1950s and since then, continues to be reported in periodic episodes in various regions of the world. Several factors are responsible for the development of the disease (Figure 1). Although the causative agent is *C. perfringes*, the other factors responsible for the proliferation of the infection and the resultant effect of the disease are poorly understood. The onset of the disease is linked with a change in normal microflora present in birds' gastrointestinal tract (Antonissen et al., 2016). Any stress to the birds can also cause immunosuppression and disrupts the intestinal environment to favor the development of NE (Tsiouris, 2016).

The NE is considered to be directly related to the factors involved in the rearing of the birds. Management factors could have a marked effect on the pathogenesis of necrotic enteritis. In most experimental models, coccidiosis and supplementation of protein-rich fish meals are essential predisposing factors (Wu et al., 2014). Coccidiosis has bad effects on the intestines that make them susceptible to NE.s The integrity of gut is compromised by injury and damage to GIT which (M'Sadeq et al., 2015) opens access to the basal layer of the intestine which can become an important infection site in the initial stages of the disease, (Van Immerseel et al., 2016) can expose collagen and extracellular molecules, which play a critical role in adherence of *C. perfringens* (Wade and Keyburn 2015; Hafez et al., 2011) can result in leakage of serum into intestinal lumen which acts as rich source of nutrients for *C. perfringens*; and (Moore, 2016; Umar et al., 2016)

cause production of mucus which serves as high protein nutrient source for *C. perfringens* proliferation (Moore, 2016). Therefore, the control of coccidiosis is imperative for the successful control of NE.

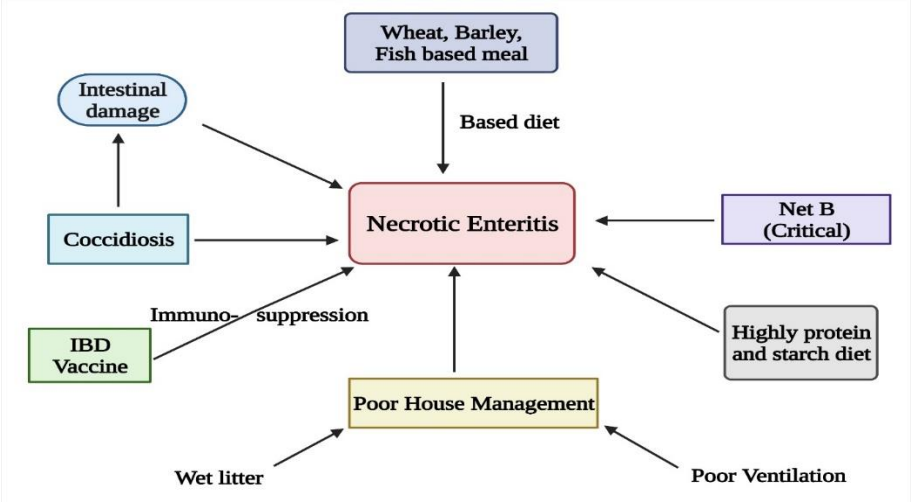

Figure 1. Pre-disposing factors or causative agents of Necrotic enteritis.

Etiology and characterization of various *C. perfringens* toxins

Necrotic enteritis is caused by some strains of *C. perfringens*, a spore-forming gram-positive bacterium. Any factor affecting the intestine, including stocking density, stress, the occurrence of coccidiosis or infectious bursal disease and changes in intestinal motility etc. can have a role in the pathogenesis of NE (Zahoor et al., 2018).

C. perfringens can produce four types of lethal toxins (alpha, beta, epsilon, and iota) and categorize them into different biotypes A, B, C, D, and E (Hafez, 2011). Besides the above-mentioned toxins, some *C. perfringens* strains also produce beta2 (CPB2) and enterotoxin (CPE), which have been reported to be involved in the pathogenesis of enteric

disorders (Zeng et al., 2016). A novel toxin named NetB was recently discovered in A strains of *C. perfringens* isolated from the birds infected with NE (Keyburn et al., 2008). It is reported to be a βpore-forming toxin of the family α-hemolysin and is necessary for the development of NE (Rood et al., 2016). Smyth and Mertin (Smyth and Martin, 2010) have reported that 58% of cases of NE were due to NetB toxin, while according to Gad et al. (2011), it is also found in normal chickens.

About 17 genes of *C. perfringens* have been classified, which encode endotoxins and exotoxins (Songr, 1996; Keyburn et al., 2010). Many molecular techniques, including multi-locus variable number of tandem repeats analysis (MVRT) (Sawires and Songer, 2005), pulsed-field gel electrophoresis (Crespo et al., 2007), and multilocus sequence typing (MLST)-(Jost et al., 2006) are described to access the genetic diversity of *C. perfringens* populations and to investigate isolates in the field outbreaks (Chalmers et al., 2008). Four major toxins (α, β.ε, and ι) are used to toxinotyped *C. perfringens* isolates. Various other minor toxins, e.g., β2 toxin, CPE, collagenase (κ-toxin), and perfringolysin O (θ-toxin) are also produced by various strains of *C. perfringens.* The term minor toxins are used for them because they are produced in less quantity or are less important (Rood et al., 2016; Uzal et al., 2014). A brief review of the activities of α and β toxins is provided below.

Alpha toxin

The alpha-toxin, a membrane-associated, chromosome encoded phospholipase, was thought to be a leading toxin inked to NE (Ellenmor et al., 1999) before the discovery of NetB- a class of βpore-forming toxins that are presently understood to be the main virulence factor documented for pathogenesis (Keyburn et al., 2008). It is the main extracellular toxin shown to be necessary for developing clostridial myonecrosis (Awad et al., 1995). Earlier research pointed out that secretions of *C. perfringens* could produce typical lesions of poultry NE. Since alpha-toxin was considered the main constituent of secretions, it was considered responsible for these lesions. Alpha toxin comprises two domains responsible for phospholipase C action (N-domain consisting of 1-250 residues) and membrane recognition action (C-domain, 251-370 residues). The terminal C-domain plays a role in maintaining the active form of toxin and works in a calcium-dependent fashion in regulating interactions with membrane-associated phospholipids. These two domains are not toxic at the individual level but are quite immunogenic in mice. However, the immune response against C-domain was effective in protecting against subsequent challenges. Due to this reason, the terminal C domain of α-toxin has undergone extensive investigation as a vaccine candidate for *C. perfringens* infection by delivering either as purified protein or by attenuated live bacteria (Jiang et al., 2015).

Net B toxin

Current studies have highlighted the role of a new toxin in NE known as NetB toxin. It was the first time reported in an Australian strain of *C. perfringens* type A (Keyburn et al., 2008). It is discovered to be associated with most of the necrotic enteritis-associated clostridial strains worldwide (Jiang et al., 2015; Rood et al., 2016). It is also considered the most important virulence factor responsible for necrotic enteritis in poultry. This pore-forming toxin is encoded by a relatively large conjugative plasmid (nearly 85 kilobase within a 42-kb pathogenicity locus designated as NELoc-1) and shows almost 38% identity to b-toxin of *C. perfringens* (Keyburn et al., 2010; Keyburn et al., 2008). This toxin also shows 29% resemblance to hemolysin II toxin of *Bacillus cereus* and 30% resemblance to alpha-toxin produced by *staphylococcus aureus*. The surveys of clostridial isolates from poultry have shown that the NetB gene is more prevalent in clostridial strains from infected birds than normal birds (Rood et al., 2016). However, a Denmark survey has shown more NetB gene incidence in clostridial isolates obtained from healthy birds (Abildgaard et al., 2010). This discovery shows that simple clostridial infection is insufficient to produce disease. So it was concluded that other predisposing factors must be present to develop the disease (Moore, 2016; Shojadoost et al., 2012). The NetB caused pathological changes in the chicken's leghorn male hepatoma (LMH) cells, rounding, and subsequent lysis of cells. Polyethylene glycol (PEG) 1500 and PEG 1000 were able to block these pathological changes

and LDH release from the cells, showing that toxin-dependent pore formation in the cell membrane is responsible for these changes.

The polyethylene glycol (PEG), an osmotic stabilizer, effectively inhibited target cell lysis if it cannot pass through toxin generated hole. Based on estimated radii of several PEG molecules, it was concluded that NetB produced a 1.6-1.8 nm diameter hydrophilic pore in the plasma membrane. The crystal structure determination of NetB pore showed an internal diameter of 26Å (Sawa et al., 2013). The detailed structure of NetB monomeric molecule has been estimated up to a resolution of 1.8Å (Yan et al., 2013). It showed that it contained rim, prestem, latch, and β-sandwich domains typically associated with α-hemolysin family of β-pore inducing proteins. The structure of this toxin is almost identical to *C. perfringens* δ-toxin despite having a different sequence of amino acids. The rim domain in most other βpore-forming toxins is linked to lipid binding while it deletes four amino acids in NetB. This fact highlights that this toxin has a different target on the cell surface. When the ability of NetB to generate pores in planar bilayers of phospholipids was analyzed, it was observed that pore channels of NetB have a high preference for cations than anions (Yan et al., 2013). The NetB structure excluding the first 20 amino acids of the N-terminus has been studied up to a resolution of 3.9Å after purification and solubilization of the complex structure through lipid vesicles (Sawa et al., 2013). Similar to monomer, the pore structure also shows resemblance with staphylococcal α-hemolysin. It consists of seven monomers of NetB assembled in a ring structure, and the transmembrane hydrophobic domain covers residues from

1121 to V146 (Numbered from N-terminal amino acids). Liposome studies have shown that NetB generated a hydrophilic hole with a functional diameter of nearly 1.6-1.8Å in the plasma membrane. When the crystal structure possessed by NetB was determined, it showed an internal diameter of about 26Å (Sawa et al., 2013), which agreed with the preliminary findings.

Along with NetB and alpha toxins, various host factors and secretions of *C. perfringens* also have a predominant role in disease pathogenesis. These secretions include proteolytic and hydrolytic enzymes (Myers et al., 2006) responsible for the damage to the basal lamina and enterocytes lateral domains (Shimizu et al., 2002). These proteolytic activities have effects on cellular junctions and also on the extracellular matrix. The *C. perfringens* affects the intestinal tissues of birds and causes an increase in collagenolytic activities of matrix metalloproteinase (MMP-2). This activity is considered to be responsible for pathological changes at basal lamina as well as at enterocyte lateral domains (Olkowski et al., 2008). Besides toxins, highly fibrous diets, poor housing, and hygienic conditions also play a role in the pathogenesis of NE.

Pathogenicity of NE

The gross pathology of NE is highly variable. The lesions vary from being focal to multifocal and convalescent, and in the severe case of the disease can be diffused throughout the small intestine. Although lesions are frequently associated with the proximal portion of the jejunum, practically all of the small intestine, including the cecum

region, can be involved. Necrotic and fibronecrotic lesions can be identified by tan discoloration of mucosa (Shojadoost et al., 2012). In few cases, mucosal thickening can occur due to the accumulation of necrotic debris and adherent fibrin. The mucosa becomes coarse and granular in texture and can be moderately moist and soft or firm and adherent. The ulcers are represented by depressed foci having roughened red surfaces, and there can be limited hemorrhages in the lumen or at the margins (Smyth, 2016). In birds having necrotic enteritis, all the lesions having a crater-like appearance are commonly designated as ulcers. At the same time, many of them may represent areas having mucosal thickening associated with sloughing of necrosed mucosa. Such areas have a smooth and glistening surface, which is somewhat depressed as compared to surrounding mucosa. Most often, the mucosal rim around these re-epithelialized craters and ulcers has tan discoloration due to necrosis. Re-epithelialized craters and ulcers are frequently visible on the serosal surface. The intestinal walls become thin and flaccid due to sloughing of necrosed mucosa and loss of tone by smooth muscles. The lumen of the intestine may accumulate sloughed necrotic debris and foul gases (Smyth, 2016). The luminal contents and mucosal surface in the duodenum and proximal jejunum are frequently discolored by dark green and thick bile.

The microscopic lesions of NE are very characteristic but not pathognomonic as other clostridia, e.g., *C. sordellii* (Rimoldi et al., 2015) and *C. colinum* (Swayne, 2013), may produce very identical lesions. Therefore, the immunohistochemical and cultural

confirmation of *C. perfringens* is necessary and intestinal lesions for accurate diagnosis of NE. Single scattered villi or groups(s) of villi or total villi in a given section may be infected. A superficial zone of variable thickening with markedly eosinophilic necrotic material may be present, coated with a thick layer of clostridia. It is separated from surrounding healthy tissues by a zone of heterophilic infiltration. Sometimes bacteria and necrosed lamina propria are found under comparatively normal epithelial tissues. Necrotic coagulum may also have huge bacterial clumps.

The craters that have undergone re-epithelialization are evident as areas with increased depth of crypts but reduced villi height. Pathological changes such as intestinal villi, separation of lamina propria and epithelium, strips of separated epithelial cells etc., should be interpreted with care because these changes are also associated with autolysis following the bird's death and can be mistakenly interpreted as pathological lesions of NE (Smyth, 2016). The pathologists must be familiar with the appearance of freshly dead birds and birds that are dead for hours or days. Also, a complete inspection of intestines for characteristic lesions and microbiological demonstration of the agent in tissues is mandatory for the correct diagnosis of the problem.

Control strategies

The following three strategies are proposed for control of poultry NE: (M'Sadeq et al., 2015) the use of biosecurity measures to minimize the environmental exposure, (Van Immerseel et al., 2016) boost up the

bird's resistance to pathogenic clostridial species by genetic selection, vaccination, and competitive exclusion, etc. and (Hafez. 2016) use of anti-bacterial approaches (probiotics, prebiotics) to lessen and even wipe out pathogenic Clostridia from infected chickens (e.g., bacteriocin treatment and bacteriophage therapy, etc.). The bird's genetics seems to influence the susceptibility to necrotic enteritis, as is shown by the difference in susceptibility of different breeding lines of poultry (Jang et al., 2013) to NE. The use of natural intervention approaches for poultry production has become necessary due to limitations on antibiotics placed by legislation (Liu et al., 2016). Therefore, there is an urgent need to control NE in all possible ways and means. Here, we discussed briefly the role of dietary supplement including prebiotics, probiotics, vaccination, and bacteriophage therapy, against this NE (Figure 2).

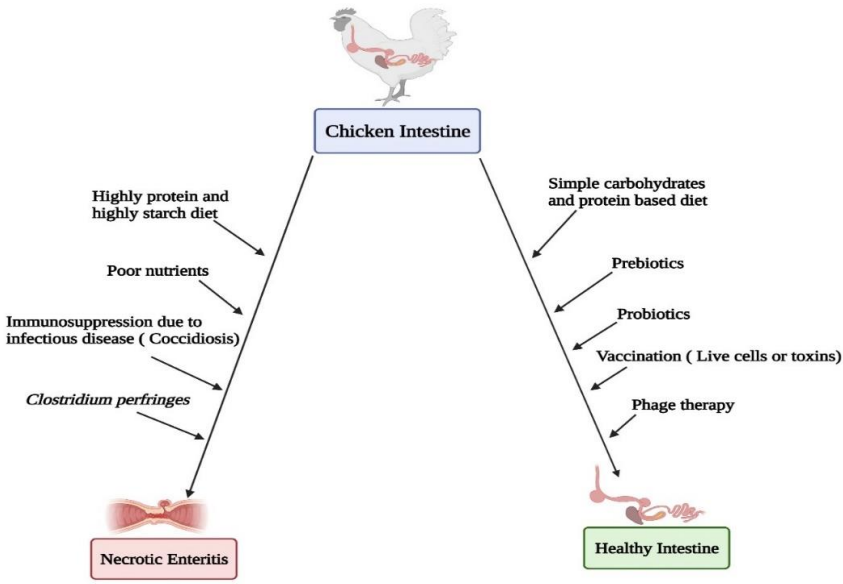

Figure 2. Possible control stratergies against Necrotic enteritis.

Dietary control

The dietary approach to minimize the devastating losses suffered by the poultry industry due to this disease is an excellent opportunity for NE control. Dietary ingredients have a critical role in the development of NE. It was observed that confining the feed of broilers effectively reduced the intensity of necrotic enteritis lesions and decreased the population of *C. perfringens* in the caecum (Tsiouris et al., 2014). The positive effect of confining feed access was due to the immune system and neuroendocrine influence and the non-availability of nutrients in the digestive tract. Moreover, confining the feed also improved circulation to the mucosa of the intestines, thus protecting it against necrosis (Tsiouris et al., 2014). The birds fed on rye oats, barley, and wheat-based diets have more NE incidence than the birds fed diets based on maize (Annett et al., 2002). The maize is understood to be a good ingredient of the broiler diet due to its high energy contents, and its inclusion in the birds' diets also decreases the NE incidence in the birds (Moore, 2016). Cereal grains contain a high quantity of non-starch polysaccharides (NSP). The presence of NSPs increases the viscosity and passage time of intestinal contents (Moore, 2016), which can help in bacterial colonization in the intestine. Hence, an increase in viscosity and passage time increases the bird's susceptibility to NE. Therefore, the reduction in amounts of cereal grains in feed can be helpful to control NE. Some experimental models have utilized a high level of animal origin proteins in the diet, especially fishmeal, as a predisposing factor (Cooper and Songer, 2009; Keyburn et al., 2006; Wu et al., 2014). High protein contents in the intestines can increase

the growth and proliferation of *C. perfringens* and alter the composition of normal microflora. These effects are due to increased nutrients supply and an increase in intestinal Ph.

The supplementation of broiler's feed with beneficial probiotics has shown to be effective in controlling the growth of pathogens and diseases (Figure 3). The health, feed conversion ratio, and weight gain are improved by supplemented feed containing probiotics bacteria (Caly et al., 2015). Many products effective against infectious diseases including NE are commercially available in the market (Table 1). Probiotics are live microbes that benefit the host by improving intestinal microbial balance (Caly et al., 2015). The probiotics interact with the host to improve intestinal morphology and immunity and thus lessen the risk of opportunistic pathogens. Probiotic bacteria also produce antimicrobial molecules, e.g., bacteriocins that target pathogens, inhibit their adhesion and toxin production (Schoster et al., 2013). Beneficial bacteria also compete with pathogens for resources within the host. Probiotics are also used as competitive exclusion (CE) cultures. The antimicrobial properties of yeasts are also well known (Hatoum et al., 2012). The cell wall of many yeasts is rich in beta-glucans that exert immunomodulatory effects (Alizadeh et al., 2016). Yeasts protect the host from pathogens (M'adeq et al., 2015) by secreting specific enzymes which destroy microbial toxins (Van Immerseel et al., 2016) by preventing microbial adhesion to the epithelial cells and (Moore, 2016; Umar et al., 2016) by competing with pathogenic organisms.

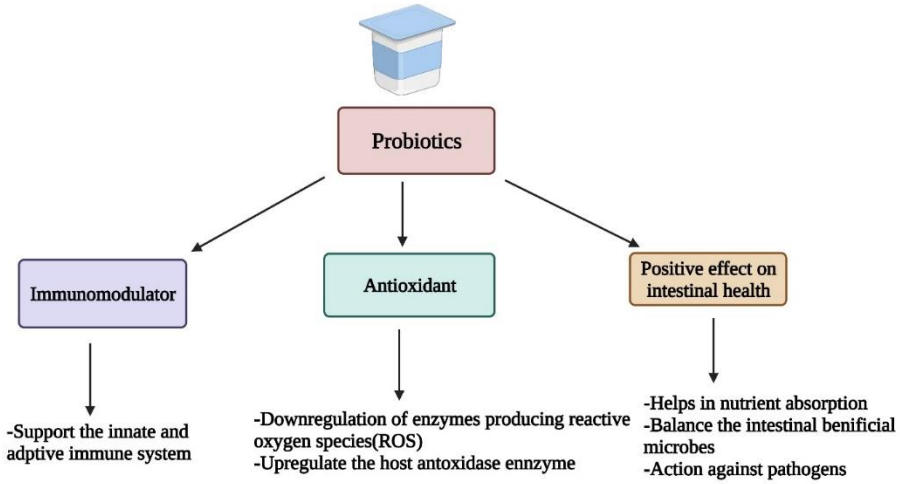

Figure 3. Role of probiotics in controlling Necrotic enteritis in the chicken.

Prebiotics refer to the indigestible oligosaccharides which selectively stimulate the growth of beneficial bacteria and complement the effects of dietary probiotics (Patel and Goyal, 2012). Various prebiotic molecules are used, including the Mannanoligosaccharides (MOS) which are components of the cell wall of yeast and are also present in yeast extracts (YE). They are frequently used in broiler feed (Table 1). The inclusion of MOS in the broiler fed improved weight gain and productivity (Fowler et al., 2015). After replication in the bacteria, phages secrete endolysins that damage bacteria's call walls by targeting peptidoglycans. The bacterial cells are lysed, and phages become free to infect other cells (Nakonieczna et al., 2015).

Various bacteriophages are defined for *C. perfringens,* some isolated from poultry strains and anti-clostridial activity (Volozhantsev et al., 2011). The bacteriophage use, although challenging to apply, can be a promising alternative. In reality, the behavior of molecules *in vivo* is

influenced by many factors and is hard to predict. More recently, essential oil carvacrol in encapsulated form has positive effects on controlling NE (Liu et al., 2016). The supplementation of organic acids in feed can prevent the growth of pathogenic bacteria and maintain the intestine's health by altering host-pathogen interactions (Timbermont et al., 2010).

Table 1. Commercially available products effective against infectious diseases including NE.

Product	**Composition**	**Performance**	**Reference**
FloraMax® B-11	11 lactic acid bacteria and inactivated *Saccharomyces cerevisiae*	Immunomodulatory, Antioxidant effect	Biloni et al., 2013
Aviguard®	Over 200 bacterial species	Competitive exclusion	Hofacre et al., 1998
MSC™	Bacteria	Competitive exclusion	Craven *et al*., 1999
Broilact®	Complex mixture of bacteria	Competitive exclusion	Kaldhusdal *et al*., 2001
PoultryStar®	6 bacterial species and 1 prebiotic (FOS)	Competitive exclusion	McReynolds *et al*., 2009
SafMannan®	Yeast extract	Immunostimulation, antimicrobial activity	Abudabos and Yehia, 2013
NuPro®	Yeast extract	Immunostimulation, antimicrobial activity	Thanissery *et al*., 2010
Immunolin®	Mixed Bacteria Species	Immunomodulatory, Antioxidant effect	Abu-Akkada and Awad, 2015

Polystar®	*Bifidobacterium bifidus* and *Lactobacillus plantarum*	Immunomodulatory, Antioxidant effect	Ritzi et al., 2016; Mohsin et al., 2021a

Infectious diseases control

There is a great need to control infectious diseases (Lin et al., 2020; Aleem et al., 2021). Coccidiosis has bad effects on the intestines (Lin et al., 2020; Chen et al., 2020), making them susceptible to NE. The integrity of the gut is compromised by injury and damage to GIT, which (M'Sadeq et al., 2015) opens access to the basal layer of the intestine, which can become an important infection site in the initial stages of the disease, (Van Immerseel et al., 2016) can expose collagen and extracellular molecules, which play a critical role in adherence of *C. perfringens* (Hafez, 2011; Wade and Keyburn, 2015) can result in leakage of serum into intestinal lumen which acts as rich source of nutrients for *C. perfringens*; and (Moore, 2016; Umar et al., 2016) cause production of mucus which serves as high protein nutrient source for *C. perfringens* proliferation (Moore, 2016). The infectious diseases that infect intestinal regions, especially coccidiosis and infectious bursal disease, can make them susceptible to NE. Therefore, the control of infectious diseases is imperative for the successful control of NE.

Immune interventions

The current situation demands us to utilize immunization as an alternative strategy to antimicrobials for controlling NE. The details of immune reaction to *C. perfringens*, pathogen recognition, and its secreted toxins and proteins are yet to be explored. In chickens that were partially immunized against NE, a specific mucosal IgA response against NetB, alpha-toxin, and many other immune-stimulating proteins was observed (Caly et al., 2015; jang et al., 2012; Kulkarni et al., 2007). However, in intestinal washings of birds that were given experimental challenge, only a meager response of mucosal antibodies (IgA) to *C. perfringens* was observed. This may suggest that serum IgY may have a more critical role in the immune response to NE than mucosal IgA. After systemically immunizing the birds against various immunogenic proteins (recombinant), serum IgY reached mucosal surface under the influence of *C. perfringens* induced inflammation (Kulkarni et al., 2007; Mot et al., 2014).

Various strategies have been utilized to vaccinate the broilers against *C. perfringens*, including live bacteria and inactivated toxins. Vaccines can be added to feed, sprayed on chicks after hatching, added in feed, and even injected into eggs (Mot et al., 2014). Mild virulence is necessary for the strains used for vaccination as non-virulent strains are proved inefficient. Many studies have proved that chickens can be immunized against NE by injecting active or inactive toxins (Mot et al., 2014; Jang et al., 2012) and various antigenic proteins (Jiang et al., 2015). The vaccines based on proteins are

frequently used due to their safety and better characterization than live vaccines and are still immunogenic (Unnikrishnan et al., 2012). They include subunit vaccines based on secreted toxins and other virulent factors and inactivated toxoids. DNA vaccines expressing Clostridium toxins other than *C. perfringens* have also been tested for vaccine development (Jin et al., 2013; Li et al., 2011). Avirulent or attenuated bacteria can act as vehicles for the efficient delivery of various vaccine candidates (Rappouli et al., 2011). Attenuated strains of Salmonella are frequently used in poultry to control salmonellosis. They can also act as effective and safe carriers for oral-based NE vaccines by expressing various heterologous antigens (Jiang et al., 2015).

The misunderstanding that alpha-toxin has an important role in pathogenesis misled the vaccine development efforts for years. Still, recent improvements in our understanding of pathogenesis have enabled us to develop effective vaccines (Moore, 2015). vaccination against alpha-toxin in recent age, NetB toxin has also become the target of extensive studies for vaccine development (Fernandes et al., 2013; Keyburn et al., 2013a). Several studies have highlighted that the vaccines using NetB toxin produce an effective immune response with a good level of protection against NE. The directly vaccinated birds (Fernandes et al., 2013; Jang et al., 2012; Jiang et al., 2015; Keyburn et al., 2013a) and the chicks from well-vaccinated hens (Keyburn et al., 2013b) have shown protection. It can be concluded that 70-80% protection level can be achieved using native NetB, recombinant

NetB, bacterin, and toxoid-containing vaccines having sufficient NetB to stimulate a good immune response. However, the development of an affordable and safe vaccine compatible with management practices is still a challenge.

CONCLUSION

Necrotic enteritis (NE) is a re-emerging economically significant poultry disease caused by the bacterium *Clostridium perfringens*. Due to drug resistance, Prebiotic and probiotic supplementation are appealing and practical approaches in controlling infectious diseases (Mohsin et al., 2021a; 2021b), including NE, positively affecting the growth performance of the birds and their role as inhibition of pathogens. Moreover, vaccination with various immunogenic proteins secreted by bacteria and modified toxins appears to be a logical preventive protocol against the disease. This review summarizes the importance of NE and recent advancements in preventive treatments against NE and elaborates the role of vaccines, prebiotics, and probiotics for the effective management of NE. However, further studies are needed to control the disease by following omics study.

ACKNOWLEDGMENTS

The manuscript has been supported by the Natural Science Foundation of China (No. 31872466), the grant from Fujian Science and Technology Department (2019N0005) and Fujian Modern Poultry Industry Technical System Construction Project (2019-2022).

REFERENCES

Abildgaard, L., Sondergaard, T.E., Engberg, R.M., Schramm, A., Højberg, O., 2010. In vitro production of necrotic enteritis toxin B, NetB, by NetB-positive and NetB- negative Clostridium perfringens originating from healthy and diseased broiler chickens. Veterinary Microbiology., 144(1): 231-235.

Abudabos, A.M. and Yehia, H.M., 2013. Effect of dietary mannan oligosaccharide from Saccharomyces cerevisiae on live performance of broilers under Clostridium perfringens challenge. Italian Journal of Animal Science, 12(2), p.e38.

Abu-Akkada, S.S. and Awad, A.M., 2015. Protective effects of probiotics and prebiotics on Eimeria tenella-infected broiler chickens. Pakistan Veterinary Journal, 35, pp.446-450.

Aleem, M.T., Jiawen, S., Yu, Z.Q., hai Wen Z., Yang Z., Meng, L., Lakho, S.A., Haseeb, M., Ali, H., Hassan, M.W., Song, X.K., 2021. Characterization of Membrane-associated Progesterone Receptor Component-2 (MAPRC2) From Trichinella spiralis and Its Interaction With Progesterone and Mifepristone.

Annett, C.B., Viste, J.R., Chirino-Trejo, M., Classen, H.L., Middleton, D.M., Simko, E., 2002. Necrotic enteritis: effect of barley, wheat and corn diets on proliferation of Clostridium perfringens type A. Avian Pathology., 31(6): 598-601.

Antonissen, G., Euckhaut, V., Van Driessche, K., Onrust, L., Haesebrouck, F., Ducatelle, R., Moore, R.J., Van Immerseel, F., 2016. Microbial shifts associated with necrotic enteritis. Avian Pathology., 45(3): 308-312.

Alizadeh, M., Rodriguez-Lecompte, J.C., Rogiewicz, A., Patterson, R., Slominski, B.A., 2016. Effect of yeast-derived products and distillers dried grains with solubles (DDGS) on growth performance, gut morphology, and gene expression of pattern recognition receptors

and cytokines in broiler chickens. Poultry Science., 95(3): 507-17.

Awad, M.M., Bryant, A.E., Stevens, D.L., Rood, J.I., 1995. Virulence studies on chromosomal alpha-toxin and theta-toxin mutants constructed by allelic exchange provide genetic evidence for the essential role of alpha-toxin in Clostridium perfringens-mediated gas gangrene. Molecular Biology., 15(2): 191-202.

Biloni, A., Quintana, C.F., Menconi, A., Kallapura, G., Latorre, J., Pixley, C., Layton, S., Dalmagro, M., Hernandez-Velasco, X., Wolfenden, A. and Hargis, B.M., 2013. Evaluation of effects of Early Bird associated with FloraMax-B11 on Salmonella Enteritidis, intestinal morphology, and performance of broiler chickens. Poultry science, *92*(9), pp.2337-2346.

Caly, D.L., D'Inca, R., Auclair, E., Drider, D., 2015. Alternatives to Antibiotics to Prevent Necrotic Enteritis in Broiler Chickens: A Microbiologist's Perspective. Frontiers in Microbiology., 6: 1336.

Chalmers, G., Martin, S.W., Hunter, D.B., Prescott, J.F., Weber, L.J., Boerlin, P., 2008. Genetic diversity of *Clostridium perfringens* isolated from healthy broiler chickens at a commercial farm Veterinary Microbiology., 127(1-2): 116-127.

Chalmers, G., Martin, S.W., Prescott, J.F., Boerlin, P., 2008. Typing of *Clostridium perfringens* by multiple-locus variable number of tandem repeats analysis.Veterinary Microbiology., 128(1-2): 126-135.

Chen, H., Huang, C., Chen, Y., Mohsin, M., Li, L., Lin, X., Huang, Z., Yin, G., 2020. Efficacy of recombinant N-and C-terminal derivative of EmIMP1 against E. maxima infection in chickens. British poultry science. Sep 2;61(5):518-22.

Cooper, K.K., Songer, J.G., 2009. Necrotic enteritis in chickens: a paradigm of enteric infection by Clostridium perfringens type A. Anaerobe., 15(1-2): 55-60.

Craven, S.E., Stern, N.J., Cox, N.A., Bailey, J.S. and Berrang, M., 1999. Cecal carriage of Clostridium perfringens in broiler chickens given Mucosal Starter Culture™. Avian Diseases, pp.484-490.

Crespo, R., Fisher, D.J., Shivaprasad, H.L., Fernandez-Miyakawa, M.E., Uzal, F.A., 2007. Toxinotypes of *Clostridium perfringens* isolated from sick and healthy avian species. Journal of Veterianry Diagniostic Investigation.,19(3): 329-333.

Engberg, R.M., Grevsen, K., Ivarsen, E., Frette, X., Christensen, L.P., Højberg, O., Jensen, B.B., Canibe, N., 2013. The effect of Artemisia annua on broiler performance, on intestinal microbiota and on the course of a Clostridium perfringens infection applying a necrotic enteritis disease model. Avian. Pathol., 41(4): 369-376.

Fernandes, d.a., Costa. S.P., Mot, D., Bokori-Brown, M., Savva, C.G., Basak, A.K., Van Immerseel, F., Titball, R.W., 2013. Protection against avian necrotic enteritis after immunisation with NetB genetic or formaldehyde toxoids. Vaccine., 31(37): 4003-4008.

Fowler, J., Kakani, R., Haq, A., Byrd, J., Bailey, C., 2015. Growth promoting effects of prebiotic yeast cell wall products in starter broilers under an immune stress and Clostridium perfringens challenge. THE JOURNAL OF APPLIED POULTRY RESEARCH., 24(1): 66-72.

Gad, W., Hauck, R., Kruger, M., Hafez, M.M., 2011. The prevalence of *Clostridium perfringens* in commercial Turkey and layer flocks. Archiv fur Geflugelkunde., 75(2): 74-7

Galindo-Cuspinera, V., Westhoff, D.C., Rankin, S.A., 2003. Antimicrobial properties of commercial annatto extracts against selected pathogenic, lactic acid, and spoilage microorganisms. Journal of food protection., 66(6): 1074-1078.

Geier, M.L., Mikkelsen, L., Torok, V., Allison, G., Olnood, C., Boulianne, M., Hughes, R., Choct, M., 2010. Comparison of alternatives to in-feed antimicrobials for the prevention of clinical necrotic enteritis. Journal of Applied Microbiology., 109(4): 1329-1338.

Hafez, H.M., 2011. Enteric diseases of poultry with special attention to *Clostridium perfringens*. Pakistan Veterinary Journal., 31(3): 175-184.

Hatoum, R., Labrie, S., Fliss, I., 2012. Antimicrobial and probiotic properties of yeasts: from fundamental to novel application. Frontiers in Microbiology., 3:421.

Hofacre, C.L., Froyman, R., Gautrias, B., George, B., Goodwin, M.A. and Brown, J., 1998. Use of Aviguard and other intestinal bioproducts in experimental Clostridium perfringens-associated necrotizing enteritis in broiler chickens. Avian Diseases, pp.579-584.

Jang, S.I., Lillehoj, H.S., Lee, S.H., Lee, K.W., Lillehoj, E.P., Hong, Y.H., An, D.J., Jeong, W., Chun, J.E., Bertrand, F., Dupuis, L., Deville, S., Arous, J.B., 2012. Vaccination with Clostridium perfringens recombinant proteins in combination with Montanide™ ISA 71 VG adjuvant increases protection against experimental necrotic enteritis in commercial broiler chickens. Vaccine., 30(36): 5401-5406.

Jang, S.I., Lillehoj, H.S., Lee, S.H,. Lee, K.W., Lillehoj, E.P., Hong, Y.H., An, D.J., Jeoung, D.H., Chun, J.E., 2013. Relative disease susceptibility and clostridial toxin antibody responses in three commercial broiler lines coinfected with Clostridium perfringens and *Eimeria maxima* using an experimental model of necrotic enteritis. Avian Diseases., 57(3): 684-687.

Jiang, Y., Mo, H., Willingham, C., Wang, S., Park, J.Y., Kong, W., Roland, K.L., Curtiss, R., 2015. Protection Against Necrotic Enteritis in Broiler Chickens by Regulated Delayed Lysis Salmonella Vaccines. Avian Diseases., 59(4): 475-485.

Jin, K., Wang, S., Zhang, C., Xiao, Y., Lu, S., Huang, Z., 2013. Protective antibody responses against Clostridium difficile elicited by a DNA vaccine expressing the enzymatic domain of toxin B. Human Vaccines & Immunotherapeutics.,9(1): 63-73.

Jost, B.H., Trinh, H.T., Songer, J.G., 2006. Clonal relationships among *Clostridium perfringens* of porcine origin as determined by multilocus sequence typing. Veterinary Microbiology., 116(1-3): 158-165.

Kaldhusdal, M., Schneitz, C., Hofshagen, M. and Skjerve, E., 2001. Reduced incidence of Clostridium perfringens-associated lesions and improved performance in broiler chickens treated with normal intestinal bacteria from adult fowl. *Avian diseases*, pp.149-156.

Keyburn, A.L., Sheedy, S.A., Ford, M.E., Williamson, M.M., Awad, M.M., Rood, J.I., Moore, R.J., 2006. Alpha-toxin of Clostridium perfringens is not an essential virulence factor in necrotic enteritis in chickens. Infection and Immunity., 74(11): 6496-6500.

Keyburn, A. L., Boyce, J. D., Vaz, P., Bannam, T. L., Ford, M. E., Parker, D., ... & Moore, R. J., 2008. NetB, a new toxin that is associated with avian necrotic enteritis caused by Clostridium perfringens. *PLoS pathogens.*, *4*(2), e26.

Keyburn, A.L., Bannam, T.L., Moore, R.J., Rood, J.J., 2010. NetB, a pore-forming toxin from necrotic enteritis strains of *Clostridium perfringens.* Toxins., 2(7): 1913-1927.

Keyburn, A.L., Yan, X.X., Bannam, T.L., Van Immerseel, F., Rood, J.I., Moore, R.J., 2010. Association between avian necrotic enteritis and *Clostridium perfringens* strains expressing NetB toxin. Veterinary Research., 41(2): 1-8.

Keyburn, A.L., Portela, R.W., Ford, M.E., Bannam, T.L., Yan, X.X., Rood, J.I., Moore, R.J., 2013a. Maternal immunization with vaccines containing recombinant NetB toxin partially protects progeny chickens from necrotic enteritis. 44:108.

Keyburn, A.L., Portela, R.W., Sproat, K., Ford, M.E., Bannam, T.L., Yan, X., Rood, J.I., Moore, R.J., 2013b. Vaccination with recombinant NetB toxin partially protects broiler chickens from necrotic enteritis. Veterinary Research., 44: 54.

Kulkarni, R.R., Parreira, V.R., Sharif, S., Prescott, J.F., 2007. Immunization of broiler chickens against Clostridium perfringens-induced necrotic enteritis. Clinical and Vaccine Immunology., 14(9): 1070-1077.

Li, N., Yu, Y.Z., Yu, W.Y., Sun, Z.W., 2011. Enhancement of the immunogenicity of DNA replicon vaccine of Clostridium botulinum neurotoxin serotype A by GM-CSF gene adjuvant. Immunopharmacology and Immunotoxicology., 33(1): 211-219.

Lin, X., Mohsin, M., Abbas, R.Z., Li, L., Chen, H., Huang, C., Li, Y., Goraya, M.U., Huang, Z., Yin, G., 2020. Evaluation of Immunogenicity and Protective Efficacy of Eimeria maxima Immune Mapped Protein 1 with EDA Adjuvant in Chicken. Pakistan Veterinary Journal. 2020 Jan 1;40(2):209-13.

Liu, D., Guo, Y., Wang, Z., Yuan, J., 2010. Exogenous lysozyme influences Clostridium perfringens colonization and intestinal barrier function in broiler chickens. Avian Pathology., 39(1): 17-24.

Liu, X., Diarra, M.S., Zhang, Y., Wang, Q., Yu, H., Nie, S.P., Xie, M.Y., Gong, J., 2016. Effect of encapsulated carvacrol on the incidence of necrotic enteritis in broiler chickens. Avian Pathology., 45(3): 357-364.

McReynolds, J., Waneck, C., Byrd, J., Genovese, K., Duke, S. and Nisbet, D., 2009. Efficacy of multistrain direct-fed microbial and phytogenetic products in reducing necrotic enteritis in commercial broilers. Poultry Science, 88(10), pp.2075-2080.

McDevitt, R.M., Brooker, J.D., Acamovic, T., Sparks, N.H.C., 2006. Necrotic enteritis: a continuing challenge for poultry industry. World's Poultry Science., 62(2): 221-247.

M'Sadeq, S.A., Wu, R., Swick, R.A., and Choct, M., 2015. Towards the control of necrotic enteritis in broiler chickens with in-feed antibiotics phasing-out worldwide. Animal Nutrition., 1: 1-11.

Mohsin, M, Li, L., Huang, X., Aleem, M.T., Habib, Y.J., Ismael, A., 2021b. Immunogenicity and Protective Efficacy of Probiotics with EtIMP1C against Eimeria tenella Challenge. Pakistan Veterinary Journal, Jan 1;41(2):274-8.

Mohsin, M, Abbas, R.Z., Yin, G., Sindhu, Z.U., Abbas, A., Huang, Z., Aleem, M.T., Saeed, Z., Afzal, M.Z., Ejaz, A., Shoaib, M., 2021. Probiotics as therapeutic, antioxidant and immunomodulatory agents against poultry coccidiosis. World's Poultry Science Journal. 2021a Feb 17:1-5.

Moore, R.J., 2016. Necrotic enteritis predisposing factors in broiler chickens. Avian Pathology., 45(3): 275-281.

Moore, R.J., 2015. Necrotic enteritis in chickens: an important disease caused by Clostridium perfringens. Microbiology Australia., 36(3): 118-119.

Mot, D., Timbermont, L., Haesebrouck, F., Ducatelle, R., Van Immerseel, F., 2014. Progress and problems in vaccination against necrotic enteritis in broiler chickens. Avian Pathology., 43(4): 290-300.

Myers, G.S., Rasko, D.A., Cheung, J.K., Ravel, J., Seshadri, R., DeBoy, R.T., Ren, Q., Varga, J., Awad, M.M., Brinkac, L.M., Daugherty, S.C., Haft, D.H., Dodson. R.J., Madupu, R., Nelson, W.C., Rosovitz, M.J., Sullivan, S.A., Khouri, H., Dimitrov, G.I., Watkins, K.L., Mulligan, S., Benton, J., Radune, D., Fisher, D.J., Atkins, H.S., Hiscox, T., Jost, B.H., Billington, S.J., Songer, J.G., McClane, B.A., Titball, R.W., Rood, J.I., Melville, S.B., Paulsen, I.T., 2006. Skewed genomic variability in strains of the toxigenic bacterial pathogen, Clostridium perfringens. Genome Research., 16(8):1031-1040.

Nakonieczna, A., Cooper, C.J., Gryko, R., 2015. Bacteriophages and bacteriophage-derived endolysins as potential therapeutics to combat Gram-positive spore forming bacteria. Journal of Applied Microbiology., 119(3): 621-631.

Olkowski, A.A., Wojnarowicz, C., Chirino-Trejo, M., Laarveld, B., Sawicki, G., 2008. Sub-clinical necrotic enteritis in broiler chickens: novel etiological consideration based on ultra-structural and molecular changes in the intestinal tissue. Research in Veterinary Science, 85(3): 543-553.

Patel, S., Goyal, A., 2012. The current trends and future perspectives of prebiotics research: a review. 3 Biotech., 2(2): 115-125.

Rappuoli, R., Black, S., Lambert, P.H., 2011. Vaccine discovery and translation of new vaccine technology. The Lancet., 378(9788): 360-368. 76.

Rimoldi, G., Uzal, F., Chin, R.P., Palombo, E.A., Awad, M., Lyras, D., Shivaprasad, H.L., 2015. Necrotic Enteritis in Chickens Associated with Clostridium sordellii. Avian Diseases., 59(3): 447-451.

Ritzi, M. M., W. Abdelrahman., K. Van-Heerden., M. Mohnl., N. W. Barrett., and R. A. Dalloul., 2016. Combination of Probiotics and Coccidiosis Vaccine Enhances Protection against an Eimeria Challenge. Veterinary Research., 47 (1): 111. doi:10.1186/s13567-016-0397-y.

Rood, J.I., Keyburn, A.L., Moore, R.J., 2016. NetB and necrotic enteritis: the hole moveable story. Avian Pathology., 45(3): 295-301.

Sawires, Y.S., Songer, J.G., 2005. Multi-locus variable-number tandem repeats analysis for strain typing of *Clostridium perfringens*. Anaerobe., 11(5): 262-272.

Schoster, A., Kokotovic, B., Permin, A., Pedersen, P.D., Dal Bello, F., Guardabassi, L., 2013. In vitro inhibition of Clostridium difficile and Clostridium perfringens by commercial probiotic strains. Anaerobe., 20: 36-41.

Shojadoost, B., Vince, A.R., Prescott, J.F., 2012. The successful experimental induction of necrotic enteritis in chickens by Clostridium perfringens: a critical review. Veterinary Research., 43(1): 1

Shimizu, T., Ohtani, K., Hirakawa, H., Ohshima, K., Yamashita, A., Shiba, T., Ogasawara, N., Hattori, M., Kuhara, S., Hayashi, H., 2002. Complete

genome sequence of Clostridium perfringens, an anaerobic flesh-eater. Proceedings of the National Academy of Sciences of the United States of America., 99(2): 996-1001.

Smyth, J.A., 2016. Pathology and diagnosis of necrotic enteritis: is it clear-cut? Avian Pathology., 45(3): 282-7.

Smyth, J.A., Martin, T.G., 2010. Disease producing capability of NetB positive isolates of *C. perfringens* recovered from normal chickens and a cow, and NetB positive and negative isolates from chickens with necrotic enteritis. Veterinary Microbiology., 146(1-2): 76-84.

Skinner, J.T., Bauer, S., Young, V., Pauling, G., Wilson, J., 2010. An economic analysis of the impact of subclinical (mild) necrotic enteritis in broiler chickens. Avian Diseases., 54(4): 1237-1240.

Songr, J.G., 1996. Clostridial enteric diseases of domestic animals. Clinical Microbiology Reviews., 9(2): 216-234.

Swayne, D.E., Glisson, J.R., McDougald, L.R., Nolan, L.K., Suarez, D.L., Nair, V.L., 2013. Diseases of Poultry. 13th ed. John Wiley and Sons; New Jersey USA.

Thanissery, R., McReynolds, J.L., Conner, D.E., Macklin, K.S., Curtis, P.A. and Fasina, Y.O., 2010. Evaluation of the efficacy of yeast extract in reducing intestinal Clostridium perfringens levels in broiler chickens. *Poultry science*, *89*(11), pp.2380-2388.

Timbermont, L., Lanckriet, A., Dewulf, J., Nollet, N., Schwarzer, K., Haesebrouck, F., Ducatelle, R., Van Immerseel, F., 2010. Control of Clostridium perfringens induced necrotic enteritis in broilers by target-released butyric acid, fatty acids and essential oils. Avian Pathology., 39(2):117-121.

Tsiouris, V., Georgopoulou, I., Batzios, C., Pappaioannous, N., Ducatella, R., Fortomaris, P., 2014. Temporary feed restriction partially protects broilers from necrotic enteritis.

Tsiouris, V., Georgopoulou, I., Batzios, C., Pappaioannous, N., Ducatella, R., Fortomaris, P., 2015. High stocking density as a predisposing factor for necrotic enteritis in broiler chickens. Avian Pathology., 44(2): 59-66.

Tsiouris, V., 2016. Poultry management: a useful tool for the control of necrotic enteritis ipoultry. Avian Pathology., 45(3): 323-325.

Umar, S.M., Younus, M., Shehzad, M., Aqil, K., Qayyum, R., Mushtaq, A., Shah, M.A.A., Munir, M.T., 2016. Role of wheat based diet on the pathology of necrotic enteritis in Turkey. Scientifica., 2016.

Unnikrishnan, M., Rappuoli, R., Serruto, D., 2012. Recombinant bacterial vaccines. Current opinion in immunology., 24(3): 337-342.

Uzal, F.A., Freedman, J.C., Shrestha, A., Theoret, J.R., Garcia, J., Awad, M.M., Adams, V., Moore, R.J., Rood, J.I., McClane, B.A., 2014. Towards an understanding of the role of Clostridium perfringens toxins in human and animal disease. Future Microbiology., 9(3): 361-377.

Van Immerseel, F., Lyhs, U., Pedersen, K., Prescott, J., 2016. Recent breakthroughs have unveiled the many knowledge gaps in Clostridium perfringens-associated necrotic enteritis in chickens: the First International Conference on Necrotic Enteritis in Poultry. Avian Pathology., 1-5.

Volozhantsev, N.V., Verevkin, V.V.., Bannov, V.A., Krasilnikova, V.M., Myakinina, V.P., Zhilenkov, E.L., Svetoch, E.A., Stern, N.J., Oakley, B.B., Seal, BS., 2011. The genome sequence and proteome of bacteriophage ΦCPV1 virulent for Clostridium perfringens. Virus Research., 155(2): 433-439.

Wade, B., Keyburn, A., 2015. The true cost of necrotic enteritis. PoultryWorld., 31(7): 16-17.

Wu, S.B., Stanley, D., Rodgers, N., Swick, R.A., Moore, R.J., 2014. Two necrotic enteritis predisposing factors, dietary fishmeal and Eimeria infection, induce large changes in the caecal microbiota of broiler chickens. Veterinary Microbiology., 169(3): 188-197.

Yan, X.X., Porter, C.J., Hardy, S.P., Steer, D., Smith, A.I., Quinsey, N.S., Hughes, V., Cheung, J.K., Keyburn, A.L., Kaldhusdal, M., Moore, R.J., Bannam, T.L., Whisstock, J.C., Rood, J.I., 2013. Structural and functional analysis of the pore-forming toxin NetB from Clostridium perfringens. mBio., 4(1): e00019 00013.

Zahoor, I., Ghayas, A., Basheer, A., 2018. Genetics and genomics of susceptibility and immune response to necrotic enteritis in chicken: a review. Molecular Biology Reports., 45: 31-37.

Zeng, J., Song, F., Yang, Y., Ma, C., Deng, G., Li, Y., Wang, Y., Liu, X., 2016. The generation and characterization of recombinant protein and antibodies of *Clostridium perfringens* Beta2 toxin. Journal of Immunology Research., 1-12.

CHAPTER 8

IoT IN AGRICULTURE: SMART FARMING

Assist. Prof. Deepa SONAL [1]

[1] Patna University, Patna Women's College, Department of Computer Science, Patna, India. deepsonapwc@gmail.com ORCID ID 0000-0002-2485-6140

1. INTRODUCTION

Agriculture, like every other sector, is being transformed by digital technology. Precision agriculture is a growing trend that uses technology to assure that crops and soil get exactly what they need to thrive. Mobile applications, sensor technologies, drones, and cloud computing technologies are all used in precision farming. This shift is occurring across the board in the agricultural industry, regardless of size. Precision agriculture is made up of three sorts of platforms: stationary, airborne, and ground-based mobile, all of which rely on IoT and APIs.

The Internet of Things (IoT) is a network of interconnected computing devices, digital and mechanical equipment, humans or animals, and objects that can detect, gather, and send data over the internet without need for human intervention. Everything is given a distinct identifier. It is an advanced examination and mechanized framework that employs detecting, organizing, immense data, and man-made awareness innovation to convey a complete administration framework. Essentially, the Internet of Things (IoT) is for extending the capabilities of the internet over smartphones and computers.

There are four main components of IoT-

- Low-power embedded systems—In the design of electronic systems, the inverse factors of high performance and low battery consumption play a crucial role.

- Data acquired from devices is saved on dependable storage servers, which is where cloud computing comes into play.
- Availability of Big Data- Because IoT relies heavily on real-time sensors. As a result, the use of electronic devices has extended throughout every field, resulting in a vast data flow.
- Network connection- Internet access is required for communication, and each physical object is allocated an IP address. With the help of these, a network connection is established between the devices.

2. IoT IN AGRICULTURE

Within few years, the world's population will have surpassed 3 billion. As a result, the agriculture business must embrace IoT in order to feed such a large population. Excessive climate conditions, weather change, and various environmental effects resulting from farming techniques are all difficulties that must be addressed in order to meet the need for more food. The future of Indian agriculture must be shaped by a thorough awareness of and excessive reliance on technologies that may increase production while also regaining farmers' interest in the industry. As a result, these smart farming approaches will help farmers reduce scrap and increase capacity. It's essentially a high-tech, capital-intensive method for mass-producing crops in a sustainable manner. Farmers can use this technology to observe ground conditions from anywhere using sensors and to water fields using an automated system. It is the use of information and communications technologies in farming.

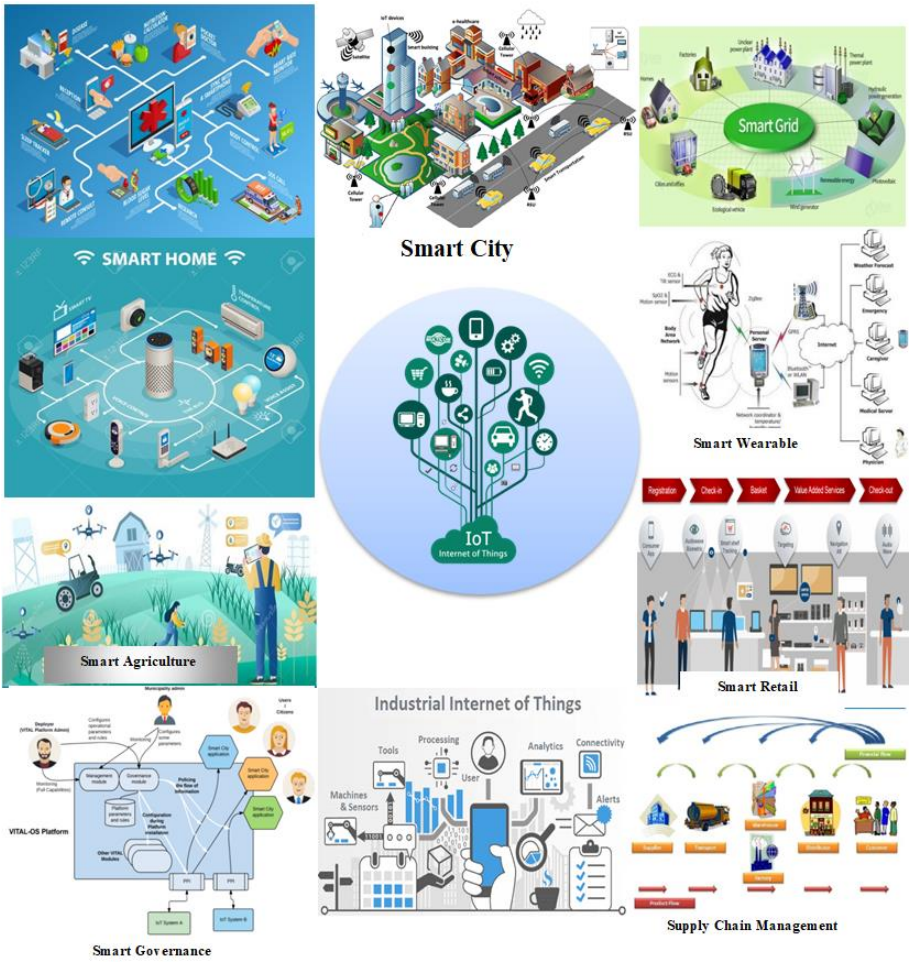

Figure 1: Application of IoT in various fields

3. IoT STRUCTURE IN AGRICULTURE

The sensor layer, transport layer, and application layer are the three levels that make up this system structure, and the functions of these layers are listed below –

1) **Sensor layer**—One of the sensor layer's challenges is to gain automated and real-time transformations of real-world agricultural manufacturing figures into digital transformations or information that can be handled in the virtual world using various methods. The information they gather is as follows:

- Sensor data includes humidity, temperature, gas concentrations, and pressure, among other things.
- Name, model, price, and features of the product.
- Working conditions - operating parameters of various machines, apparatus, and so on.
- Information on the location

The primary goal of the Information Layer is to identify various types of information or data, collect the information and labeled information in the real world using sensing techniques, and then remodel those for processing into digital information. RFID tags, cameras, two-dimensional code labels, and sensor networks are some of the tactics used in this sensor layer.

2) Transport layer- This layer's job is to gather and consolidate agricultural data from the previous layer in preparation for processing. It is thought to be the IoT's nerve center. This layer consists of a telecommunication management center, as well as an internet network, an information center, and smart processing centers.

3) Application layer- This layer's job is to assess and interpret the data gathered in order to foster digital consciousness of the real world.

It's a hybrid of the Internet of Things and agricultural market intelligence.

4. CURRENT IoT SYSTEMS OVERVIEW

Various IoT solutions have been proposed by researchers in recent years. The system architecture is determined by the category of communication technology currently offered on-site, the communication protocol, the cost of hardware and software, the amount of land used, the crop type (open-field or indoor agriculture), the sensors used, and whether the systems are research or application-oriented.

The FarmBeats system, according to Vasisht et al. (2017), has two communication layers: the base stations in the farmland were linked to the farmhouse via TV White spaces, and they were attached to the field sensors (including cameras) and drones via Wi-Fi. Temporarily underutilized radio frequencies of professionally allocated frequencies for broadcast television channels are known as TV white spaces (Sonal et al. , 2021) Microsoft Azure was the fifth cloud service used. Local backup at the farm was utilized to save data amid internet outages.

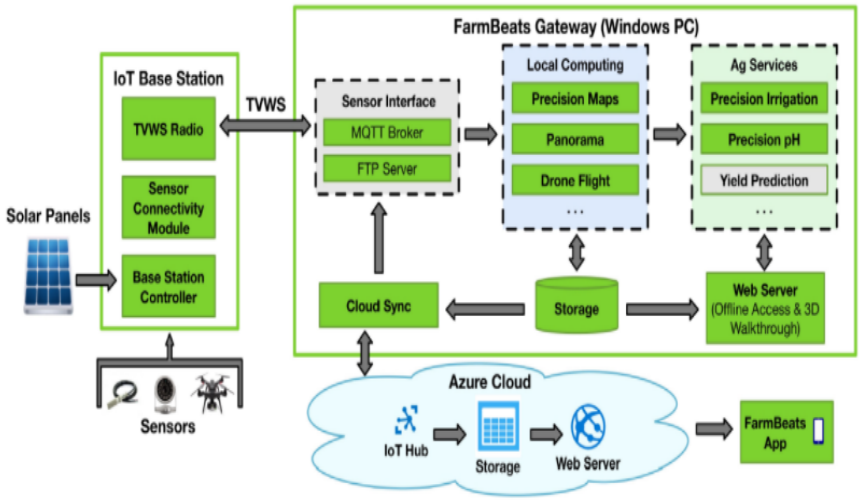

Figure 2: Schematic diagram of Architecture of Existing IoT System (Vasisht et al., 2017)

Popovic et al. (2017) presented an IoT-enabled platform architecture for smart farming and environmental tracking research. It had an identical framework to Farmbeats, but the sensor nodes built by (Libelium, 2021) were integrated into the system. The research paper (Popovic et al., 2017) was significant since the authors examined IoT system architecture from several, concurrent perspectives.

5. LAYERS OF THE INTERNET OF THINGS

The perception layer (sensors and actuators), the network layer (data transfer), and the application layer (data storage and processing) are the three levels that make up a typical IoT system architecture. Two more levels were required to form an IoT system: the middleware

layer, which sits between the network and business layers, and the application layer, which comes just after the middleware layer.

- **Perception Layer**

Sensors and actuators make up the perception layer. This layer is in charge of gathering and processing data that can be transmitted. The general architecture of perception layer devices is described in Figure 3. The perception layer aids in the spatial and temporal resolution of agricultural data collection.

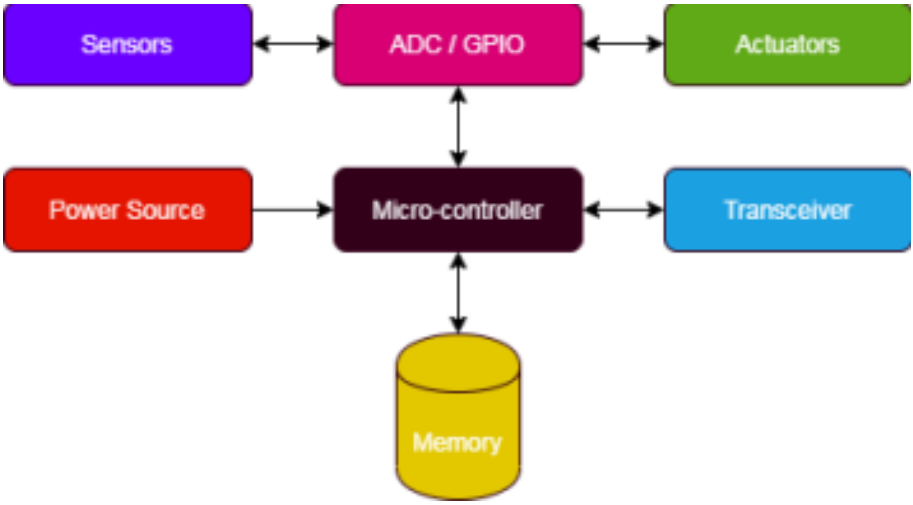

Figure 3: Perception layer device architecture

In comparison to conventional sensors, IoT perception layer devices have a unique identification number to identify them on the internet (AliKhattak et al., 2019). Wi-Fi-connected sensor nodes, for example, have an IP address to indicate their uniqueness, whereas LPWAN perception layer devices have a unique identification number.

- **Network Layer**

The network layer is used to send data obtained by sensors from the perception layer to the application layer over an existent communication network, whilst the application layer sends decisions or control signals to actuators in the perception layer (Leo et al., 2014). For monitoring-only systems, bidirectional communication is not required. Communication Technology (CT) and Communication Protocols are the two fundamental components of the network layer.

- **Middleware Layer**

There are three kinds of IoT middleware, according to (Ngu et al., 2017). The first is service-based, which is characterized by a service-oriented architecture (SOA). LinkSmart is an example of how it enables developers and consumers to implement various IoT devices as services (LinkSmart, 2021). The second category is a cloud-based solution that restricts users in terms of the type and quantity of IoT devices they may install but allows them to simply link, gather, and analyze the data obtained because certain use cases can be defined and programmed without any knowledge of sensor data.

- **Application Layer**

The application layer's primary function is data formatting and presentation. Data transmission among nodes, gateways, and cloud data storage, as well as between cloud data storage and end-user applications, is handled by the application layer. These protocols

manage data requests, responses, publishes, and subscriptions. Application layer protocols such as CoAP, MQTT, XMPP, REST, AMQP, and Web socket are widely used (Karagiannis et al., 2015).

- **Business Layer**

The business layer's key goals are to ensure the long-term viability of the entire IoT system, comprising applications, business and profit models, and user privacy (Navani, Jain, & Nehra, 2017). For the purposes of this chapter, the business layer's scope is somewhat less important.

6. CONCLUSION

The Internet of Things (IoT) is a crucial and quickly expanding technology with several applications in various fields, including agriculture. VI monitoring via satellites, handheld sensors, ground-based systems, mobile platforms, and Autonomous Aerial Vehicles has become common in agrarian and ecological applications over the last three decades. Due to a lack of understanding and the high cost of field VI monitoring systems with multispectral sensors, only a small percentage of farmers use them. Furthermore, farmers need real-time monitoring data in making decisions.

REFERENCES

Vasisht, D., Kapetanovic, Z., Won, J., Chandra, R., Kapoor, A., Sinha, S., . . . Stratman, S. (2017). FarmBeats: An IoT Platform for Data-Driven Agriculture. 14th {USENIX} Symposium on Networked Systems Design and Implementation (pp. 515-529). Boston: USENIX Association. Retrieved from https://www.usenix.org/system/files/conference/nsdi17/nsdi17-vasisht.pdf

Navani, D., Jain, S., & Nehra, M. (2017). The Internet of Things(IoT) : A Study of Architectural Elements. 13th International Conference on Signal-Image Technology and Internet-Based Systems (pp. 473-478). Jaipur, India: IEEE. doi:10.1109/SITIS.2017.83

Karagiannis, V., Chatzimisios, P., Vazquez-Gallego, F., & Alonso-Zarate, J. (2015). A Survey on Application Layer Protocols for the Internet of Things. Transaction on IoT and Cloud Computing, 3(1), 11-17.

LinkSmart, I. (2021, 1 22). Linksmart. Retrieved 01 22, 2021, from https://linksmart.eu/

METER Group, I. U. (2020). SRS Spectral Reflectance Sensor Operator's Manual.Pullman WA: METER Group, Inc. USA. Retrieved from http://manuals.decagon.com/Manuals/14597_SRS_Web.pdf

Ngu, A., Gutierrez, M., Metsis, V., Nepal, S., & Sheng, Q. (2017). IoT Middleware: A Survey on Issues and Enabling Technologies. IEEE INTERNET OF THINGS JOURNAL, 4(1), 1 - 20. doi:10.1109/JIOT.2016.2615180

Leo, M., Battisti, F., Carli, M., & Neri, A. (2014). A federated architecture approach for Internet of Things security. 2014 Euro Med Telco Conference (EMTC) (pp. 1-5). Naples, Italy: IEEE. doi:10.1109/EMTC.2014.6996632

AliKhattak, H., AliShah, M., Khan, S., Ali, I., & Imran, M. (2019). Perception layer security in Internet of Things. Future Generation Computer Systems, 100, 144- 164. doi:https://doi.org/10.1016/j.future.2019.04.038

Libelium. (2021, 01 16). Retrieved from https://www.libelium.com/

Popovic, T., Latinovic, N., Pešic, A., Zecˇevic, Z., Krstajic, B., & Djukanovic, S. (2017). Architecting an IoT-enabled platform for precision agriculture and ecological monitoring: A case study. Computers and Electronics in Agriculture, 140, 255– 265. doi:https://doi.org/10.1016/j.compag. 2017.06.008

M.A. Haque, D. Sonal, S. Haque, M.M. Nezami, K. Kumar, An IoT-Based Model for Defending Against the Novel Coronavirus (COVID-19) Outbreak, Solid State Technol., pp. 592–600, 2020.

J.A. Luis, J.A.G. Galán, J.A. Espigado, Low power wireless smoke alarm system in home fires, Sensors (Switzerland) 15 (8) (2015) 20717–20729, https://doi.org/10.3390/s150820717.

S. Giordano, I. Seitanidis, M. Ojo, D. Adami, F. Vignoli, IoT solutions for crop protection against wild animal attacks, 2018 IEEE Int. Conf. Environ. Eng. EE 2018 – Proc., vol. 1, no. 710583, pp. 1–5, 2018, doi: 10.1109/EE1.2018.8385275.

D. Sonal, D. N. Pandit, and M. A. Haque, "An IoT Based Model to Defend Covid-19 Outbreak," Int. J. Innov. Technol. Explor. Eng., vol. 10, no. 7, pp. 152–157, May 2021, doi: 10.35940/ijitee.G9052.0510721

EasyChair Preprint The Role of Internet of Things (Iot) to Fight Against Covid-19 The Role of Internet of Things (IoT) to Fight Against COVID-19. Available from:

https://www.researchgate.net/publication/354208629_EasyChair_Preprint_The_Role_of_Internet_of_Things_Iot_to_Fight_Against_Covid-19_THE_ROLE_OF_INTERNET_OF_THINGS_IoT_TO_FIGHT_AGAINST_COVID-19 [accessed Sep 13 2021].

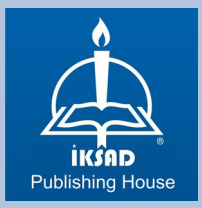

ISBN: 978-625-7562-95-9